

For Reference

NOT TO BE TAKEN FROM THIS ROOM

Ex LIBRIS
UNIVERSITATIS
ALBERTAEASIS



Level Mountain is a Late Cenozoic shield volcano located near 131° THE UNIVERSITY OF ALBERTA volcanic belt of northwestern British Columbia. The volcano rises with an

LATE CENOZOIC ALKALINE VOLCANICS OF THE LEVEL MOUNTAIN RANGE, NORTHWESTERN BRITISH COLUMBIA: GEOLOGY, PETROLOGY AND PALEOMAGNETISM

region of peaks and ridges to a maximum elevation of 7300' (2220m), and is situated on a series/belt of alkali basalts and ultramafic rocks which cut through the belt and span the period from 4.5 million years ago to recent times. Fazle basaltic rocks are older, basic and associated approximately postdate continental glaciation. A paleomagnetic study of the basalts

A THESIS

SUBMITTED TO THE FACULTY OF GRADUATE STUDIES AND RESEARCH
IN PARTIAL FULFILMENT OF THE REQUIREMENTS FOR THE DEGREE

OF DOCTOR OF PHILOSOPHY

isotope series and are of continental affinity. Oxygen isotope values over 0.6‰ have been measured for unaltered rocks including basalt, gabbro, and ultramafic inclusions. This would seem to indicate that the volcano under northwestern British Columbia is rooted with respect to oxygen and that it has been mainly derived, meteorically.

EDMONTON, ALBERTA

FALL 1981

V.2

salic, underevaporated and **ABSTRACT** metasaline and
metalluminous rocks attest to the complexity of petrogenetic

Level Mountain is a Late Cenozoic shield volcano located near $131^{\circ}20'W$, $58^{\circ}31'N$ in the Stikine Volcanic Belt of northern British Columbia. The volcanic plateau with an average elevation of 4500', (1372m), is younger than Upper Miocene in age and is comprised of up to four sequences of alkali basalt and ankaramite flows and tuffs. The central region of peaks and ridges rises to a maximum elevation of 7200', (2195m), and has a repetitive bimodal distribution of alkali basalt and peralkaline salic lavas and tuffs that spans the period from 4.5 million years b.p. to recent times. Feeble basaltic vents with spatter, bombs and scoria apparently postdate continental glaciation. A paleomagnetic study on two stratigraphic sections that span the entire range of volcanism samples the earth's major polarity reversals for the past 6 MY.

Petrochemically the lavas belong to the sodic alkali basalt series and are of continental affinity. Oxygen isotope values near $5.6^{\circ}/_{\text{o}}$ $\delta^{18}\text{O}$ SMOW have been measured for unaltered rocks including basalts, salics, and ultramafic inclusions. This would seem to indicate that the mantle under northwestern British Columbia is normal with respect to oxygen and that the Level Mountain magmas are mantle derived. Corroborating evidence is available from the whole rock strontium isotope studies which show a total range of $^{87}\text{Sr}/^{86}\text{Sr}$ from .7025 to .7071. The presence of basic and

salic, undersaturated and ovesaturated, peralkaline and metaluminous rocks attests to the complexity of petrogenetic processes at Level Mountain. Although the two volumetrically important lava types appear to be primary and mantle derived, the presence of some rhyolites enriched in ^{18}O , granitic gneiss inclusions in basalts and tristanites and great variation in whole rock lead isotope ratios are probably all indicative of some degree of interaction between magmas and crustal rocks. Major and trace element geochemical variations and mineralogy indicate an upper mantle origin at shallower than 15 kbar pressure from an undersaturated ultramafic source that possessed an abundance of alkalis and incompatible elements. The mineralogy and chemistry of the major rock types indicate conditions of low oxygen fugacity and a dry gas phase composition for both peralkaline flows and basalts. The field relations of some comendite flows implies fluid behavior and seems to indicate a viscosity two to three orders of magnitude lower than would be predicted on the basis of silica content and whole rock chemistry. This could be partially reconciled if the gas phase had been halogen rich and dry.

Calculations of the volume and energetics of the volcanism of the Stikine Belt indicate that less than 15% of the modern heat flow is necessary to maintain the levels of volcanicity since Pliocene times.

Table of Contents

Volume II

	Page
Abstract	xxv
List of Tables	xxix
List of Figures	xxx
List of Plates	xxxi
List of Maps	xxxii
CHAPTER 8. CRYSTALLIZATION AND MELTING EXPERIMENTS AT ONE ATMSPHERE TOTAL PRESSURE ON SELECTED ROCKS FROM LEVEL MOUNTAIN	321
INTRODUCTION	321
PREVIOUS WORK. CRYSTALLIZATION AND MELTING RELATIONSHIPS OF PERALKALINE ROCKS	321
EXPERIMENTAL TECHNIQUES.....	325
RESULTS.....	326
CHAPTER 9. THE PHYSICAL BEHAVIOR OF LEVEL MOUNTAIN LAVAS.....	335
VISCOSITIES: ESTIMATED AND EXPERIMENTAL.....	335
Theoretical Viscosity Calculations.....	335
Experimental Viscosity Determinations.....	337
CONSTRAINTS ON THE RISE TIME OF LEVEL MOUNTAIN LAVAS..	342
Introduction.....	342
Nodule Transport and the Ascent of Magmas.....	344
VOLUME ESTIMATES OF LEVEL MOUNTAIN VOLCANISM.....	357
THE ENERGETICS OF MELTING AND RISE.....	366
The Energetics of Volcanism at Level Mountain and for the Stikine.....	366
MODELLING OF A HEAT FLOW AND A GEOTHERMAL GRADIENT FOR LEVEL MOUNTAIN AND THE STIKINE.....	374

CHAPTER 10. GEOTHERMOMETRY AND GEOBAROMETRY ESTIMATES.....	380
INTRODUCTION.....	380
REVIEW OF PREVIOUS DATA FOR THE INTERMONTANE BELT.....	388
GEOBAROMETRY AND GEOTHERMOMETRY FROM THE ACTIVITIES OF SILICA AND ALUMINA IN LEVEL MOUNTAIN LAVAS.....	396
CHAPTER 11. A PALEOMAGNETIC STUDY OF THE LEVEL MOUNTAIN VOLCANICS.....	411
INTRODUCTION.....	411
METHODOLOGY FOR THE PALEOMAGNETIC STUDY OF LEVEL MOUNTAIN.....	414
MAGNETOSTRATIGRAPHY FOR LEVEL MOUNTAIN.....	419
The Stratocone Section, (PB)-Meszah Peak.....	419
The Plateau Section, (PA)-Little Tahltan Canyon...	426
A Comparison of the Paleomagnetic Sections from Level Mountain and Mount Edziza.....	428
CHAPTER 12. SUMMARY AND CONCLUSIONS REGARDING THE PETROGENESIS OF THE LEVEL MOUNTAIN VOLCANICS AND THEIR RELATIONSHIP TO THE TECTONICS OF THE INTERMONTANE BELT....	433
BIBLIOGRAPHY.....	440
APPENDIX 1. FIELD AND REMANENCE NOTES ON LEVEL MOUNTAIN STRATOCONE SECTION.....	475
APPENDIX 2. FIELD AND REMANENCE NOTES ON LEVEL MOUNTAIN PLATEAU SECTION.....	479
APPENDIX 3. REMANENCE DATA FOR LEVEL MOUNTAIN LAVAS.....	483

List of Tables

Table 8-1 - Liquidus and solidus data for basic and intermediate lavas	328
Table 8-2 - Liquidus and solidus data for salic lavas ...	330
Table 9-1 - Predicted viscosities for Level Mountain lavas	336
Table 9-2 - Physical properties of Level Mountain lavas .	345
Table 9-3 - Characteristics of xenoliths from Level Mountain	347
Table 9-4 - Model ascent velocities for Level Mountain lavas	350
Table 9-5 - Volume estimates for Level Mountain lavas ...	358
Table 9-6 - Volume and mass estimates for map units (eruptive pulses) at Level Mountain	361
Table 9-7 - Volume estimates for the Stikine Volcanic Belt	363
Table 9-8 - Energy dissipated by Level Mountain volcanism	368
Table 9-9 - Energy requirements of volcanism at Level Mountain and the Stikine Volcanic Belt	371
Table 9-10 - Cordilleran and other Canadian heat flow data	375
Table 10-1 - Geothermometry of spinel lherzolites	384
Table 10-2 - Chemical analyses of minerals from spinel lherzolites	390
Table 10-3 - Calculated equilibration temperatures for spinel lherzolites from the IMB	393
Table 10-4 - Geothermometry and geobarometry estimates for Level Mountain lavas	404
Table 11-1 - Paleomagnetic remanence data for Level Mountain	420

List of Figures

Figure 8-1 - Peralkaline trachyte liquidus curves in P-T space	324
Figure 8-2 - Buffered crystallization sequences for Level Mountain lavas	327
Figure 9-1 - Plot of reciprocal temperature versus log viscosity	340
Figure 9-2 - Plot of cumulative energy dissipated versus time for Level Mountain volcanism	369
Figure 9-3 Model geothermal gradient for the Stikine Volcanic Belt	378
Figure 10-1 - P-T plot with stability fields for mantle peridotites	395
Figure 10-2 - Buffer curves for $\log a\text{SiO}_2$ and $\log a\text{Al}_2\text{O}_3$, versus P and T	401
Figure 10-3 - Calculated P-T conditions for Level Mountain lavas and spinel lherzolites	406
Figure 10-4 - Geobarometry and geothermometry estimates for the origin of the Level Mountain lavas	409
Figure 11-1 - Location map for Level Mountain paleomagnetic sections	412
Figure 11-2 - Magnetogram:VGP latitude versus elevation for Level Mountain	421
Figure 11-3 - Reference geomagnetic polarity time scale ..	423
Figure 11-4 - Magnetograms for Mount Edziza	429
Figure 11-5 - Correlation for Level Mountain to Mount Edziza and the geomagnetic polarity time scale	430

List of Plates

Plate 8-1 - Photomicrograph of experimentally crystallized aenigmatite	332
Plate 8-2 - Photomicrograph of experimentally crystallized aenigmatite	333
Plate 11-1 - Location of the plateau section: Little Tahltan Canyon	415
Plate 11-2 - Location of the stratocone section: Meszah Peak - Kakuchuya Creek	416

List of Maps

Map 1 - Geologic map and cross sections of the Level
Mountain volcanic centreMap packet

Map 2 - Topographic map of the Level Mountain Range with
traverse controlMap packet

CHAPTER 8. CRYSTALLIZATION AND MELTING EXPERIMENTS AT ONE
ATMOSPHERE TOTAL PRESSURE ON SELECTED ROCKS FROM LEVEL
MOUNTAIN

INTRODUCTION

A series of more than one hundred reconnaissance experiments was conducted to determine the crystallization behavior of fourteen Level Mountain lavas. Six of the lavas were peralkaline salics and five were basaltic. The remaining three were an alkaline trachyte, a tristanite and a phonolite. Additionally, thirty-five experiments were conducted to determine the solidus temperatures of six xenoliths of mafic and ultramafic composition. For these experiments, the conditions covered the temperature interval from 800°C to 1300°C with the principle range of oxygen fugacities between the FMQ and MW buffers. Twenty-nine experiments were additionally performed under more oxidizing conditions to assess the effect of variable fO_2 . For the most part these experiments were rock-air buffered somewhere between FMQ and HM.

PREVIOUS WORK. CRYSTALLIZATION AND MELTING RELATIONSHIPS OF PERALKALINE ROCKS

A number of studies have been conducted on the melting characteristics of peralkaline rocks. Rather different behavior has been demonstrated for plutonic versus volcanic

undersaturated peralkaline rocks (agpaites).¹ The most prominent initial observation from experimental work was that agpaites had much longer melting intervals than common rock types (Piotrowski and Edgar, 1970; Sood et al, 1970). The large liquidus - solidus interval has been attributed in part to peralkalinity and in part to high concentrations of uncommon or incompatible geochemical elements (Ti, Zr, REE, Fe³⁺, Cl). The halogens and water in these systems may be preferentially retained in the melt, thus affecting an abnormal depression of the solidus, particularly at higher pressures (Anderson, 1974; Manning, 1981). Edgar and Parker (1974) successfully verified this hypothesis for eight crystalline rocks, four plutonic and four volcanic. The melting intervals were typically greater for the plutonic rocks than for the volcanics of similar composition. Presumably this was due to differences in previous cooling history of samples versus incorporation of halogens into crystals and the glass. The experiments reported by Piotrowski and Edgar and by Edgar and Parker were conducted at either one atmosphere or at one kilobar water pressure, unbuffered. Their two-point hydrous liquidus curves appear to be normal, with negative slopes ($dP/dT < 0$). In the determination of the liquidus for the crystalline samples,

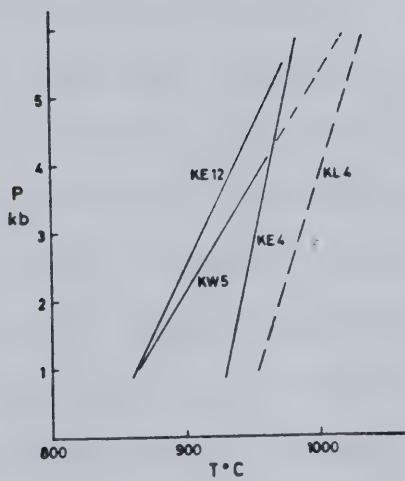
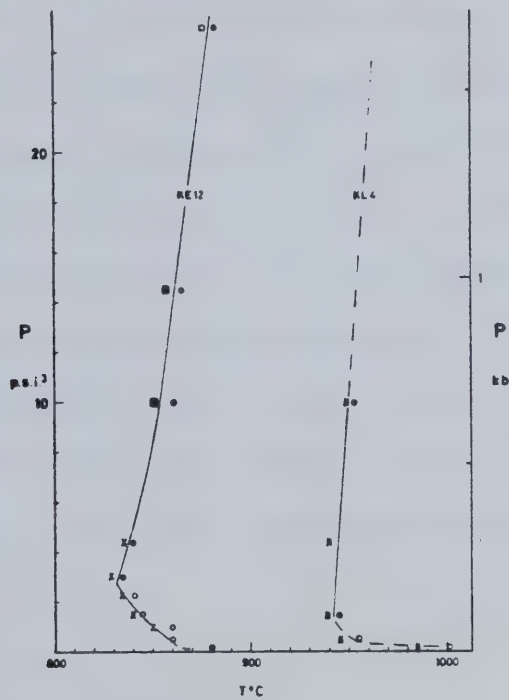
¹ Peralkaline plutonic rocks have been termed agpaites (Sorenson, 1970). They are characterized by a peralkalinity index greater than unity (Act:Ns in the norm), high concentrations of Fe, Ti, Zr, REE, F, Cl and unusual mineralogy which may include eudialite, rinkite, rosenbuschite. Typical occurrences of these rocks are found at Khibina, Kola and Ilimaussaq.

For the four Tenerife phonolites the one-atmosphere liquidus temperature ranged from 1030° to 1200°C. The crystallization sequence at one atmosphere was feldspar followed by nepheline then amphibole. When pH₂O is low, clinopyroxene may crystallize before amphibole or in place of amphibole. The order of appearance of clinopyroxene on the liquidus is quite variable. The phonolites were of the mildly peralkaline type with A.I. ranging from 1.03 to 1.19. Melting intervals determined for three of the phonolites ranged from 305°C to 475°C.

The silica oversaturated peralkaline system has been studied experimentally by Bailey et al (1974). Their studies were anhydrous but unbuffered and conducted over a range of pressures from one atmosphere to approximately 1.5 kilobar. Their samples were pantellerites and pantelleritic trachytes from East Africa (Menghi, Longonot, Eburru). The work of Bailey et al (1974) was done on very peralkaline compositions with A.I. = 1.38 to 2.18. While the solidus temperature was not determined, the liquidus temperature showed a strong linear decrease with increasing peralkalinity. For all compositions studied, plagioclase was the silicate liquidus phase to one kilobar. Sample 83, Eburru Pantellerite, also had phenocryst quartz at one kilobar. There was something noteworthy and rather unusual about the liquidus curves reported in Bailey et al (1974) and Bailey and Cooper (1979), see Figure 8-1. The boundary of the liquidus line in PT space, and also the

Figure 8-1.

Liquidus curves for peralkaline trachytes (KL4, KE4) and more siliceous pantellerites (KE12, KW5) taken from Bailey et al (1974). As pressure increases the liquidus temperature goes through a minimum, then increases linearly to about 5kbar. Depending on the ascent path, such melts could develop considerable superheat. Note convergence of liquidus curves to higher P and T.



crystallization surfaces for alkali feldspar and quartz, are concave to higher temperatures with a temperature minimum at about 0.3 kilobar. If this is indeed the case, a peralkaline magma could possibly acquire some degree of superheat upon ascent (Waldbaum, 1971; Marsh and Kantha, 1978). Partially resorbed alkali feldspar and quartz phenocrysts are a common feature of sparsely crystalline and glassy peralkaline salic lavas. Comendites and pantellerites typically display flow morphologies characteristic of fluid behavior, which contrasts with the more viscous nature of calc-alkaline rhyolites of similar SiO₂ content (Shaw, 1973; Schmincke, 1974). Both of these observations might arise from such a heat input implied by the liquidus determinations of Bailey et al (1974).

EXPERIMENTAL TECHNIQUES

Experiments were conducted on the Deltech furnace under controlled fO₂ conditions achieved by the use of known mixtures of CO and CO₂. The samples, either pressed mineral powder briquettes or glasses quenched from 1300°C, were sintered onto a Pt wire loop and suspended in the thermally uniform position of the furnace after the technique of Donaldson et al (1975). Experiment durations were generally one to three hours. Rapid quenching was achieved by severing the suspension wires so that the sample fell into a mercury filled receptacle at the base of the furnace.

RESULTS

The results of the melting experiments on Level Mountain lavas are summarized as a series of bar graphs in Figure 8-2. The basaltic lavas had the crystallization sequence oxide, olivine, clinopyroxene, plagioclase. The crystallization data is summarized in Table 8-1. An oxide phase crystallized above 1260°C. Compositionally these were magnetite - ulvöspinel solid solutions. Forsterite-rich olivine was the first silicate phase on the liquidus between 1250°C and 1265°C. With the exception of Ne-normative hawaiite, 8/25-50/6397, diopsidic clinopyroxene appeared as the second silicate phase. The clinopyroxene liquidus fell in the interval 1250° to 1165°C. Towards the lower temperature end of this range an intermediate plagioclase, labradorite to andesine composition, was on the liquidus. This compares favorably with the one atmosphere crystallization experiments conducted on alkali basalt by Thompson and Flower (1971) and Duke (1974). Residual phases such as alkali feldspar and nepheline did not appear until near the solidus, between 1100°C and 1050°C. Often two distinct forms were present in the crystallized phases. While the high temperature titanomagnetites tended to be well formed cubes or octahedra, a second dendritic or quench textured magnetite formed particularly in the runs quenched from the lower temperature range of the melting interval. Olivines formed as discreet prisms of equant to acicular habit, while clinopyroxenes crystallized as blades both

Figure 8-2.

Buffered crystallization sequences and melting intervals for Level Mountain lavas. Comendites: (1) 9/2-99 and (2) 8/25-54/6345; Pantellerites: (3) 25/5e and (4) 8/5-8/5150; Comenditic Trachyte: (5) 24/2 o/c and (6) 25/7; Trachyte: (7) 24/hi; Tristanite: (8) LMIII A; Phonolite: (9) LMI20i; Hawaïite: (10) 8/25-50/6397; Alkali Basalts: (11) and (14); Ankaramites: (12) and (13). T range of experiments indicated by length of line. Highest T occurrence of a mineral plotted as appropriate symbol.

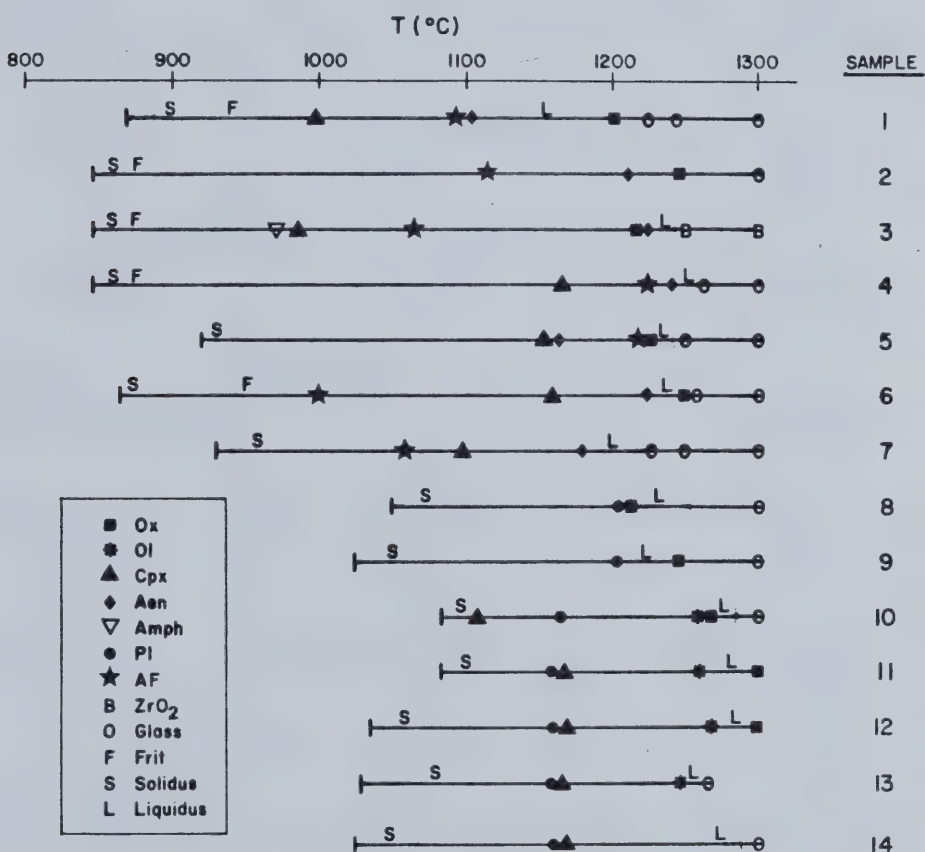


Table 8-1 Liquidus and Solidus Data for Basic and
Intermediate Lavas from Level Mountain

Sample	TL °C	T _S °C	T _m °	TL °C Calc*
LMI20i phonolite	1225 ±20	1050 ±25	175 ±45	1173 pl 1086 cpx 1006 ol
LMIIIA tristanite	1230 ±25	1041 ±31	189 ±56	1364 pl 1050 cpx 876 ol
8/25-59/6397 hawaiite	1270 ±15	1080 ± 7	190 ±22	1165 ol 1140 pl 1135 cpx
PAP Alkali basalt	1275 ±15	1100 ±15	175 ±30	1210 ol 1205 cpx 1173 pl
01 Ankaramite	1250 ±10	1062 ±12	188 ±22	1327 ol 1230 cpx 1048 pl
h ankaramite	1255 ±10	1092 ± 5	163 ±15	1264 pl 1171 ol 1165 cpx
29/1-f early hawaiite	1275 ±13	1083 ±73	192 ±86	—

* French (1971)

singly and as feathery, quench textured aggregates.

Plagioclase crystallized both as blades and dovetail prisms. The crystallization sequences found experimentally correspond to the natural behavior inferred from the petrography of the respective lavas; however, the actual crystal forms may differ due to kinetic effects (Donaldson, 1976). The average measured silicate liquidus temperature for five Level Mountain basalts was $1265^{\circ}\pm5^{\circ}\text{C}$, with a corresponding average solidus of $1083^{\circ}\pm6^{\circ}\text{C}$. The average of the five basalt melting intervals was $182^{\circ}\pm5^{\circ}\text{C}$.

The crystallization sequence of the phonolite and tristanite were oxide, plagioclase, alkali feldspar, clinopyroxene. The oxide appeared between 1212°C and 1247°C . Plagioclase and andesine to oligoclase composition appeared above 1205°C with the silicate liquidus temperatures for phonolite and tristanite set at $1225^{\circ}\pm20^{\circ}$ and $1230^{\circ}\pm25^{\circ}$ accordingly. The averages for these two intermediate lavas are liquidus temperature: $1228^{\circ}\text{C}\pm3^{\circ}$, solidus temperature: $1045^{\circ}\text{C}\pm5^{\circ}$ and melting interval: $183^{\circ}\text{C}\pm7^{\circ}$. The liquidus and solidus are marginally lower than for the basalts and the melting interval is the same.

The crystallization behavior of the salic lavas is summarized in Figure 8-2 with temperature data listed in Table 8-2. The average silicate liquidus temperature for the seven Level Mountain lavas was $1216^{\circ}\pm13^{\circ}\text{C}$. The average salic solidus was $894^{\circ}\pm15^{\circ}\text{C}$ and the average melting interval was $308^{\circ}\pm22^{\circ}\text{C}$. The largest melting range observed was for

Table 8-2 Liquidus and Solidus Data for Salic Lavas
From Level Mountain

Sample	TL °C	T _S °C	T _m °	TL °C Calc*
24/1 hi trachyte	1190 ± 10	965 ± 35	225 ± 45	1189 1050 995
24/2 o/c	1235 ± 10	930 ± 10	305 ± 20	—
25/5e pantellerite	1235 ± 10	862 ± 13	273 ± 23	1149 1071 978
25/7	1233 ± 7	875 ± 10	358 ± 17	1138 1027 986
9/2-99 comendite	1155 ± 50	900 ± 30	255 ± 80	1150 1056 986
8/5-8/5150 pantellerite	1250 ± 10	862 ± 13	388 ± 23	1147 1044 962
28/25-54/6345 comendite	1215 ± 10	862 ± 13	353 ± 23	1131 1060 994

* French (1971) Plagioclase; Clinopyroxene; Olivine

pantellerite 8/5 -8/5150 ($388^{\circ}\pm23^{\circ}\text{C}$). The liquidus determinations are somewhat higher than previously reported (Bailey et al, 1979). This is presumably due to the present study being anhydrous and buffered at lower fO_2 . The long melting intervals are comparable to data on peralkaline phonolites and plutonics reported by Edgar and Parker (1974).

Aenigmatite was the first silicate to crystallize for six out of seven samples under the conditions of low fO_2 . The aenigmatite crystallized as a deep reddish brown pseudo-hexagonal thin platelets both singly and in "squadron formation", where platelets in small regions of the glass were all in parallel orientation, see plates 8-1 and 8-2. This presumably indicates regions of intermediate to long range order in the glass. The aenigmatite may be preceded by an oxide phase, although a reaction is usually indicated due to disappearance of the oxide at and below the temperature of aenigmatite crystallization. At the silicate liquidus temperature the oxide reacts with the peralkaline component (Ns) of the melt to form aenigmatite. The incongruent melting of aenigmatite has previously been reported (Lindsley, 1971; Lindsley and Haggerty, 1971). Incongruent melting has also been noted for acmite (Bailey, 1969). Aenigmatite is followed by intermediate to potassic alkali feldspar and sodic hedenbergite in either order. The pyroxenes are prismatic while the feldspars are either lathlike, in the upper end of the melting range, or a matte



Plate 8-1.

Photomicrograph (P.P.L., 340x240 microns) of a crystallization experiment on peralkaline trachyte 8/5-8/5150. Aenigmatite reddish brown pseudohexagonal platelets occur on the liquidus for T-fO₂ conditions between M-W and FMQ.

Plate 8-2.

Photomicrograph (P.P.L., 68x48microns) of a crystallization experiment on pantellerite 25/5e at 1201°C and $\log fO_2 = -8.78$. Pseudohexagonal brown aenigmatite is followed at slightly lower temperatures by the crystallization of an oxide phase. Possibly having crossed the boundary curve for $Aen+O_2 = TiMt+Nds+SiO_2$, as a result of the specific fO_2 conditions or early aenigmatite crystallization having lowered the peralkalinity sufficiently to shift the equilibria.



of microlites near the solidus. A bluish alkali amphibole, presumably riebeckite, was observed in one charge of pantellerite (25/5e) and in the mid-melting range of some of the earlier unbuffered experiments. The unbuffered experiments had slightly lower liquidus temperatures (average of five determinations $1138 \pm 35^\circ\text{C}$) with the sequence oxide, alkali feldspar, clinopyroxene, alkali amphibole or oxide, aenigmatite, alkali feldspar. In considering just the latter low fO_2 experiment, there is a great deal of variation in crystallization sequence and in temperature intervals between sequential appearance of the various silicate phases. This degree of variability in the crystallization behavior of these seven samples would not be expected from the small degree of compositional variation in the major element contents of these lavas.

CHAPTER 9. THE PHYSICAL BEHAVIOR OF LEVEL MOUNTAIN LAVAS

VISCOSITIES: ESTIMATED AND EXPERIMENTAL¹

Theoretical Viscosity Calculations

For lavas of known composition, viscosities have been predicted according to the model of Shaw (1972). These calculations were performed using a fortran computer programme supplied by J. Nicholls to give a log-linear expression of the form:

$$\ln n(\text{pascal-sec}) = A/T^\circ\text{K} - B$$

which corresponds to newtonian behavior. This type of relationship has been shown to be valid above the liquidus temperature while below the liquidus the viscosities increase more rapidly due to the presence of crystals and the behavior is no longer newtonian (Shaw, 1969; Scarfe, 1973; Murase and McBirney, 1973). The conversion from SI to cgs units, which have been conventionally used is:

$$10^e \exp(\ln n(\text{pascal-sec})) = n(\text{poise})$$

To characterize the expected variation in viscosity for Level Mountain lavas and to compare it to other British Columbia lavas, the theoretical anhydrous viscosity has been calculated at 1300°C. The range of predicted viscosities is tabulated as a function of rock type for Level Mountain and other Cordilleran lavas, table 9-1. The lowest predicted

¹ Throughout this chapter the symbol n is used to denote viscosity.

Table 9-1 Range of Predicted Viscosities as a Function of Rock Type

<u>Rock Type</u>	<u>ln (pascal-sec)¹</u>	<u>median</u>
Alkali Basalts and Ankaramite	0.4 to 2.4	1.7
Hawaiites	1.8 to 3.4	2.7
Mugearites, Benmoreites and Phonolites	4.2 to 6.4	5.3
Trachytes and Tristanites	6.6 to 8.8	7.3
Comendites and Rhyolites	9.0 to 10.8	9.7

1. Viscosity calculated from chemical analysis on an anhydrous basis at 1300°C after the method of Shaw, 1972.

viscosities are for ankaramites and other basalts. Melts of basaltic composition have a high proportion of network modifier cations and a less polymerized polyanionic melt framework (Scarfe, 1973, 1977; Scarfe et al, 1979; Mysen et al, 1980). The highest predicted viscosities are for metaluminous rhyolites with comendites being slightly lower. The samples from Edziza and other late Cenozoic lavas in British Columbia display the same range of variation as seen at Level Mountain. For the purposes of comparison, all of these viscosities were calculated using dry chemical analyses. The effect of water is to de-polymerize the silicate melt by increasing the proportion of non-bridging oxygens. The calculated effect of this depolymerization for these relatively dry alkaline lavas is generally less than a few percent lowering in $\ln n$ and the inaccuracy introduced by comparing lavas at a single temperature of 1300°C should outweigh this. The value of 1300°C was chosen to be above, but close to, the liquidus for all of the alkaline lavas. This is about 35°C above the average basalt liquidus and 85°C above the average salic liquidus.

Experimental Viscosity Determinations

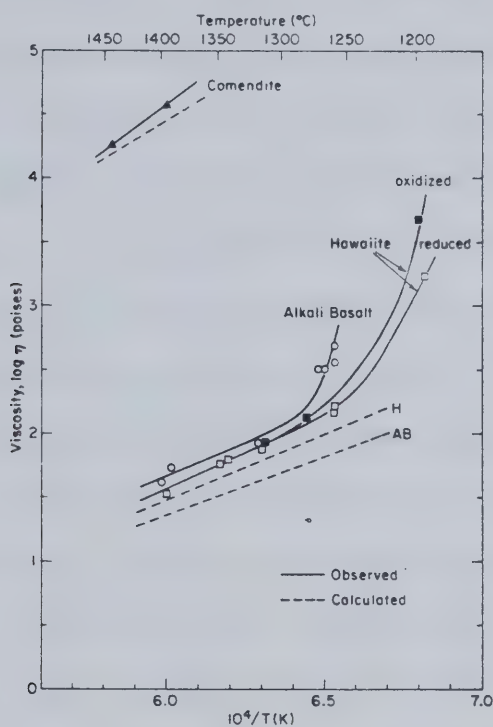
Three rocks were chosen to represent the basalt to comendite sequence at Level Mountain: hawaiite (8/25 - 50/6397), alkali basalt (PAP), and comendite (8/25 - 54/6345). For chemical analyses please see chapter on petrochemistry. Rock powders (which passed the 325 mesh screen) were prepared from these specimens. Experimental

work was performed by C.M. Scarfe at Sheffield University (Scarfe and Hamilton, 1980). Glasses free from bubbles and crystals were fused from whole rock powders, under reducing conditions, in a gas furnace at $1400^{\circ} - 1600^{\circ}$, for two hours. Fusions were performed in alumina crucibles and the liquid was poured into a steel mold to make a glass slug whose diameter matched the internal dimensions of the outer cylinder of a concentric cylinder viscometer (Scarfe 1977). Under measurement conditions, the 8cc glass slug filled the cavity between the inner and outer platinum cylinders of the viscometer. During a measurement, shear across the silicate liquid transmits torque to the inner cylinder which results in an angular displacement. The displacement is recorded as a light spot deflection on a linear scale. At constant temperature, there is a linear relationship between rotation speed of the outer cylinder and angular displacement of the inner cylinder. This corresponds to a plot of shear stress versus shear rate, which for newtonian fluids is a straight line through the origin. All experimental determinations were performed in air. Viscosities are considered accurate to $\pm 5^{\circ}\text{C}$ in the range 1200°C to 1400°C . Starting glasses for the hawaiite sample were prepared under both oxidizing and reducing conditions. The resulting difference in measured viscosities was very small, with the reduced aliquot being slightly less viscous at any temperature. This could be related to enhancing the behavior of Fe as a network modifier under reducing conditions (Fe^{2+} rather than Fe^{3+}).

Results for the three Level Mountain lavas are presented in Figure 9-1. The apparatus was calibrated using NBS Standard 710, a soda-lime silica glass, for which the viscosity-temperature relationship is accurately known. Curves through experimental points are fit by hand. Dashed lines correspond to theoretically predicted viscosities. Viscosities calculated using the method of Shaw (1972) agree with experimental determinations to within 0.25 log units, with the predicted values being lower than measured values in all cases. A linear relationship exists between the logarithm of the viscosity and the reciprocal absolute temperature in the range 1300° to 1400°C. The temperature dependence of the viscosity can be described by an Arrhenius relationship of the form $n = n_0 e^{-E_a/RT}$ where n_0 is constant for a given melt, and E_a is the activation energy for viscous flow. Activation energies for the Level Mountain lavas are in the range 98 kcal/mol for the comendite to 54 kcal/mol for the hawaiite. At any temperature above the liquidus the viscosity of the comendite is about three orders of magnitude greater than the basalts. For example, at 1300°C the comendite has $\ln n = 5.3$ poise as compared with $\ln n = 2.05$ and 2.60 for the basalts; ($\ln n = 9.4$, 3.6, 2.3 pascal - sec respectively). Despite the fact that theoretical and experimental data agree in predicting a high viscosity for comendite, this does not account for the apparent fluid nature of comendite flows at some locations on Level Mountain. Both experimental and theoretical data

Figure 9-1.

Plot of reciprocal absolute temperature versus log viscosity (in poise) comparing experimentally determined viscosities to Shaw model predictions, taken from Scarfe and Hamilton (1980).



relate to a degassed dry sample. Under natural conditions of emplacement and extrusion, dissolved volatiles in the comendite melt, particularly fluorine and chlorine (Bailey and MacDonald, 1975; Scarfe, 1977), may have reduced viscosities considerably below 10^5 poise. Degassing could eventually increase viscosity to the point where flow will cease (Nash and Evans, 1977). The other possibility is that comendite may acquire some degree of superheat (Marsh and Kantha, 1978) due to a peculiarity of the liquidus geometry in PT space and ascent path (Bailey et al, 1974). The only problem is that for the viscosity-temperature relationships presented here, an extrusion temperature of 1500°C would still give a viscosity too high to explain fluid features, lava tubes, thin flows (less than 3m thick), long low volume flows, lineations, flow folds and thin dykes (less than 1m thick) which have been observed in the field. Comendites should have a more polymerized melt than basalts due to high silica contents, high $R=(\text{Si}+\text{Al})/\text{O}$ (atomic) (Shaw, 1965; 1972) and low ratios of non bridging oxygens to tetrahedrally coordinated cations, principally Si and Al (NBO/T, Mysen et al, 1980). The precise effects of high $\text{Fe}/(\text{Si} + \text{Al})$, $(\text{Na} + \text{K})$, (Na/K) halogen content, and eruptive temperatures, as compared with these values in calc-alkaline rhyolites of similar silica contents, are unknown; however, all of these characteristics could contribute to a lower viscosity (Schmincke, 1974). Also there is probably a pressure effect which contributes to decreasing the

viscosity of salic melts due to a collapse of their one-atmosphere 3D polymer structure at higher pressures (Virgo et al, 1979). Characterizing the viscosities for the Level Mountain lavas is important to an understanding of their flow properties, extrusion rates and nodule transport.

CONSTRAINTS ON THE RISE TIME OF LEVEL MOUNTAIN LAVAS

Introduction

This section is devoted to placing physical and fluid mechanical constraints on the rise times and emplacement velocities of the various lava types found in the alkaline association at Level Mountain. Settling calculations have been performed for selected flow-nodule pairs. Some diapiric rise and heat transfer calculations are also presented. The data used in this section comes from a variety of places. Liquidus and solidus determinations were made on glassy charges suspended in a Deltech vertical tube quench furnace equipped for gas mixing. Oxygen fugacity was controlled to lie between FMQ and MW buffers using mixtures of CO and CO₂, after Dienes et al (1974). Viscosities are calculated at the liquidus and, when available, experimental values are used. Due to the dry nature of these lavas (see chapter on petrochemistry), the effect of wet versus dry viscosities is small, especially when compared to other assumptions made in model calculations. All of the liquidus data, eleven values covering the entire range of lava compositions, were plotted

as $10^4/T^\circ\text{K}$ versus $\ln n$ (SI units) to give the following linear relationship at the liquidus:

$$\ln n = 18.75 (10^4/T^\circ\text{K}) - 117.91$$

with a coefficient of determination of $r^2 = 0.79$ as determined by least squares linear regression. This empirical expression was used along with the Shaw equation

$$\ln n = A/T^\circ\text{K} - B$$

for each lava to predict liquidus temperature and viscosity where such data was not otherwise available. Reasonable liquidus estimates were also obtained using this expression and other B.C. alkaline lavas, the McKinney basalt, and some calc-alkaline andesites as well. It is conceivable that an expression relating viscosity and temperature should exist for a given volcano. This could be due to the mechanism of magma genesis for a related suite or perhaps due to the effect of common plumbing. Estimates of liquidus temperature and viscosity could also be made by comparison with other lavas without recourse to speculative and empirical expressions. The determination of the significance of this type of expression would require further research with additional data on viscosity and liquidus temperatures. The rational for using such empirical calculations on Level Mountain lavas was to be able to use values for actual host lava-nodule pairs.

Xenolith densities were analytically determined using a weight and volume displacement technique. Lava densities were calculated at the liquidus temperature after the method

of Bottinga and Weill (1970). The Bingham model of Sparks, Pinkerton, and MacDonald (1977) was calculated using their empirical graphs and SI units. Other calculations were done for convenience in cgs units.

Nodule Transport and the Ascent of Magmas

The majority of lava flows on Level Mountain are aphyric to fine grained and relatively free of phenocrysts. Newtonian flow models should be adequate for these lavas, however Sparks et al(1977) made a case for phenocryst laden alkaline lavas behaving as a Bingham fluid. It is conceivable that up to several flow volumes of alkali magma could be transported through the crust as crustal rich diapirs. Information relating to the physical properties of lavas used in model ascent calculations is presented in Table 9-2.

Petrographic and field relations suggest that most lavas were at or near their liquidus temperature at the time of eruption. Pleistocene basalts from Meszah Peak contain xenoliths of anorthositic gneiss, troctolite and gabbro. Of these the troctolite and gabbro are considerably denser than their host flow. Similar basalts of the adjacent Stikine canyon occasionally contain lherzolite nodules (Littlejohn and Greenwood, 1974). At three locations on Level Mountain peralkaline trachytes were found to contain armoured nodules of ultramafic composition and a positive density contrast with their host flows. A two meter wide tristanite dyke contained 5 cm long gneiss fragments with a positive density

Table 9-2. Physical Properties of Level Mountain Lava

Sample #	Rock Type	Phenocrysts	Liquidus T°C	Solidus T°C	Density (at liquidus) g/cc	** Liquifidus Viscosity Log (poise)	** Liquifidus Viscosity Log Predicted Measured
8/25-54/6345	Comendite	None (Obsidian)	1215° ± 10°	862° ± 13°	2.34	5.61	5.77
8/6-12	Comenditic Trachyte	Anorthoclase	1200°	-----	2.38	5.07	-----
8/16-44/6250	Tristanite	Andesine, Barkvikite	1231°	-----	2.36	4.01	-----
8/5-8/5150	Paralkaline Trachyte	Anorthoclase, Sodic Ferrohedenbergite	1250° ± 10°	862° ± 13°	2.36	3.94	-----
PAP	Alkali Basalt	Forsterite	1275° ± 15°	1100° ± 15°	2.63	1.67	2.23
8/25-54/6397	Hawaiite	Labradorite	1270° ± 15°	1080° ± 7°	2.71	1.99	2.17
Hypothetical Lava	Alkali Basalt		1255°		2.70	1.00	

** Calculated after model of Bottlinga & Weill (1970)

*** Calculated after model of Shaw (1972)
(Viscosities and densities are calculated using water+ of chemical analyses where any was present).

contrast. Further description of these nodule flow pairs is presented in Table 9-3 and in the chapter on petrography.

The existence of xenolith fragments in certain flows places two constraints on the rise times of these magmas. Where the nodule density is greater than the host lava and the nodule is sufficiently large, a slow ascent velocity would permit the nodule to settle out. If the solidus temperature of the nodule is below the liquidus temperature of the host magma, as it appears to be for most examples given here, the nodule should react, melt and possibly disaggregate. The rates of these phenomena depend on nodule size, relative thermal conductivities, grain size, fabric, chemical diffusivities and heat capacities of nodule and melt, as well as on the melt viscosity and flow regime. For the nodules to arrive intact at the surface, their residence time in the melt must be short enough to prevent either settling out or destruction.

For flow models involving a viscous compressible fluid and low concentration of spherical particles, the settling behavior changes as a function of frictional drag and Reynolds number. The Reynolds number is given by $Re = (ZrVe/n)$ (Bird, Stewart and Lightfoot, 1962). For $Re \leq 1.0$ the frictional drag is effectively a linear asymptotic function of Re and the Stoke's Settling Law behavior is valid. For intermediate Re (1.0 to 1000.0) the relationship is a power law, where the friction factor (f) is given by $f = 1.85Re \exp(-0.6)$, reflecting the existence of a turbulent

Table 9-3. Characteristics of Xenoliths from Lavas of the Level Mountain Formation

Sample #	Rock Type	Modal Phases	T°C Solidus * °C	g/cc STP	Max Size (cm)	Most Flow	Relationship
Level Mountain: MPM	Tracholite	Plag-ol-Cpx-Opx-Ap	1086°±8°	3.13	15 cm	Hawaiite 8/25-50/6397	CPX in Reaction w/Melt PLAG Partially Resorbed
8/6-12 N	Ultramafic	Cpx-Amph-Plag-Ne-Opx-Phlog	1078°±5°	2.53	10 cm	Comenditic Trachyte 8/6-12/5290	nodules armoured by glassy reaction rims
8/16-44 1	Gneiss	Plag-A-Fldg.-Q-Amph-Opx	1080°±40°	2.66	5 cm	Tristanite 8/16-44/6250	no petrographic sign of melting
Heart Peaks: HP 13 A	Essexite	Plag-Cpx-Or-Amph-Opx	1085°±75°	2.85	> 10 cm	Hawaiite ? no petrographic sign of melting Sample from J. Casey	no petrographic sign of melting Sample from J. Casey
Telegraph Creek: TCL 1004-41	Lherzolite	Ol-cpx-Cpx-Sp	1210°±22°**	3.37	5 cm	Alkali Basalt H.J. Greenwood	no petrographic sign of melting. Sample from H.J. Greenwood
Hypothesis BC Lava	Lherzolite	Ol-Opx-Cpx-Sp	1245°	3.3	3 cm	Alkali Basalt	CPX in Reaction w/Melt

* Hamilton 1980

** This solidus determination is comparable to the 1 bar data of Kushiro et al 1968 of 1200±5 & 1250±5
Scarf et al (1972) 1215±10

flow around the equator and in the lee of the particle. For high Re the friction is nearly independent $f = 0.44$ and the type of settling is in keeping with Newton's Law. The cutoff of $Re = 2000$ marks the onset of turbulent flow. Particle Reynold's numbers for relatively aphyric melts are typically smaller than 10^{-5} for salic compositions and between 2×10^{-1} and 2×10^1 for basalts. For these crystal and nodule poor cases Stoke's law settling behavior should be reasonably valid. The greatest uncertainty is not the choice of the settling law, but the assumptions of viscosity and density contrast. For multiphase flow of crystal and xenolith mushes, the disperse particle theory no longer applies and particle boundary layers and particle interactive forces come into play. An alternate way of stating this is that in phenocryst laden melts, there is significant crystal-crystal interaction which impedes flow. Bingham model ascent rates have been calculated for the Level Mountain examples according to the models of Sparks et al (1977). For the basaltic magmas a rapid ascent time is still implied. The Bingham model is not very informative when applied to the salic magmas. The minimum ascent velocities for nodule transport, rather than settling, imply maximum rise times on the order of tens of thousands of years. Upon consideration of cooling and crystallization processes and thermal conductivities of the materials in question, this is sufficiently long to cool salic magams by conduction alone. If ascent were this slow, plutonism rather then volcanism

would have occurred.

The model of Takeuchi et al (1972) assumes buoyant rise of melts through a lithosphere of greater density. In their model the minimum velocity for magma rise is given by

$$V = \Delta \rho g d^2 / 12n,$$

where d is the characteristic dimension of the conduit. These calculations have also been presented in Table 9-4 using an hypothetical conduit dimension of 10m, which is typical of high level vents on Level Mountain, and an assumed crustal density of 2.9g/cm^3 , after the crustal model for the Intermontane Belt in Southern B.C. (Keen and Hyndman, 1979). Again the assumptions regarding geometry and viscosity have far greater effects than actual magnitude of density contrast. In all cases this buoyant magma rise model predicts velocities that are orders of magnitude faster than the minimum velocity limits set by nodule transport. This model presupposes a magma-filled conduit extending through the crust. The driving force is the magmastic head (difference in lithostatic and magmastic pressure at depth). For basalts this magmastic head may be as high as a few kilobars (Maaloe, 1973). The model does not account for frictional effects or the pressure required to hold the conduit open. All limitations considered, this model should put a maximum constraint on ascent velocity. In this case the velocities calculated for the hawaiite and the "typical basalt" are 20 to 30% of the expected seismic velocities (V_p) in the crust. Velocities of this magnitude are also

Table 9-4. Model Ascent Velocities and Rise Times for Level Mountain Lavas

Sample #	Rock Type	Re	Newtonian Stokes	Bingham	Maximum Residence Time (Days) r=10m Nodule Melting
8/25-50/6397	Hawaiite 30km	21.92	52.7:34.3.33.0 (1 day)	2.78x10 ⁻² (3.4 yr)	1.67x10 ⁵ (18 sec)
8/16-44/6250	Tristanite 5km	4.6x10 ⁻⁵	4.0x10 ⁻² (-145 day)	6.72x10 ⁻⁶ (2.36x10 ¹ yr)	4.31x10 ³ (116 s)
8/6-12/5290	Comenditic Trachyte 30km	1.4x10 ⁻⁶	7.0x10 ⁻³ (13.7 yr)	1.16x10 ⁻⁶ (8.15x10 ⁴ yr)	3.61x10 ⁷ (2.3 hr)
8/25-54/6397	Comendite 30km	1.5x10 ⁻¹	2.5x10 ⁻¹ (38.0 yr)	-----	1.12x10 ² (7.4 yr)
A.O.B. plus Lherzolite Nodules	Alkali Basalt 30km	3.97x10 ⁻¹	4.91 (7.1 days)	1.20x10 ⁻³ (79.2 yr)	2.59x10 ⁵ (12 sec)
<hr/>					

- Velocities in cm/sec
- A depth of nodule incorporation is assumed for each sample to calculate rise times or velocity
- Re = Reynolds Number

expected from the arguments for magma emplacement in the crust governed by fracture propagation (Anderson and Grew, 1977). Using the model with its buoyancy drive mechanism, all types of magmas encountered at Level Mountain can rise from mantle depths in a matter of hours.

Rise times can also be estimated by calculating the time required to heat a nodule through its melting point. This is essentially a "Newton's Law of Cooling" calculation. Several assumptions and preliminary observations should be noted. In Clark (1966) it is shown that refractory minerals have higher thermal conductivities than melts of higher silica content. In keeping with this observation, an inclusion made up of refractory minerals will tend to have a very flat thermal profile as it heats up in a melt. Forced convection of the magma and turbulent flow will tend to transport heat to the nodule faster than assumed in these calculations, which will diminish the residence time to melting. For any positive density contrast (nodule greater than melt) some crossflow must exist so that this time estimate will be a maximum. Spherical nodules have the highest volume to surface area ratio so that any other geometry will enhance heat transfer and diminish time to melting. For this model the characteristic time is the duration of the heating process, only up until the nodule solidus is achieved. For real nodules once the solidus has been reached there will still be a finite time of melting associated with kinetic effects such as diffusion and

reactive melting. In this model, for steady state conduction, the rate of change of temperature with time is given by Tuma (1976) as

$$\frac{dT}{dt} = -hc\Delta T A / V\rho C_p$$

where hc = heat conduction coefficient, cal/cm²-sec-°C

ΔT = initial temperature differential, °C melt - nodule

A, V = surface area and volume of nodule, cm², cm³ respectively

ρ = density of nodule

C_p = heat capacity of nodule

The heat capacity, density and geometry of the nodule are assumed to be constant up until melting. To extend the model through melting, the heat capacity would have to be replaced by a term including the heat of melting and any excess heats of mixing associated with diffusion processes. For a spherical nodule geometry $A/V = 3/r$. Newton's Law of Cooling states

$$\Delta T(t) = \Delta T_0 e^{-\alpha t}$$

where $\alpha = (dT/dt)/\Delta T_0$.

The only remaining quantity to be evaluated is hc . Kreith (1973) gives $hc = kN/D$ where k is thermal conductivity and N is Nusselt's number, which for Reynold's numbers $Re \leq 10.0$ is approximately equal to 2.0. Values of k for minerals and some rocks are published in Clark (1966). A sample calculation is presented for a general alkali basalt and a lherzolite nodule assuming the basalt to be at a liquidus

temperature of 1225°C, the lherzolite initially at 1045°, with a solidus at 1245°C (CO_2 , 9.1kbar, Yoder, 1976). Then:

$$hc = (0.011)2/15 = 0.00147 \text{ cal/cm}^2\text{-sec}^{-1}\text{°C}$$

$$\begin{aligned} dT/dt &= (-0.00147)3(210)/7.5(3.3)5.9(10) \\ &= 6.48 \times 10^{-4} \text{ °C/sec} \end{aligned}$$

$$\alpha = 3.08 \times 10^{-6}, T(t) = 10^\circ \text{ and } T_0 = 210^\circ.$$

Finally the heating expression can be rewritten in terms of t to give:

$$t = \ln (\Delta T(t)/\Delta T_0)/-\alpha$$

which with substitution of the appropriate values,

$$t = \ln(10/210)/-3.08 \times 10^{-6} \text{ gives}$$

$$t = 9.87 \times 10^5 \text{ seconds or 11.43 days.}$$

Assuming the lherzolite to have become incorporated at a depth of 30km yields a minimum ascent velocity of 3.039 cm/sec. Depending on the assumed depths of incorporation for the inclusions the model ascent velocities are generally between those estimated by Stoke's Settling and buoyant rise, see table 9-4.

Carmichael et al (1977) present an ascent model whereby spherical magmatic diapirs rise buoyantly, yet frictionally retarded, through a very viscous upper mantle. The relationship they derive is $R^2 = 3Vn/g\Delta\rho$, where R is the effective radius of the magma diapir, V is the ascent velocity and n is the viscosity of the upper mantle. The value of n , derived from isostasy, and typically used in geodynamic arguments is 10^{21} poise (Cathles, 1975). A few trial calculations, using reasonable density contrasts and

assuming a value for either V or R to solve for the other, reveals unreasonably large radii, of hundreds to thousands of km, or unreasonably slow velocities, which for depths of 30 to 100km imply rise times of tens of millions to billions of years. The Cordilleran lithosphere is thinner and the upper mantle is softer, with lateral variations in the effective viscosity spanning two orders of magnitude at the 100km depth range (Ranalli, 1980). The diapiric transport calculation can be rearranged to estimate a viscosity for the upper mantle that would be volcanologically more reasonable. Consider a peralkaline trachyte flow, PBE from Meszah Peak. The volume of the flow is $4.8 \times 10^{-3} \text{ km}^3$ for an equivalent spherical radius of 105m. Assuming a slow ascent velocity of $1.16 \times 10^{-6} \text{ cm/sec}$, and densities for mantle and melt of 3.3g/cc and 2.4g/cc respectively, results in a calculated estimate for $n(\text{mantle})$ of $2.78 \times 10^{16} \text{ poise}$. For a hypothetical diapir volume of 1 km^3 , a velocity of 10^{-6} cm/sec and the same density contrast, the value of is $1.13 \times 10^{18} \text{ poise}$. This begins to look plausible for the situation of a partially molten upper mantle and transport of diapirs having about 10 flow volumes worth of magma. For the ascent velocity of about 10^{-6} cm/sec , it would require approximately 42,000 years to traverse 13km of upper mantle. The evidence from age dating attempts suggests that the major eruptive periods are separated in time by tens of thousands of years. This coincidence lends support to the buoyant diapir concept and calculations discussed.

Assuming that all of the Level Mountain lavas rose as a single magma diapir from a hypothetical depth of melting and segregation of 105km to 30km. The total volume of volcanics is 1500 km^3 for an equivalent diapir radius of 7.1km. As the lavas are predominantly basic, a more reasonable density contrast is 0.6 g/cm^3 . For a normal upper mantle viscosity (10^{21} poise), the calculated ascent velocity is $9.89 \times 10^{-8}\text{ cm/sec}$ and the traverse time to the base of the crust is $7.58 \times 10^3\text{ sec}$ or 2.4MY. The age for the lowest flows sampled in the Little Tahltan Canyon is interpreted from paleomagnetic evidence to be about 6.4MY. The combination of these two ages, 8.8MY, should be close to the origin time for the Level Mountain magmas. In Hamilton, Baadsgaard, and Scarfe (1978) a whole rock Rb-Sr age of $9.4 \pm 1.0\text{ MY}$ was reported and interpreted as possibly representing some precursor thermal event in the upper mantle. The coincidence of the reported and the modelled date may lend some support to the mantle diapir model.

Carmichael et al (1977) in using the same model, and reasonable model parameters for alkali basalts and tholeiites, derived an apparent viscosity for the upper mantle of $5.3 \times 10^9\text{ poise}$. They concluded that, while this is unlikely to represent the viscosity of the whole upper mantle, it could represent the viscosity of a thin lubricating sheath of partially fused mantle material surrounding the diapir. They also did a conductive heat loss calculation, inferring a drop of about 2°K for flow sized

bodies ascending at typical nodule settling velocities.

Carmichael et al (1977) also calculated convective heat loss for these magma diapirs with thin boundary layers. For diapirs in the volume range 0.03 to 0.185km³, the boundary layers were all less than 40cm thick, which is one per mil of the diapir radius. The temperature losses associated with laminar boundary layer convection were 21° and 7° respectively. The losses corresponding to a turbulent boundary layer were higher, 86° and 39° respectively. Using the appropriate physical parameters for the Level Mountain hawaiite flow, 8/25-50/6397, and a model transport from 100km, the laminar convective boundary layer model gives a temperature drop of 3° while the turbulent case was 23°C. Convective heat losses offset by proportional crystallization could be a significant driving force and mechanism for differentiation even at mantle depths. This might be a means to derive large volumes of hawaiite from a more primary composition while still in the mantle depth range.

In addition to conductive and convective heat losses some other types of heat changes need to be considered. The adiabatic gradient is given by Yoder (1976) to be between 0.2 and 0.5°C/km. This is equivalent to -20° to -50° for a 100km path. For isenthalpic decompression, Waldbaum (1971) cites a value of adiabatic heating on decompression which may be as great as 22°C per kilobar. Clearly this is a mechanism to offset convective heat losses and even perhaps

to provide superheat for an ascending magma body. This mechanism could provide sufficient heat for a magma to assimilate significant quantities of wall rock, whether in the upper mantle or crust. Here the ascent velocity would be the crucial parameter. Again it is pointed out that any rising magma must undergo decompression and, if this can generate heat and drive assimilation processes, it may be difficult indeed to transport and erupt a primary magma. Thermal changes due to viscous heating and transportive friction may also be significant but their effect is thought to be less than adiabatic and convective effects (Carmichael et al., 1977).

VOLUME ESTIMATES OF LEVEL MOUNTAIN VOLCANISM

Volume estimates have been made for thirty-five typical eruptive events from Level Mountain. Estimates have been made for single eruption flows, tuffs, domes, and dykes representing the entire range of compositional types. Although estimates cover the time span of volcanic activity, the younger events are more heavily represented due to preservation and mappability. Dyke and vent pipe thicknesses were estimated at the base of the plateau as this was the volume of material added to the volcanic pile during an eruptive event. Volume estimates are presented in Table 9-5 along with characterizing information for locality, map unit = age, and composition. The entire range of volumes is $6.12 \times 10^8 \text{ m}^3$ (0.612 km^3) to $1.02 \times 10^6 \text{ m}^3$ (0.001 km^3). Typical

Table 9-5. Volume Estimates of Some Level Mountain Eruptive and Hydabyssal Events

historic basalt flow volumes from Hawaii and elsewhere are given as 0.03 and 0.185km³ (Carmichael et al, 1977). The average volume of five post-glacial basalt, basanite and nephelinite cinder cones from the Cariboo, Chilcotin and Stikine regions of B.C. is 0.0134 km³. A large Pleistocene basaltic tuff cone near Jacques Lake (Campbell, 1961) has a volume of 0.126km³. Compared to these, the Level Mountain events appear to be of ordinary size. The volume estimates have been subdivided into basic and salic types as well as into flows versus hypabyssal intrusions. It is apparent that at Level Mountain the dykes, stocks and domes are an order of magnitude larger in volume than the flows and ejecta. Flow volumes are taken to be single eruptive events, while dykes and stocks may be intermediate in size between eruptive events and eruptive episodes. There is no statistical difference in size for basic versus salic types in either the eruptive or hypabyssal group. This would seem to indicate that eruptive volumes are determined by common energetics of magma rise or by a common set of volcanic plumbing, rather than by the relative volumes of melting or differentiation events.

The volume of eruptive episodes, taken to be synonymous with the sequential map units, have been estimated using topographic maps at 1:50,000 scale for elevation control and a grid overlay for area. Volumes have been reconstructed to include materials eroded from the plateau margins and youthful alpine glacial valleys. Model densities have been

assigned to each unit on the basis of average physical and chemical properties for rock types present. Time spans for map units have been estimated from all available sources of field and laboratory data. The average time intervals between flows have been calculated for a typical flow volume of 0.01km^3 in size. This data is summarized in Table 9-6.

There have been approximately 85,000 flow sized eruptions at Level Mountain over a time period of about 6 to 7MY. The lifespan of the volcano is clearly divided into 39% initial plateau building and a 61% later stratocone development. The average time span calculated for flows of the plateau building period is 43 years while for the stratocone development phase the interval is 226 years. Field mapping and geomorphology indicate that the activity was likely to have been more intense with widespread contemporaneous eruptions separated by periods of hundreds of years of quiescence. The figure of 43 years for the plateau period seems reasonable as there was insufficient time between sequential flows for extensive soil development or vegetation to have occurred.

Of the total 857.6km^3 of volcanics, 80.8% was basaltic while 19.2% was salic and dominantly peralkaline. The plateau building site was wholly basaltic. The stratocone stage, with a repeated bimodal process, was 85% salic in character.

In addition to the Level Mountain Volcanism, the volumes have been estimated for the other major centres in

Table 9-6. Volume and Mass Estimates for Level Mountain Volcanisms as a Function of Time

Map Unit or Magma Pulse	Time Span M.Y.B.P.	Duration	Dominant Composition	Volume (km ³)	Model Density	Mass in Kg	Years/Flow
8-10	1.2 -0.0	(1.2)	basic	0.83	2.84	2.36×10^{12}	14,458
7a-c	2.4 -1.2	(1.2)	salic	55.85	2.61	146.0×10^{12}	215
6b	3.25-2.4	(1.05)	basic	14.17	2.86	40.5×10^{12}	188
6a			salic	41.68	2.56	107.5×10^{12}	
5b	4.2 -3.25	(.95)	basic	15.00	2.82	42.4×10^{12}	116
5a			salic	67.11	2.44	164.0×10^{12}	
4	4.6 -4.2	(.4)	basic	165.79	2.71	$449. \times 10^{12}$	24
3	5.6 -4.6	(1.0)	basic	165.79	2.77	$459. \times 10^{12}$	60
2	6.3 -5.6	(0.7)	basic	207.19	2.78	$576. \times 10^{12}$	34
1	7.0 -6.3	(0.7)	basic	124.18	2.73	$339. \times 10^{12}$	56
				-----	-----	-----	-----
Total	857.59	Avg	2.71	Total	2325.26 $\times 10^{12}$		

for an average flow volume of 0.01 km³,
and an time span of 7×10^6 yr.
this means an average of one flow per 82 years

the Stikine Volcanic Belt. This information is presented in Table 9-7 along with some estimates of dimensions pertaining to the source region. The total 1710km³ of volcanics outcrops over an area of 8629km² in the Stikine Volcanic Belt which has a total area of 70,000km². The volumes and areas of the eleven major volcanic centres of the Stikine show a logarithmic distribution. Level Mountain and Mount Edziza are the largest in both area and volume. Using the total volume estimated and a time span of 5MY, it is apparent that the Stikine Volcanism is small in comparison to the Columbia River Plateau or the East African Rift and that the extrusion rates are lower by two orders of magnitude.

The volume data on the Stikine volcanism can be used to evaluate two possible source models. The two models are (i) partial melting of a slab of upper mantle and (ii) upper mantle diapirs below each of the eleven major centres. The slab hypothesis (using the surface outcrop area as an estimate of source region extent) implies the removal of a layer up to 180m thick beneath the volcanic centres. If the volume is derived over the extent of the Stikine Volcanic Belt, the removed layer may be as thin as 23m. When these slab calculations are performed for each centre, the calculated layer thickness varies from 76m to 532m with a mean of 235m and a standard deviation that is 33% of the range. Assuming that 5% to 25% partial melting accounts for the volcanics, and that this volume may be efficiently

Table 9-7. Total erupted volumes for the Major Centers of the Stikine Volcanic Belt

Center	Lat.N/Long.W	Vol (km ³)	Surface Area (km ²)	Source Region Estimates	Slab Thickness (m)	Spherical drapir radius (km)
Kawdy Plateau	58°52' / 131°10'	35	997	35	2.029	
Heart Peaks	58°38' / 132°00'	100	499	200	2.879	
Level Mountain	58°25' / 131°15'	860	3324	259	5.899	
Tahltan Plateau	58°05' / 131°35'	50	484	272	2.285	
Stikine River	58°00' / 131°00'	5	66	76	1.061	
Mt. Edziza	57°30' / 130°40'	500	1773	282	4.924	
Tanzilla Plateau	58°30' / 129°35'	35	166	211	2.029	
Castle Rock	57°52' / 130°15'	10	50	200	1.337	
Klastiline Plateau	57°25' / 129°50'	50	1440	35	2.285	
Hoodoo Mtn.	56°44' / 131°20'	40	83	482	2.122	
Iskut River/Mt. Dunn.	56°38' / 130°45'	25	47	532	1.814	
Total	1710	Total	8629	Mean 235 S.d. 162	Mean 2.606 S.d. 1.484	

removed, implies a thickness for the melting region of between 0.94km and 4.70km for the mean figure quoted, or 0.092 to 0.460km for the minimum case of partial melting below the entire belt. When the eleven estimates are considered as a population, the distribution is normal and 85% of the entire Stikine Volcanism is accounted for within a thickness variation of ± 0.5 standard deviation of the mean. All of the thickness estimates lie within ± 2 standard deviations of the mean. From these model data it appears geologically reasonable that the Stikine Volcanism could originate from a thin zone of partial melting.

For the thermal model presented in this chapter, the partial melting zone could be as thick as 6km. Using this as a maximum estimate, and keeping the same levels of partial melting, an estimate of melt extraction efficiency can be made. A relatively inefficient melt extraction process has been inferred from studies of lherzolite textures (Waff and Holdren, 1980). For the case that melt generation is localized, the efficiency of melt extraction is between 78.3% and 15.7%, while for the case of a general partial melting zone beneath the entire Stikine, the melt extraction efficiency is between 7.7% and 1.5%. In either case a period of partial melting results in a considerable amount of material that may be left behind. For basaltic partial melts, the melt that stays behind could generate regions of gabbro in a more ordinary peridotite upper mantle. The idea of inefficient melt extraction is important to the concept

of upper mantle differentiation but has been proposed on other terms (Mysen and Boettcher, 1975; Lloyd and Bailey, 1975; Boettcher and O'Neill, 1980). Sufficient preconditioning of the upper mantle to generate gabbroic pods (plagioclase plus pyroxene) could result in the derivation of more salic magmas in subsequent partial melting events. It is noteworthy that the three largest centres of the Stikine have both the long spans of activity and the salic lavas one would expect from such a two stage process.

The second source model for the Stikine postulates separate diapirs below each of the centres which, successively tapped, could account for the cumulative individual volumes. For a spherical diapir model, the radii so calculated for the 11 Stikine centres are normally distributed. The mean radius is 2.61km and the range is 1.06km to 5.90km with a standard deviation that is 31% of the range. Unlike the slab calculation, only 12% by volume of the Stikine Volcanism is accounted for by average sized diapirs. Another way of stating this conclusion is that, if diapirism explains the Stikine volcanism, the diapir size is highly variable. This implies that 88% of the volcanism must be accounted for by two mega diapirs of extraordinary size. Therefore the first source mode (slab partial melting) in localized or widespread regions seems to be the more reasonable hypothesis.

THE ENERGETICS OF MELTING AND RISE

The Energetics of Volcanism at Level Mountain and for the Stikine

Volcanism can be considered as an energy dissipation process. The thermal requirements to initiate and maintain this process include mantle preheating, phase change energy associated with melting, and the work performed in magma transport to the surface. The total energy released at the surface can be considered as a contribution to the total heat flow.

As a monitor of the Level Mountain volcanism, the total energy dissipated will be considered as a function of time. The timing comes from magnetostratigraphy and limited age dating control. Mass estimates for successive units were derived from field mapping and laboratory density measurements. Three energy terms are considered. The cooling of lavas from their liquidus temperatures to surface conditions is expressed as a heat capacity integral, using heat capacities for typical flows from each unit as calculated in ROCK. Due to the small variation ($\pm 50^\circ$) in liquidus temperatures, regardless of lava composition, the value of 1200°C was used for all calculations. The heat of fusion values apply to liquidus temperatures for specific compositions considered representative of each unit. The transport work is expressed as a potential energy term (mgh) for the total mass of each map unit and the constant depth

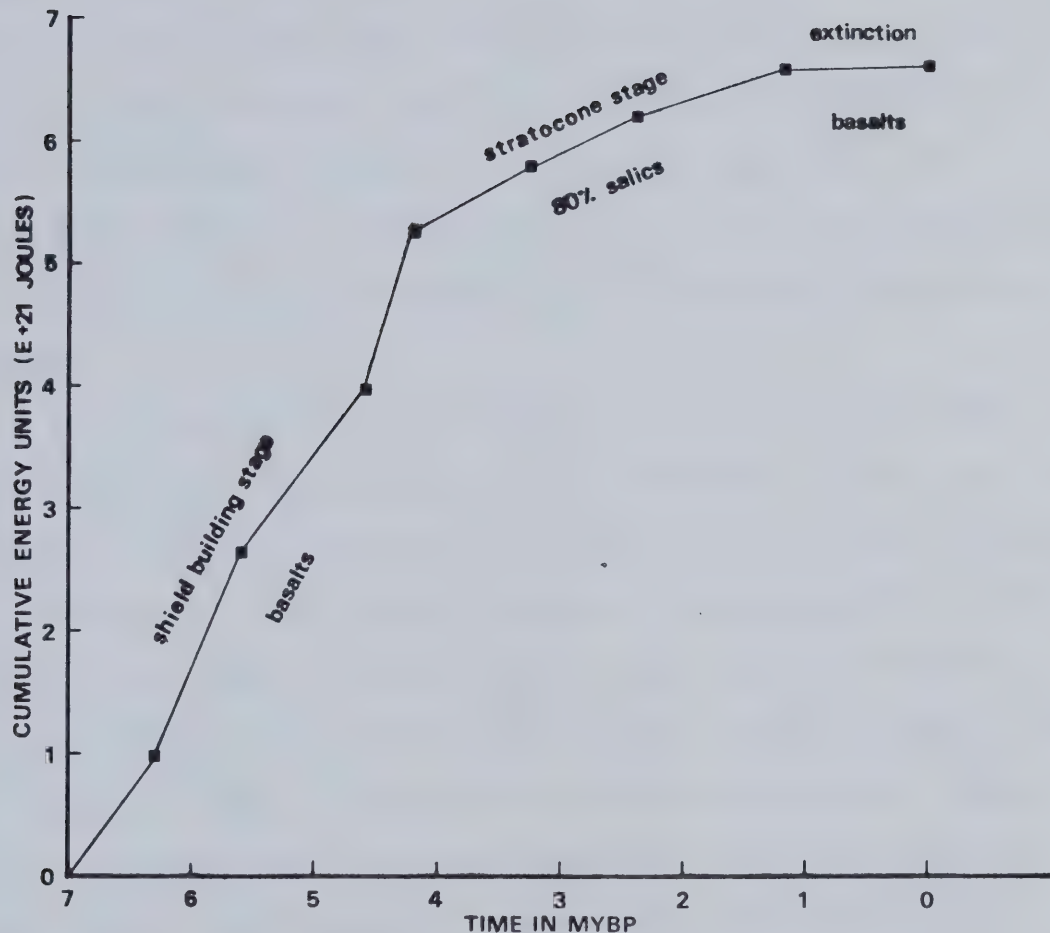
of 35km. These data and calculations are summarized in Table 9-8. The largest energy contribution for each unit is the cooling term which is about five times the heat of fusion. Map units 5a, 6a, and 7a-c are dominated by salic lavas. The energy components of salic lavas are distinctive. Due to the low heats of fusion for salic lavas, the lift energy required for magma transport exceeds the phase change energy. For the remaining units, dominated by basaltic compositions, the reverse is true.

A graphical representation of the cumulative energy dissipated by Level Mountain volcanism is presented in Figure 9-2. The energy plotted is the sum of three terms discussed above. The graph should be read as: 0.979×10^{21} J was dissipated between the onset of volcanism and 6.3 MY before present, etc. Two and possibly three distinct stages are present. The shield building basaltic volcanism (units 1 to 4) has the highest rate of energy dissipation, such that 79% of the total energy expended had occurred by 4.2MY before present. The overall rate (which appears to be constant) was 1.87×10^{21} J/M.Y. For the plateau surface area of 3324 km², this rate is equivalent to 17.8 mW/m². The closest heat flow measurements in northern British Columbia are Dease and Hotailluh which average 73.5 mW/m² (Jessop, Souther et al, 1980 in prep.). Presuming the heat flow to be similar at Level Mountain during plateau building times, then volcanism represents 24% of the total heat flow. The next stage, roughly equal in duration, corresponds to the

Table 9-8. Energy Dissipated by Level Mountain Volcanism

Map Unit or Magma Pulse	Mass (10 ¹² kg)	CP (J/kg K)	E by cooling SepdT (10 ¹⁸ J)	H (10 ¹⁸ J)	Mgh (10 ¹⁸ J)	E by pulse (10 ¹⁸ J)
8-10	2.36	1390	4.92	0.89	0.81	6.62
7a-c	146.0	1360	299.	39.7	50.1	388.80
6b	40.5	1411	85.7	15.3	13.9	114.90
6a	107.0	1381	222.	29.1	36.7	287.80
5b	42.4	1424	90.6	16.0	14.6	121.20
5a	164.0	1345	332.	44.8	56.3	433.10
4	449.0	1405	947.	169.	154.	1270.0
3	459.0	1450	999.	173	158.	1330.0
2	576.0	1433	1240.	217	198.	1655.0
1	339.0	1446	735.	128	116.	979.0
						6586.42X10 ¹⁸ J

Figure 9-2.
Cumulative energy dissipated by Level Mountain volcanism.



bimodal volcanism and stratocone building. Eighty two percent of the energy dissipated in this stage is by salic lavas. The rate here (also constant), is $0.45 \times 10^{21} \text{ J/MY}$, which is only 25% of the previous stage. However the surface area of the stratocone cap is only 20% of the plateau as a whole; expressed in heat flow units the rate for the stratocone stage is 7.15 mW/m^2 . This is still less than half of the shield rate, and only 9.7% of the modern heat flow values.

The final 1.2MY, with its low volume hawaiites and alkali basalts, represents another reduction in the rate and possibly signifies the extinction of Level Mountain. However if the rate of the stratocone stage is extrapolated to the present, the time period is about right for the release of another fifty cubic kilometers of lava. Mountain and for the Stikine as a whole. While the preceding discussion dealt with the development of Level Mountain volcanism and the total energy dissipated by the process, the following section considers the minimum thermal requirements to initiate and maintain the volcanism. Basic data for these calculations and the results are presented in Table 9-9. Assuming the mantle source region to be at the solidus temperature, two additional energy requirements must be met: (i) the heat of fusion for the melts and (ii) the potential energy change associated with the magma transport. The energy dissipated through normal heat flow is calculated for Level Mountian and the total volcanic area within the

Table 9-9. Energy Requirements of Volcanism

	Level Mountain	Stikine Total
LAVA Volume (Km ³)	860	1710
LAVA Mass (10 ¹² Kg)	2325	4634
Surface Area (Km ²)	3324	8629
TIME SPAN (my)	7.0	7.0
Heat of Fusion (cal/g)	85.5	86.6
SOURCE Volume * Km ³	15,623	40,556
SOURCE MASS 10 ¹² Kg	57,556	133,835
Cp J/kg°K for 1050° C 4 phase spinel peridotite	1300	1300
Modern heat flow mw/m ²		73.5
Total heat flux for 7my (J)	5.4 × 10 ²²	1.4 × 10 ²³
a) H (J)	8.32×10 ²⁰	1.68×10 ²¹
2) Mgh (J)	7.98×10 ²⁰	1.59×10 ²¹
I. BASE CASE HEAT (J) 1+2	1.63×10 ²¹	3.27×10 ²¹
equivalent heat flow mw/m ² T from 12% of H.F. (°K) available for source heating	2.2 (3% of HF) 96	1.7 (2.3% of HF) 97
II. Total heat budget for 96° heating (J)	860 8.11×10 ²¹	1710 2.0×10 ²²
equivalent heat flow mw/m ²	11.0(15% of HF)	10.5(14% of HF)

* Source volume has same surface area and 4.7 km thickness

Mass conversion assumes mantle source density of 3.3 g/cc

Stikine for the last 7MY. For the Stikine this value is 1.4×10^{23} J. For Level Mountain this works out to 3% while for the total Stikine Volcanic region it is 2.3% of present heat flow for northern British Columbia.

Additional energy would be required for pre-heating of the mantle source region. For this calculation model source region dimensions are estimated from the surface outcrop of volcanism and a slab thickness of 4.7km. Source region density was assumed to be 3.3g/cc. The heat capacity for a four phase spinel peridotite was calculated from data in Robie, Hemingway and Fisher (1978) to be 1300 J/kg-°K in the temperature range of interest. The heat capacity integral was solved for a temperature interval by assuming an amount of heat potentially available. Less than 40% of a surface heat flow value of 73.5 mW/m² probably arises from a steady state mantle contribution. A value of 12% of the total heat flow is equivalent to 30% of the mantle heat flux. This implies that less than 100° of heating can be performed over a 7MY period. Obviously heating of this type requires geologically long periods of time, or high heat fluxes, or small source regions in some combination. For the 12% pre-heat budget cited above, the pre-heat requirement is 80% and 84% of the total energy requirements for Level Mountain and the Stikine respectively. If the energy requirement for volcanism is expressed in heat flow units, these heating models represent about 15% of the modern heat flow discussed above.

The low volume alkali magmatism for the Late Cenozoic and the Stikine could be initiated and maintained by a thermal contribution equivalent to a small percentage change in the normal heat flow. If the source region must be heated to the peridotite solidus through an interval of a few hundred degrees, in the space of a few million years, an increase equivalent to 25% of the normal heat flow may be required. On the other hand, an increase in available heat as low as 2.5% could initiate and maintain alkaline volcanism from a source region already at the periodite solidus.

As a final note, the total energy dissipated through volcanism in the Stikine can be compared to a change in tectonic strain or potential energy. This can be likened to a release of mantle strain energy through subsidence of the crust over the entire Stikine Volcanic Belt. The area of the entire Stikine Volcanic Belt is estimated to be $7.19 \times 10^{10} \text{ m}^2$. For 25km of crust of mean density 2800 kg/m^3 the total mass of crust under the Stikine is $5.03 \times 10^{18} \text{ kg}$. Using the expression $E = mgh$ to equate the dissipated heat and potential energy (where: $E = 1.11 \times 10^{22} \text{ J}$ $m = 5.03 \times 10^{18} \text{ kg}$ and $g = 9.81 \text{ m/s}^2$) h can be calculated to be 225m. The efficient release of about 0.2km of strain build up over an area the size of the Stikine Volcanic Belt is equivalent to the energy released as volcanism. Whether such tectonic strain preceded the Late Cenozoic volcanism or actually was responsible is unknown. The release of a geologically small

amount of tectonic strain through a melting process could be responsible for this type of low volume alkaline volcanism without recourse to unusual compositions or events in the upper mantle, or large scale lateral geological movements such as treated in plate tectonics theory. A model of strain release through volcanism is particularly appealing for the Intermontane Belt as the strain release through seismicity is anomalously low (Milne et al, 1970).

MODELLING OF A HEAT FLOW AND A GEOTHERMAL GRADIENT FOR LEVEL MOUNTAIN AND THE STIKINE

The intent of this section is threefold, first to review existing Cordilleran heat flow data, second to calculate a steady state conduction model and third to construct a preferred PT model for the geothermal gradient under the Stikine and relate it to the origin of the Level Mountain volcanics. The steady state conduction model is in general, representative of continental geotherms. These continental geotherms are characterized by surface heat flow in equilibrium with heat flowing into the base of the lithosphere, plus a term for internally generated heat from radioactive decay (Pollack and Chapman, 1977).

A review of existing Cordilleran and Canadian heat flow measurements is presented in Table 9-10. It is noteworthy that the value of 73.5 mW/m^2 , used for the Stikine in the preceding section, is virtually identical to the Western Canadian average. The Cordilleran values are somewhat higher

Table 9-10. A summary of Cordilleran and Other Canadian Heat Flow Data

Cordillera	mW/m ²	Corrected ¹	Gradient °C/km
Buckley lake	67	74	
Dease	91	100	
Hotailuh	56	62	
Penticton*	67	79	34.7

Canadian, average heat flow by region, uncorrected

Maritimes	(3)	38.5	Eastern Canada
Quebec	(4)	32.2	
Ontario	(12)	41.0	36 ± 2
Manitoba	(1)	33.5	
Alberta	(2)	64.1	Western Canada
N.W.T.	(1)	83.7	73 ± 6
Cordillera	(4)	70.3	

data from (Jessop, Souther et al 1980 in prep.)
 (Jessop and Judge, 1971)
 (Lee and Clark, 1966)

1. Corrected for the effect of Pleistocene glaciation after the measurement of Jessop (1971).

than the continental average of 42 mW/m^2 , but not so high as many of the circum-Pacific regions which may have values as high as 170 mW/m^2 . Northern B.C. lies on the northern extension of the Western North American thermal high, with a regional heat flow of about 70 mW/m^2 (Pollack and Chapman, 1977). For the Cordilleran thermal anomaly zone, there is a sharp eastward gradient of decreasing heat flow (Roy et al, 1968). Within the thermal anomaly both the crust and mantle are hotter than to the east. The corrected shallow geothermal gradient deduced for Penticton (Jessop and Judge, 1971) is also high for a continental geotherm.

A model for heat flow at Level Mountain has been constructed assuming a simple three layer geometry. The model, in general form, is steady state conductive heat transfer through a series of arbitrarily wide parallel plates of known thickness and conductivity. The solution to Laplace's equation is given by:

$$Q/At = \Delta T / \text{SUM}(l(i)/k(i)).$$

The lefthand side of the equation is heat flux per unit area per unit time, and the right hand side is the net temperature difference across all the layers, divided by the sum of the individual layer thickness-thermal conductivity quotients. Q/At is replaced by a heat flow value and the k corresponds to geologically reasonable choices for layer compositions. With these values set, the thicknesses and temperatures are no longer independent variables so that a geothermal gradient can be calculated within acceptable

petrological and geophysical constraints.

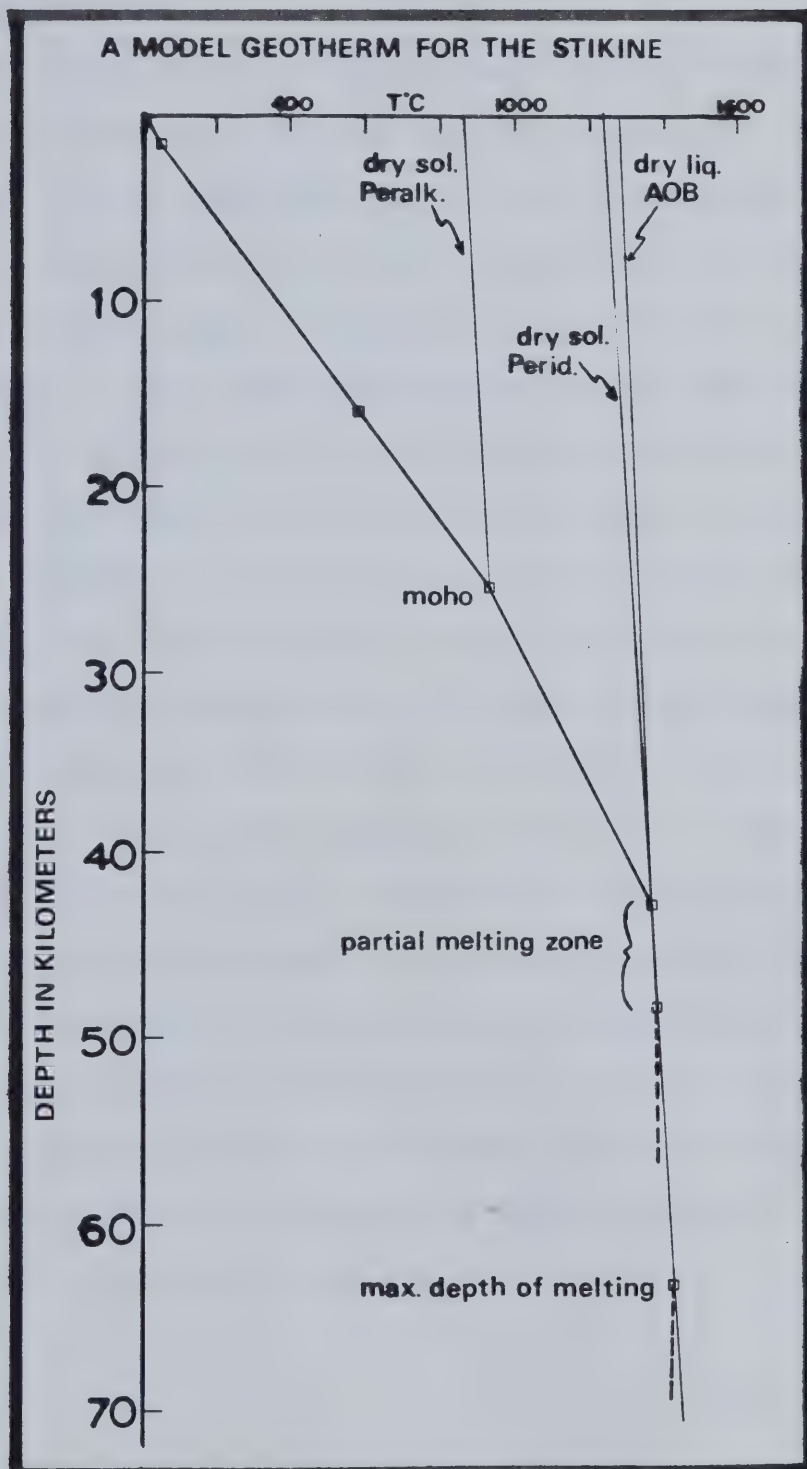
The preferred model for steady state heat flow is 81.7 mW/m² with a two layer crust and one layer upper mantle characterized by:

	l (km)	k (W/m°K)
crust 1	1.50	3.14
crust 2	23.95	2.2
upper mantle	-----	3.22

The major limitation of this model is probably the steady state assumption. The model and selected solidus/liquidus data are presented in figure 9-3. Higher heat flow values would cause unrealistically high geothermal gradients that do not agree with geophysical or petrogenetic constraints. Lower heat flow values (10%) would depress the melting zone to depths below 48km which is considered unlikely. Variations at this level correspond to lateral temperature gradients of less than 0.6°C/km, which could explain the narrowness of the volcanic areas in the Intermontane Belt. Such small differences be supported by the natural variation in thermal conductivity with temperature for peridotites, by changes in proportion and composition of phases, or by very small amounts of tectonic stress (<1.0km). Caner's (1969) estimate for the Curie isotherm depth appears to be too great and his 750°C Moho isotherm appears to be too cool. The implication of this model is that the Moho under Level Mountain is about 25.4km, which would make it one of the shallowest values for the Cordillera. This model is

Figure 9-3.

Geothermal gradient for the Stikine for model calculations and assumptions as discussed in text.



generally consistent with a mantle derivation for the Level Mountain lavas formed by the anhydrous partial fusion of spinel peridotite.

A characteristic of these steady state conduction models is a steeper geothermal gradient over most of the crust than in the upper mantle. For any reasonable choice of thermal conductivities, this geothermal gradient behavior holds for a wide range of hypothetical heat flow values (73 to 112 mW/m²), Curie isotherm depths (16 to 18km) and crustal thicknesses (25 to 30km). The very shallow geothermal gradient is predicted to be lower in the volcanic pile as compared to adjacent areas with basement outcrop, or immediately beneath the pile in the crust. This is due to the high thermal conductivity for lavas. The Intermontane Belt in Southern and Central B.C. generally lacks a high velocity lid and the LVZ begins at the base of the crust. To more accurately fit such a constraint, the gradient in the upper mantle would probably be even more gradual. For a metasomatized alkali- and silica-rich upper mantle the thermal conductivity would be closer to lower crustal values and thus support a higher geothermal gradient. Varying the model in this direction would also lend support to a mantle derivation of peralkaline melts.

Chapter 10. GEOTHERMOMETRY AND GEOBAROMETRY ESTIMATES

INTRODUCTION

Spinel lherzolites are a common inclusion type for nodule-bearing alkaline lavas of the Intermontane Belt. Studies of phase chemistry and trace element concentrations have been reported by Littlejohn and Greenwood (1974), Fiesinger and Nicholls (1977), Fujii and Scarfe (1981) and Fujii et al (1981). Microprobe analyses of coexisting minerals from two spinel lherzolites nodules, one from Telegraph Creek and one from Grizzly Hill in Central B.C. are presented here. The various geothermometers relevant to spinel lherzolites are reviewed here. Equilibration temperatures have been estimated for the two Stikine localities: Telegraph Creek and Castle Rock (Littlejohn and Greenwood, 1974), the Selkirk material (Sinclair et al, 1977) and Grizzly Hill. The purpose of this is to estimate P,T conditions in the upper mantle beneath the Cordillera to determine the conditions of alkali basalt genesis for the Late Cenozoic, particularly at Level Mountain.

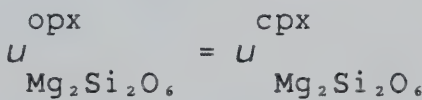
At equilibrium, the partitioning of Al, Mg, Fe etc. between the four phases olivine, orthopyroxene,, clinopyroxene and spinel, is a function of bulk composition, temperature and pressure. Considerable attention has been given to pyroxenes as geothermometers (Boyd, 1973; Wilshire and Jackson, 1975; Presnall, 1975; Stroh, 1976). Thermodynamic models may be constructed using tabulated

information from mineral thermodynamic studies (Robie et al., 1978) and experimental data from simplified analogs of the natural peridotite system, $\text{MgO}-\text{Al}_2\text{O}_3-\text{SiO}_2$, (MacGregor 1974; Fujii and Takahashi, 1978) and the enstatite-diopside join (Mori and Green, 1977, 1976; Davis and Boyd, 1966; Lindsley and Dixon, 1975).

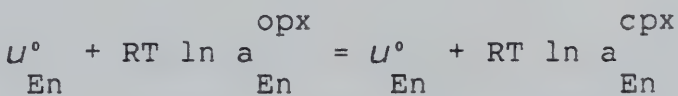
Consider the partition of magnesium between coexisting orthopyroxene and clinopyroxene



At equilibrium, (P, T , composition fixed),



the chemical potential of enstatite into both pyroxenes is equal (the sum of the $u(i)$ for the reaction is zero). Taking the standard state for each component to be equal to the pure phase, at some arbitrary temperature, the reaction can be rewritten as:



and the free energy for the reaction is then given by:

$$\frac{(\Delta G^\circ)}{T} = -RT \ln \left[\frac{a_{\text{cpx}}}{a_{\text{En}}} / \frac{a_{\text{opx}}}{a_{\text{En}}} \right]$$

dividing through by RT and recalling the Second Law of Thermodynamics:

$$\Delta G^\circ = \Delta H^\circ - T\Delta S^\circ$$

the preceding expression can be rewritten as

$$\frac{\Delta G^\circ}{RT} = - \ln \left(\frac{a_{\text{cpx}} a_{\text{opx}}}{a_{\text{En}}^{\text{cpx}} a_{\text{En}}^{\text{opx}}} \right) = \frac{\Delta H^\circ}{RT} - \frac{\Delta S^\circ}{R}$$

to give the basic form of the solid assemblage geothermometry expressions. Knowledge of ΔH° and ΔS° for the particular reaction in question may come from tabulated sources for minerals (such as Robie et al, 1978). Alternatively, ΔH° and ΔS° may be estimated from P-T slopes of reaction boundaries in experimental phase equilibrium studies using the Clapeyron relation.

The general form of the solid phase assemblage geothermometers is:

$$\ln K = \frac{\Delta H^\circ}{RT} - \frac{\Delta S^\circ}{R}$$

where K is the equilibrium constant (expression of activity products) for the reaction, and ΔH° and ΔS° are the enthalpy change (heat of reaction) and entropy change (order at a given T and P). As long as the ΔH° and ΔS° are accurately known and the simple mixing approximation applies, the geothermometers should be concisely expressed as simple log-linear expressions $\ln K = A/T + B$, where A and B are constants. This is the form generally given in geothermometry papers (Wells, 1977; Mori, 1977; Herzberg and Chapman, 1976) but it is important to keep in mind that A and B are not just arbitrarily selected numbers chosen to best fit a particular collection of data, but that they have

fundamental thermodynamic significance to them. Where the ideal mixing assumptions break down, or data on simple experimental fail to fit the more complex natural assemblages, empirical formulations have been made using polynominal expressions and adding additional terms, such as Mori (1977) or Wells (1977). It should be remembered that these extra terms are really without physical meaning and have only been added to force a mathematical fit to a collection of data. The need for such modifying terms only underlines the inaccuracies in our knowledge of ΔH° , ΔS° and in the assumed solution models. Herzberg and Chapman (1976) point out their fits imply $\Delta S > 8 \text{ cal/mol}^\circ$ which does not seem high in this temperature range. Mori's values (1977) imply even higher $\Delta S (> 9.4 \text{ cal/mol}^\circ)$. This probably demonstrates the oversimplification of the mixing model, rather than inaccuracy in the thermodynamic or experimental data. The familiar thermodynamic form of the geothermometer can be rewritten as an equivalent polynomial in $\ln K$ so that all geothermometers can be expressed in a common form:

$$10^4/T^\circ K = a(\ln k)^2 + b(\ln k) + c$$

where $c = 10^4 \Delta S^\circ / \Delta H^\circ$

$b = 10^4 R / \Delta H^\circ$

and a is an additional term with no thermodynamic meaning.

The state of the art in geothermometry of spinel lherzolites is summarized in Table 10-1. In addition to the magnesium partition between pyroxenes used in the derivation above, (reaction 1, Table 10-1) the two most accurate

Table 10-1. GEOTHERMOMETRY OF SPINEL LHERZOLITES

ASSEMBLAGE: Forsteritic Olivine - ol
 Cr-Al Diopside - cpx
 Magnesian Orthopyroxene - opx
 (Mg, Fe, Al, Cr) Spinel phase - sp

REACTIONS: AT EQUILIBRIUM TO DEFINE P, T

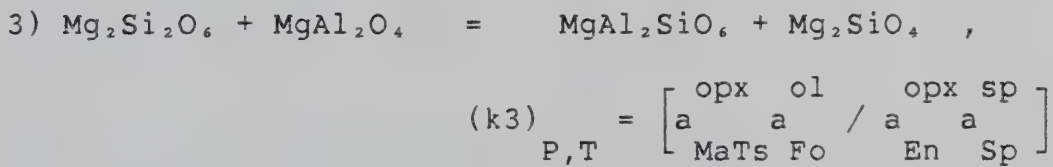
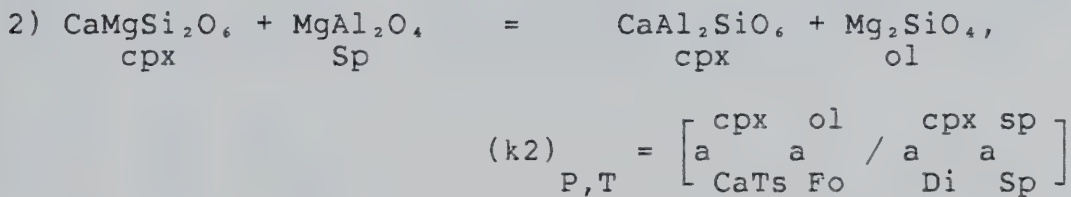


Table 10-1. (continued)

ACTIVITY DEFINITIONS¹

(Pyroxenes): M1(Al³⁺, Cr³⁺, V³⁺, Ti⁴⁺, Fe³⁺, Fe²⁺, Mg²⁺, Ni²⁺),
 M2(Mn²⁺, Ca²⁺, Na⁺, Ba²⁺, Fe²⁺, Mg²⁺)

cpx	M2	M1	In all cases Al ³⁺ is partitioned
a = X . X			between the tetrahedral site and M1
En	Mg	Mg	octahedral site on the basis of
cpx	M2	M1	silica content in the pyroxene
a = X . X			analysis assuming the tetrahedral
Di	Ca	Mg	site is completely filled by
cpx	M2	M1	Si ⁴⁺ and Al ³⁺ . After assigning
a = X . X			the site specific cations Mg ²⁺ ,
CaTs	Ca	Al	Fe ²⁺ are partitioned according to
			their proportions between M1 and M2,
			assuming ideal mixing.
opx	M2	M1	
a = X . X			
En	Mg	Mg	
opx	M2	M1	
a = X . X			
Mats	Mg	Al	

(Olivine)

ol	ol		
a = (X) ²		ideal solution	(M) ₂ SiO ₄
Fo	Fo		

(Spinel)

sp	A	B	
a = X (X) ²			for formula AB ₂ O ₄ normal spinel
MgAl ₂ O ₄	Mg	Al	

Table 10-1. (continued)

Calibrated Geothermometers:

Linear or polynomial regression fits of the form:

$$\frac{10^4}{T^\circ K} = a(\ln k)^2 + b(\ln k) + c$$

P = 12 Kbar

	a	b	c
*k ₁	0	-1.192	4.337
*k ₂	0	-1.171	4.754

after Herzberg and Chapman (1976)

P = 16 Kbar

+k ₁	0.41	0.37	5.7
*k ₁	0	-1.177	4.215
+k ₂	0	-1.08	5.12
*k ₂	0	-1.083	4.799
†k ₃	0.357	0.177	5.04
#k ₃	0	-2.06	2.69

1 = Activity definitions conform to Nicholls and Carmichael (1972), Bacon and Carmichael (1973) and reference cited below

* = Herzberg and Chapman (1976), data from experimental and natural spinel peridotites

+ = Mori (1977), experimental data base

† = Mori (1977), after MacGregor (1974)

= Mori (1977), after Obata (1976)

geothermometers are based on magnesium and aluminum partitioning between coexisting clinopyroxene spinel and olivine (reaction 2, Table 10-1) or aluminum and magnesium partitioning between coexisting orthopyroxene, spinel and olivine (reaction 3, Table 10-1). Reactions 2 and 3, involving the solubilities of alumina in pyroxenes, are not yet tested for Fe- and Cr-bearing systems. Application of these geothermometers to the Cr bearing system may give too high a temperature estimate (Fujii and Takahashi, 1978). The definitions of activities are consistent with the geothermometry papers previously cited. Activity expressions are calculated for ideal structural formulae and using concepts of equivalent sites. For example the expression

$$a_{\text{ol}} = \frac{x_{\text{M1}} x_{\text{M2}}}{x_{\text{Fo}} x_{\text{Mg}}} = \left(\frac{x_{\text{M1}}}{x_{\text{Mg}}} \right)^2 \quad \text{for } M1 = M2$$

shows the activity of the forsterite component in olivine assuming a random mixing for iron and magnesium between two octahedral sites. There is ambiguity in calculating structural formulae, particularly for pyroxenes, and several methods have been proposed (Cawthorn and Collerston, 1974; Fleet, 1974a,b). They have shown for pyroxenes of intermediate iron content, that random partitioning of Fe^{2+} between the two octahedral sites is not a very accurate assumption, because Fe^{2+} partitions in favour of Mg^{2+} into the M2 site. Magnesium and aluminum rarely exist in spinel analyses in stoichiometric proportions unbalanced by other cations. Problems arise in trying to fit data from different

laboratory studies. Additional difficulties may be encountered when fitting natural spinel lherzolites which have many additional components such as Ni, Mg, Na, Cr, Ti, V, Ba.

REVIEW OF PREVIOUS DATA FOR THE INTERMONTANE BELT

Fiesinger (1975) and Fiesinger and Nicholls (1977) performed geothermometry calculations both on solid assemblages and silica activities with coexisting lavas for spinel lherzolite and gabbroic xenoliths from Late Cenozoic lavas of the Wells Grey - Quesnel Highlands area B.C. Calculated equilibration temperatures ranged from 1050° to 1650°C with a total range of equilibration pressures from 13 to 50 kbar. The larger values for P and T here lie outside the spinel lherzolite stability field even though no garnet lherzolites are reported. There is too much variation in calculated P and T to be explained by any fractionation processes at either high or low pressure or to be explained by the inaccuracy in the assumptions and calculations of the geothermometers. The implication is that the nodules have been sampled from different depths and that the geotherm varies both in time and space for the Intermontane Belt. Similar conclusions have been obtained by Fujii et al (1981) using data for two localities from central and southern B.C. Takomkane (Boss Mountain) and Clark Creek (West Kettle River). Littlejohn and Greenwood's (1974) data for Jacques Lake (Quesnel Highlands) and Castle Rock (Klastline Plateau,

Stikine Volcanic Belt) indicate high and variable equilibration temperatures according to the olivine-spinel geothermometer of Jackson (1969). These estimates should be considered with some doubt however, due to possible subsolidus reequilibration of olivine and spinel and the assumption of ideal solution in the spinels. Sinclair et al (1977) also calculated high equilibration temperatures for nodules from the Selkirk cone.

Chemical analyses of four phases were made by electron microprobe on polished block mounts of nodules from Grizzly Hill and Telegraph Creek. Data and structural formulae are reported in table 10-2. All of these analyses gave high totals between 101 and 106% due to problems with an oil film on the beryllium window on the microprobe at the time the data were collected. Despite the high totals, the recast analyses compare favorably with other mantle inclusions reported from the literature including samples from the Cordillera (Littlejohn and Greenwood, 1974).

Activities have been calculated, from the structural formula and site occupancy restrictions as summarized in Table 10-1, for these nodules and for the four Castle Rock samples from Littlejohn and Greenwood (1974), and the two samples from the Selkirk Cone (Sinclair et al, 1978). Temperatures have been calculated for the geothermometers of Herzberg and Chapman (1976), Mori (1977) and Wells (1977) for all four localities, see table 10-3. The Castle Rock and Selkirk temperatures are derived from averages based on all

Table 10-2. CHEMICAL ANALYSES OF FOUR PHASES FROM INCLUSIONS

A. OLIVINES

	TCL 1004-41	GHL	
SiO ₂	40.58	40.48	TCL 1004-41 also contained interstitial plagioclase <1% of An(55)Ab(43)Or(2) and mono sulfide solid solution phase approximately Py(64)Pn(36) having detectable Ni,Co,Zn and micro-inclusions of sphere
FeO	10.95	11.25	GHL additionally contained <1% of interstitial alkali feldspar of An(0.7)Ab(41.0)Or(58.3) and a similar mono-sulfide solid solution to TCL
MnO	.09	.13	
NiO	.40	.47	
MgO	47.90	47.67	
CaO	.09	0.0	
	-----	-----	
	100.01	100.00	

STRUCTURAL FORMULAE PER 4 OXYGENS

Si ⁴⁺	1.001	1.0	1.000	1.0
Fe ²⁺	.226		.232	
Mg ²⁺	.002		.033	
Ni ²⁺	.008	2.0	.009	2.0
Mg ²⁺	1.761		1.756	
Ca ²⁺	.003		0.0	

Table 10-2. (continued)

B. Pyroxenes

	cpx		opx	
	TCL 1004-41	GHL	TCL 1004-41	GHL
SiO ₂	53.58	53.49	55.64	55.14
TiO ₂	0.28	0.35	0.0	0.0
Al ₂ O ₃	5.31	5.28	4.14	4.12
Cr ₂ O ₃	0.73	0.67	0.28	0.16
V ₂ O ₃	0.07	0.11	0.0	0.0
FeO	2.79	2.76	7.02	7.29
MnO	0.0	0.0	0.12	0.09
MgO	14.25	14.28	32.05	32.53
CaO	22.23	22.40	0.67	0.60
NiO	0.0	0.04	0.09	0.07
Na ₂ O	0.69	0.63	0.0	0.0
BaO	0.06	0.0	0.0	0.0
	-----	-----	-----	-----
	99.99	100.01	100.01	100.00

STRUCTURAL FORMULA PER 6 OXYGENS

Si ⁴⁺	1.931	1.932	1.924	1.911
Al(IV)	.069	2.0	.068	2.0
Al(VI)	.157	.157	.093	.079
Ti ⁴⁺	.010	.012	---	---
Cr ³⁺	.021	.019	.008	.005
V ³⁺	.002	.003	---	---
Fe ²⁺	.084	1.946	.083	2.0
Mn ²⁺	---	---	.004	.003
Mg ²⁺	.765	.769	1.652	1.680
Ca ²⁺	.858	.867	.025	.022
Ni ²⁺	---	.002	.003	.002
Na ⁺	.048	.044	---	---
Co ²⁺	.001	.044	---	---

Table 10-2. (continued)

C. Spinels

	TCL	GHL
	1004-41	
TiO ₂	0.09	0.0
Al ₂ O ₃	54.52	59.35
Cr ₂ O ₃	11.55	8.99
V ₂ O ₃	0.0	0.0
Fe ₂ O ₃	4.46	8.99
FeO	7.27	9.28
MnO	0.12	0.09
MgO	21.32	20.62
NiO	0.43	0.45
ZnO	0.10	0.05
CaO	0.14	--
	-----	-----
	100.00	100.02

STRUCTURAL FORMULA PER 32 OXYGENS

	TCL	GHL
	1004-41	
Ti ⁴⁺	0.02	0.0
Al ³⁺	13.37	14.36
Cr ³⁺	1.90	15.99
V ³⁺	---	1.46
Fe ³⁺	0.70	16.00
		0.0
Fe ²⁺	1.26	0.18
Mn ²⁺	0.02	1.59
Mg ²⁺	6.61	0.02
Ni ²⁺	8.00	6.31
Zn ²⁺	0.07	8.00
Co ²⁺	0.02	0.07
		0.01
		0.0

Table 10-3. Calculated Equilibration Temperatures ($T^{\circ}\text{C}$) for Spinel Lherzolites from the Intermontane Belt.

	(1) SELKIRK CONE, YUKON	(2) TELEGRAPH CREEK, B.C.	(3) CASTLE ROCK, B.C.	(4) GRIZZLY HILL, B.C.
--	-------------------------------	---------------------------------	-----------------------------	------------------------------

12 Kbar

*K ₁	1120	1039	1272	1041
*K ₂	1304	1366	1261	1318

16 Kbar

*K ₁	1151	1066	1308	1069
+K ₁	1126	1010	1301	1013
*K ₂	1323	1381	1281	1336
+K ₂	1246	1299	1208	1258
#†K ₃	1275	1246	1324	1146
#K ₃	1309	1267	1388	1137

0-40 Kbar

#K ₁	962	878	1095	878
-----------------	-----	-----	------	-----

- (1) Sinclair, Tempelman-Kluit, Medaris (1977) for mineral analyses of 2 Lherzolite nodules in Pleistocene cinder cone, central Yukon
- (2) Stikine region: Lherzolite nodule from Miocene or younger basalt flow at Telegraph Creek, B.C. Sample TCL 1004-41 from H. Greenwood
- (3) Littlejohn and Greenwood (1974) for mineral analyses from 4 Lherzolite Nodules in Quaternary AOB breccia at Castle Rock (Stikine Region) on northern edge of Klastline Plateau
- (4) Central B.C., Lherzolite nodule from Miocene basalt dyke at Grizzly Hill Hamilton (1979)

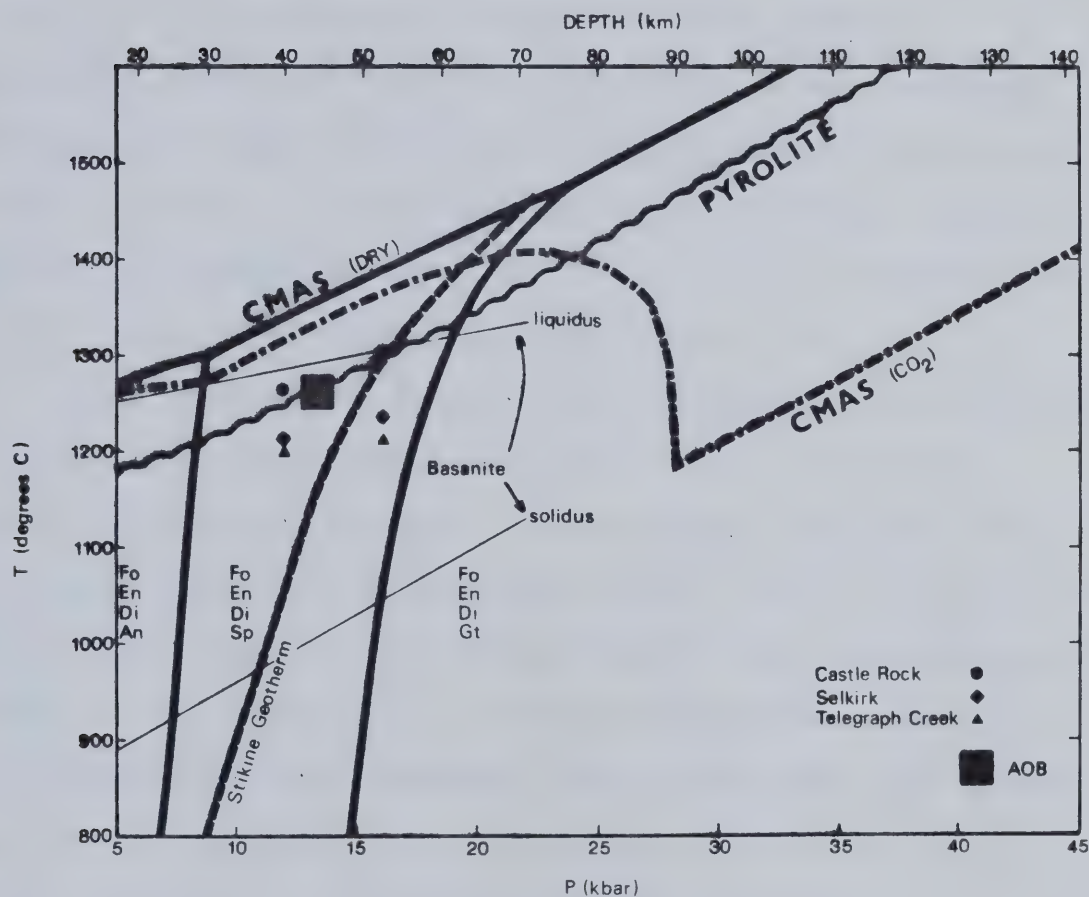
† Wells (1977)
 $10^4/T^{\circ}\text{K} = -1.362 \ln k + 4.570 + 3.324 \text{ Fe/Fe} + \text{Mg (opx)}$
 Of the natural compositions he tests this on, lherzolites and peridotites give the largest $T^{\circ}\text{K}$ discrepancies compared to other mineral geothermometers.

of the reported mineral data. The calculated temperatures fall in a tighter range than for previously reported values. Taking the Telegraph Creek, Castle Rock and Selkirk values as representative of the Upper Mantle beneath the Northern Cordillera in the vicinity of Level Mountain, the three mineral thermometers (k_2, k_3) give values in the range 1200° to 1400°C at 12 to 16 kbar, while the pyroxene thermometers give lower estimates of 875° to 1300°C. Using a surface temperature estimate (5°C), the average of all 12 kbar estimates (1219°C), and the average of all 16 kbar estimates (1228°C) for each locality, results in geothermal gradients in the range of 25°/km (82.4°/kbar) down to the intersection with the lherzolite solidus, see Figure 10-1. Owing to the Cr content of these natural samples, this geothermal gradient estimate is probably a maximum. For the simple four component experimental analog of the lherzolite system (CMAS)'this intersection would be at 15.8 kbar (51.8 km). Considering the effect of other components such as alkalis, iron, titanium, phosphorous and volatiles in depressing the solidus, this intersection is likely to be even shallower (see pyrolite solidus of Green and Ringwood, 1967). If some of the higher geothermometry estimates are accurate, the geotherm could be as steep as 31°/km with a solidus intersection as shallow as 41km (12.5 kbar). On the basis of trace element data, all of these spinel lherzolites appear to be high temperature refractory residua from previous

¹CaO - MgO -Al₂O₃ - SiO₂

Figure 10-1.

P-T plot showing phase fields and solidus for mantle peridotite along with liquidus data for basaltic lavas and range of PT estimates for lherzolites from northern Cordillera.



partial melting events and they are too depleted to be source rocks for normal basalt genesis.

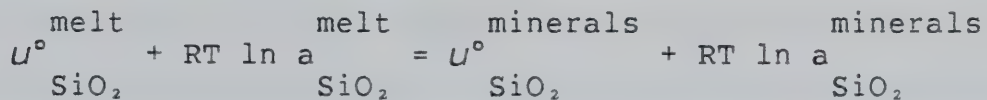
For comparison with natural rock systems the melting relations (solidus and liquidus) of a basanite are shown in Figure 10-1. The basanite comes from Mount Shadwell, Australia (Arculus, 1975). The intersection of the basanite solidus with the hypothesized Stikine geotherm lies in the stability field of ol + Cpx + Sp + Pl + L and the liquidus - geotherm intersection is in the field of ol + L, according to the phase relations of Arculus (1975).

From the work of DePaolo (1979) the intersection of the liquidus of an AOB having $\log a \text{SiO}_2 = -0.4$ with the anhydrous pyrolite solidus, is at 13.5kbar (44.5km). This point marking the alkali olivine basalt depth of origin lies within the field of the northern Cordilleran geothermometry estimates and slightly to the high temperature side of the hypothesized Stikine geotherm. Using these data the melting region for generating the Stikine basic lavas can be approximated to lie between 36 and 50 km depth.

GEOBAROMETRY AND GEOTHERMOMETRY FROM THE ACTIVITIES OF SILICA AND ALUMINA IN LEVEL MOUNTAIN LAVAS

Expressions for the variation of $\log a\text{SiO}_2$ into the melt with temperature have been published by Carmichael et al (1970) and for temperature and pressure by Nicholls et al (1971), Nicholls and Carmichael (1972) and Bacon and Carmichael (1973). The basic assumption is that for the

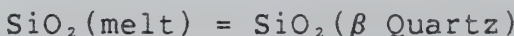
coexistence of minerals and silicate melts at equilibrium, the compositions of the minerals define a buffer on the activity of SiO_2 into the melt. Thermodynamically this can be stated:



and for more than one solid phase the right hand size would contain additional activity terms. If the chemical potential of silica in the standard state is taken to be that of SiO_2 glass for both melt and crystals, then the activity terms are equal. The activity of silica into the melt (or solids) may be defined by:

$$\left[\log a_{\text{SiO}_2}^{\text{melt}} \right]_{P,T} = \frac{\Delta G^\circ}{2.303RT} + \frac{\Delta V^\circ}{2.303RT} (P-1) + \log K$$

where $\Delta C_p = 0$ and K is the equilibrium constant for the reaction in question, defined by stoichiometry, and the activity terms are for pure mineral components into actual crystal phases, after Bacon and Carmichael (1973). Examples of such reactions that buffer silica are:



after Nicholls et al (1971). Note that in using real mineral compositions, the activity depends on both the solution model assumed and the stoichiometry. The thermodynamic form of the silica activity stated above gives rise to a unique expression for each reaction of the general form:

$$\left[\log a_{\text{SiO}_2}^{\text{melt}} \right]_{P,T} = (A/T + B) + (C/T(P-1)) + \log K$$

In keeping the same form, it can be seen that A and B come from the free energy term, while C comes from the volume change. Values of A, B and C have been calculated from existing thermodynamic data for the various silica buffering reactions. In the absence of a mineral-melt reaction which defines (buffers) the activity of SiO_2 into the melt, the following expression is used

$$\left[\log a_{\text{SiO}_2}^{\text{melt}} \right]_{P,T} = \left[\log X_{\text{SiO}_2}^{\text{melt}} + \frac{\psi(\text{SiO}_2)}{T} \right] + \frac{V-V^\circ}{2.30RT} (P-1)$$

after Bacon and Carmichael (1973). The V term is evaluated using the partial molar volume data of Bottinga and Weill (1970). The other term is a function of composition

where $X_{\text{SiO}_2}^{\text{melt}}$ is the mole fraction of silica into the melt,

and the composition function is defined:

$$\phi(\text{SiO}_2)/T = \log \left[a_{\text{SiO}_2}^{\text{melt}} / X_{\text{SiO}_2}^{\text{melt}} \right]$$

The function $\phi(\text{SiO}_2)$ may be evaluated at any single temperature if the activity of SiO_2 into the melt is known. Nicholls et al (1971) and Bacon and Carmichael (1973) have evaluated the activity of SiO_2 at the quench temperature of a lava. For this purpose they used T quench and $\log f\text{O}_2$, from Buddington and Lindsley's (1964) Fe-Ti oxide data, and equilibrium groundmass mineral compositions for olivine and

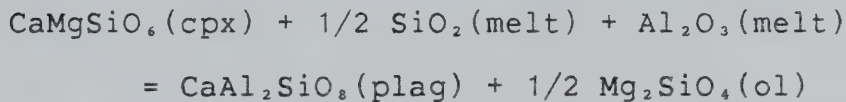
titanomagnetite with the fayalite-magnetite-silica buffer.

The buffer expression is:

$$\log a_{\text{SiO}_2}^{\text{melt}} = A/T + B + \log a_{\text{Fa}}^{\text{ol}} + 1/3 \log f_{\text{O}_2} - 2/3 \log a_{\text{Mt}}^{\text{TiMt}}$$

Note the reciprocal dependance on T and $\log f_{\text{O}_2}$. A small error in estimating T and/or $\log f_{\text{O}_2}$, while it changes the one bar activity into the melt, does not have as great an effect on estimating $\phi(\text{SiO}_2)$ for the lava. The confidence of $X(\text{SiO}_2)$ depends only on the accuracy of the bulk chemical analysis.

Alumina activities are evaluated in a parallel fashion for mineral reactions that buffer Al_2O_3 . For the unbuffered case, $\log a_{\text{Al}_2\text{O}_3}$ into the melt must be evaluated at some known temperature to get at $\phi_{\text{Al}_2\text{O}_3}$. In basic and intermediate lavas a useful defining reaction is:



where the equilibrium groundmass assemblage is used and $\log a_{\text{SiO}_2}$ into the melt must be known. The expressions

$$\log a_{\text{Al}_2\text{O}_3}^{\text{melt}} = A/T + B + \log \left[\frac{a_{\text{An}}^{\text{pl}} (a_{\text{Fo}}^{\text{ol}})^{1/2}}{a_{\text{Di}}^{\text{cpx}}} \right] - 1/2 \log a_{\text{SiO}_2}^{\text{melt}}$$

and $\phi_{\text{Al}_2\text{O}_3} = \left[\log a_{\text{Al}_2\text{O}_3}^{\text{melt}} - \log X_{\text{Al}_2\text{O}_3}^{\text{melt}} \right] T$

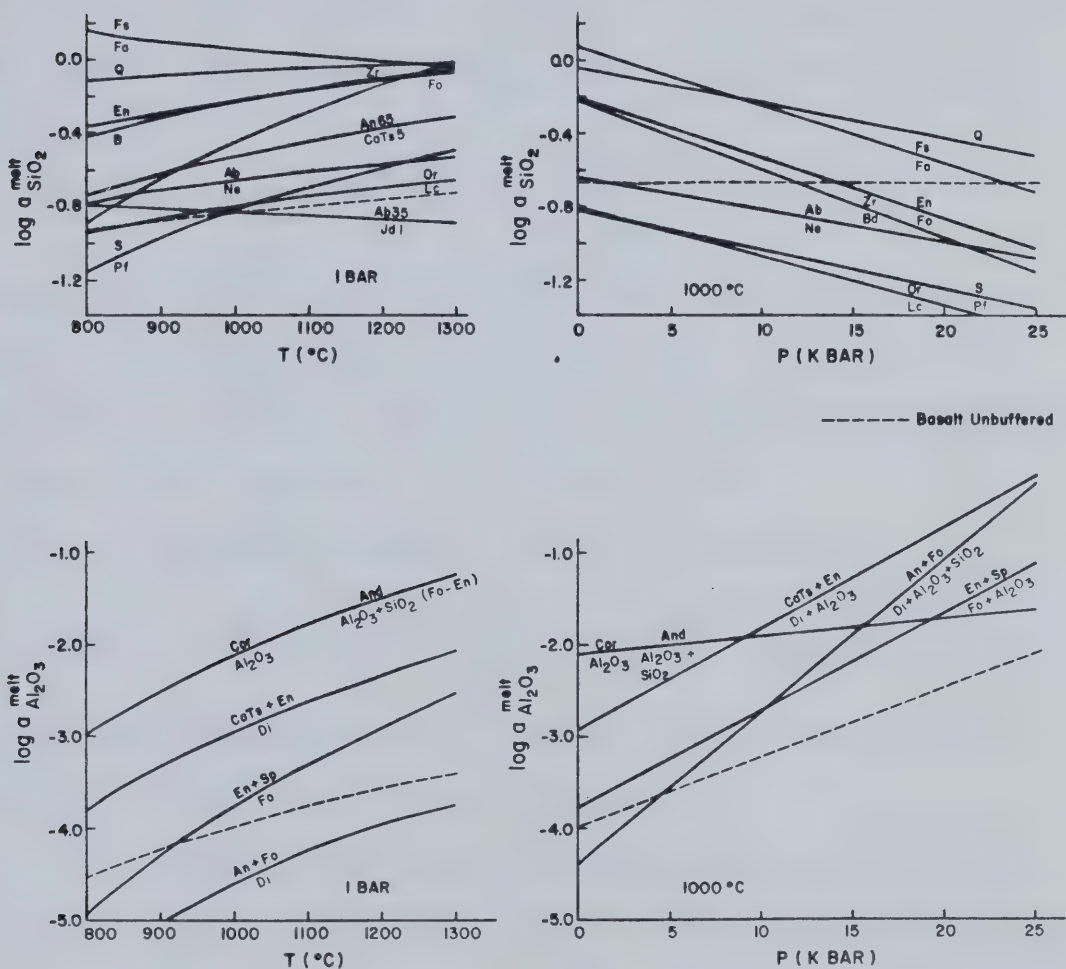
are evaluated using published values for A,B (Bacon and Carmichael, 1973) and compositions data for a specific basalt and its constituent mineral phases.

The variation of mineral-melt buffers for $a\text{SiO}_2$ and $a\text{Al}_2\text{O}_3$, are shown with temperature and pressure in figure 10-2. These diagrams have been constructed using the data of Bacon and Carmichael (1973), Nicholls and Carmichael (1972) and Nicholls et al (1971). Judging from common phenocryst assemblages, these curves likely span the $a\text{SiO}_2$ and $a\text{Al}_2\text{O}_3$ ranges commonly encountered for igneous melts from basalts to rhyolites. The unbuffered curves shown for basalt are for examples from Level Mountain. While the convergence of the common silica buffers at high temperature limits the applications of $\log a\text{SiO}_2$ into the melt as a geothermometer, the strong pressure dependence for the mineral-melt buffers compared to unbuffered lavas lends itself to use as a geobarometer. $\log a\text{SiO}_2$ varies inversely with pressure, while $\log a\text{Al}_2\text{O}_3$ varies directly. The use of silica and alumina buffers together improves the precision of pressure estimates.

Having defined the unbuffered variation in $\log a\text{SiO}_2$, and $\log a\text{Al}_2\text{O}_3$, into the melt as a function of P and T for a given lava, the expressions for both $\log a\text{SiO}_2$, and $\log a\text{Al}_2\text{O}_3$ may be solved simultaneously with reactions that define the activities of those components in the melt for mineral buffers, using assumed or analysed phenocryst or mantle assemblages, to give unique curves in PT space. As an example, Bacon and Carmichael (1973) solve the forsterite-enstatite buffer for SiO_2 , (defined previously) and the alumina buffer given by

Figure 10-2.

Calculated alumina and silica activity mineral-melt buffer curves. Pure phases unless otherwise shown. Data from Nicholls and Carmichael (1972) and Carmichael (1973).





with the unbuffered log activity expressions for the lava to give an assumed P and T of equilibration with mantle lherzolite. From the joint solution of the expressions for any mineral assemblage buffer, the general P-T curve is given by:

$$(P-1) = \frac{(B - \log X(\text{SiO}_2) + \log K)T - (\phi_{\text{SiO}_2} - A)}{D + ET}$$

where T is in °K, P in bars, A,B and K refer to the particular mineral-melt buffer and D+ET comes from the difference in the C coefficients for unbuffered melt and the chosen buffer reaction. In the case of the forsterite-enstatite buffer this expression is:

$$(P-1) = \frac{(0.597 - \log X(\text{SiO}_2) + \log K)T - (\phi_{\text{SiO}_2} + 1034)}{0.0377 + 1.34 \times 10^{-6}T}$$

where $\log K$ depends on the composition of olivine and pyroxene in the lherzolite. Similarly the olivine-orthopyroxene-spinel alumina buffer and the log alumina activity expression for the unbuffered melt can be solved to give:

$$(P-1) = \frac{(2.632 + \log K - \log X(\text{Al}_2\text{O}_3))T - (\phi_{\text{Al}_2\text{O}_3} + 8131)}{0.462 - 0.67002 \times 10^{-4}T}$$

where $\log K$ is given by:

$$\log K = \log a(\text{Sp in sp}) + \log a(\text{En in opx}) + \log a(\text{Fo in ol})$$

The equilibrium P-T curve for the lherzolite can also be defined by the reaction:



and $-\log K = -2156/T + 0.869 - 0.00778(P-1)$

The geobarometry of salic lavas presented in Nicholls et al (1971) depends on the simultaneous solution of two mineral-melt silica buffers. The fayalite-magnetite and quartz-silica buffers were used for a variety of acid lavas from different localities including a pantellerite from Pantelleria with $P_{eq.} > 7.3$ kbar.

Following the method described above, similar geobarometry calculations have been attempted for a few representative lavas from Level Mountain. The data used in these calculations and the results are presented in table 10-4. The quench temperatures inferred here are generally less than or equal to solidus estimates for Level Mountain lavas of similar composition. The oxygen fugacity inferred is slightly greater than or equal to that of the melting experiments. buffers for FMQ and MW by gas mixing.

While no lherzolite inclusions were found in the Level Mountain lavas proper, lherzolites have been found in similar lavas from the Selkirk Cone (Sinclair et al, 1978), Castle Rock (Littlejohn and Greenwood, 1974) and at Telegraph Creek. The mineral compositions from those localities have been used with Bacon and Carmichael's data for



to give the following lines in PT space for the spinel lherzolites from the Northern Cordillera (for T in °K and P in bars).

Table 10-4 Geothermometry and Geobarsometry Estimates for Level Mountain Lavas

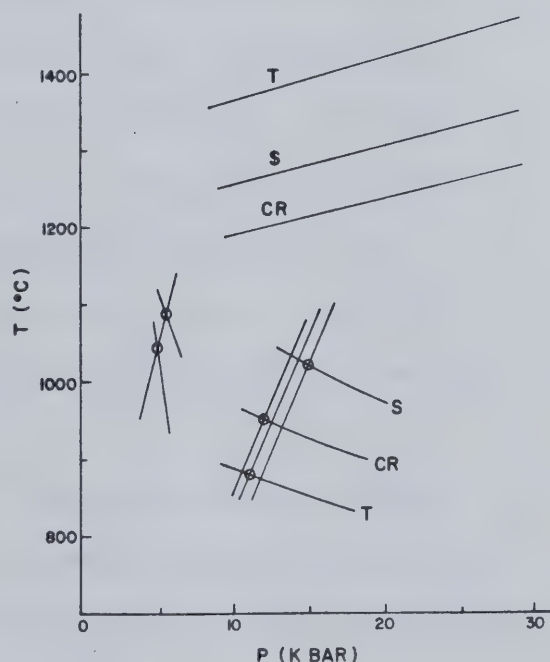
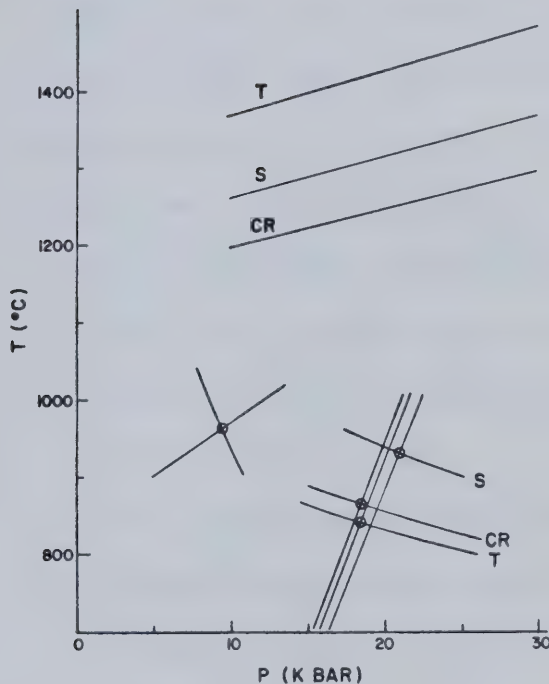
Sample ID	T quench 1 bar °C	log f02	plag X An	ol X Fo	cpx X Fa	cpx X Di	cpx X En	cpx X cat's	Tint X mt	log S102 a S102	θ S102	log Al2O3 a Al2O3	X Al2O3 θ Al2O3	T °C	*C/km	Phenocryst Megacryst or Herzolite used	
8/25-50/6397	985	-11.89	.599	.716	.274	.463	.102	.095	.33	-.6875	.5184	-.506	-.3,883 P<5.8	.0982	-3617	10.96	883
Hawaiite			.600	.591	.394											24.56 Telegraph Creek	
PBP 6480 (PBO for some minerals)	975	-12.93	.185	.338	.634	.444	.050	.022	.398	-.6897	.6746	-.647	-.4,4173 phenos P<10.6	.1082	-4308	9.86	805
Hawaiite			.220	.349	.627	.405	.572		.337	.201						25.5 CR	
PAP 4370	996	-12.06	.383	.546	.439	.509	.041	.061	.237	-.6109	.5481	-.444	-.3,955 phenos P<10.5	.1075	-3790	9.39	914
Hawaiite			.474	.507												24.28 Castle Rock	
PAR 4030	1050	-10.91	.599	.827	.764	.612	.084	.052	.225	-.1,3331	.5087	-.1375	-.1,6879 phenos P<4.25 Kbar	.1180	-3485	16.54	906
Alkali basalt																25.20 S	
PAO 4115	1041	-10.42	.526	.773	.220	.607	.076	.047	.386	-.8158	.5354	-.715	-.4,1027 phenos (minerals) T<1,185°C	.0956	-4051	14.35	803
Basalt			.707	.281												17.07 S	
PAX 3675	950	-13.00	.557	.762	.230	.467	.084	.052	.240	-1.2446	.5529	-1207.4	-.4,1007 phenos T<1,237°C	.0937	-3758	18.41	841
Basalt																13.93 CR	
PBX 5385	980	-12.40	.457	.418	.565	.517	.066	.027	(.300) -	.4891	.5358	-.273	-.4,7383 phenos T<1,150°C	.0931	-4645	No equil. w/ Herzolites	
Hawaiite																	
PAC 4465	986	-9.13	.457	.540	.444	(.514)	(.044)	(.053)	.819	.2484	.5737	617	-.4,9659 phenos P = 23.8 Kbar	.1027	-5008	No equil. w/ Herzolites or phenos?	
Hawaiite									.944								
8/26-56/6336	1090	-10.00			.753				.235	.0974	.7076	337.5			6.1 Kbar		
Trachyte															Q - SiO ₂ /Fa	Mg-SiO ₂	
8/7-19/5830	1110	-10.00			.726				.15	.1074	.7500	321.3			6.5 Kbar		
C.Trachyte															Q - SiO ₂ /Fa Mt. SiO ₂		
8/30-82/6150	860	-13.86	.232	.394	.574	.435	Jd=.04	.436	-.3716	(.7224)	-261	-5.6133	(.0967)	-5210	6.4 Kbar Ab-Jd/Fa Mt. SiO ₂		

Telegraph Creek:	P = 175.94	T = 277122
Castle Rock:	P = 195.71	T = 277122
Selkirk:	P = 187.31	T = 277122

The Castle Rock assemblage gives a very similar slope ($\Delta P / \Delta T$) to the San Quentin lherzolites of Bacon and Carmichael (1973), while the slopes for Telegraph Creek and Selkirk are slightly less. Graphical presentation of the P-T solutions for a basalt from the base of the Level Mountain plateau (unit 1) and a hawaiite from the central stratocone (unit 8) are given in Figure 10-3. Not only do these examples span most of the time of the Level Mountain volcanism, but they also span the range of depth estimates for the basaltic lavas. Two of the hawaiites presented in the table do not have real solutions (lying in positive P-T space) for lava-lherzolites or lava-phenocrysts. Those two hawaiites are assumed to be derived by substantial fractional crystallization from more primitive compositions, and in their final erupted compositions are likely to be out of equilibrium, with respect to silica and alumina activity for their phenocrysts and their presumed mantle source. As with the San Quintin lavas presented by Bacon and Carmichael, there may be some problems with the calculated pressures and temperatures. For the Level Mountain basaltic lavas all of the pressures fall into the spinel lherzolite stability field, but the temperatures seem too low for genesis of basaltic magmas. The pressures are similar to those calculated for other alkaline lavas from the

Figure 10-3.

Calculations of P-T equilibration conditions for spinel lherzolites from the northern Cordillera and two Level Mountain lavas. Upper set of 3 subparallel curves are for spinel lherzolites alone, assuming the reaction $\text{CaTs} + \text{Fo} = \text{Di} + \text{Sp}$. The plot on the left for PAX, from the lower plateau, shows the range of equilibration pressures for the unbuffered melt and lherzolite minerals, using all 3 lherzolites. Points are the intersection of $\text{Fo} + \text{SiO}_2 = \text{En}$ with $\text{Fo} + \text{Al}_2\text{O}_3 = \text{Sp} + \text{En}$. An estimate of pressure of equilibration for unbuffered melt and phenocrysts is given by the intersection of $\text{Jd} + \text{SiO}_2 = \text{Ab}$ for the plagioclase with $\text{Di} + \text{SiO}_2 + \text{Al}_2\text{O}_3 = \text{An} + \text{Fo}$ for the pyroxene. The plot on the right is for stratocone hawaiite 8/25-50/6397. The pressure estimate for melt equilibration with lherzolite minerals is lower. The lower of the pairs of curves for phenocryst buffers (with negative slope) is for $\text{CaTs} + \text{SiO}_2 = \text{An}$ other reactions as before. T = Telegraph Creek, S = Selkirk, CR = Castle Rock.



Intermontane Belt (Fiesinger and Nicholls, 1977); Nicholls et al, 1981 in prep.). The pressures calculated for three salic lavas from Level Mountain are all in the range from 6.0 to 6.5 kbar. This corresponds to the average depths calculated for diverse salic lavas in Nicholls et al (1971). The uncertainty associated with the depth (pressure) estimates for Level Mountain salic lavas is far greater than for the basalts. The two reasons for this are that the fayalites for these lavas were in reaction (petrographically) with their respective groundmass compositions (as judged by riebeckite or sodic pyroxene overgrowths), and the mineral buffers used to calculate depths were only assumed to be in equilibrium with said lavas, and this may not have been the case. The salient features of these calculations for Level Mountain are

1. that most of the basalts could have been in equilibrium with a spinel lherzolite mantle at pressures in excess of 9.4 kbar
2. that phenocryst assemblages from most basalts imply crystallization in the 4 to 6 kbar region, which could indicate the existence of crustal level magma chambers and
3. that salic lavas could have come from the lower crust or upper mantle according to the silica activity geobarometry calculations for three trachytes.

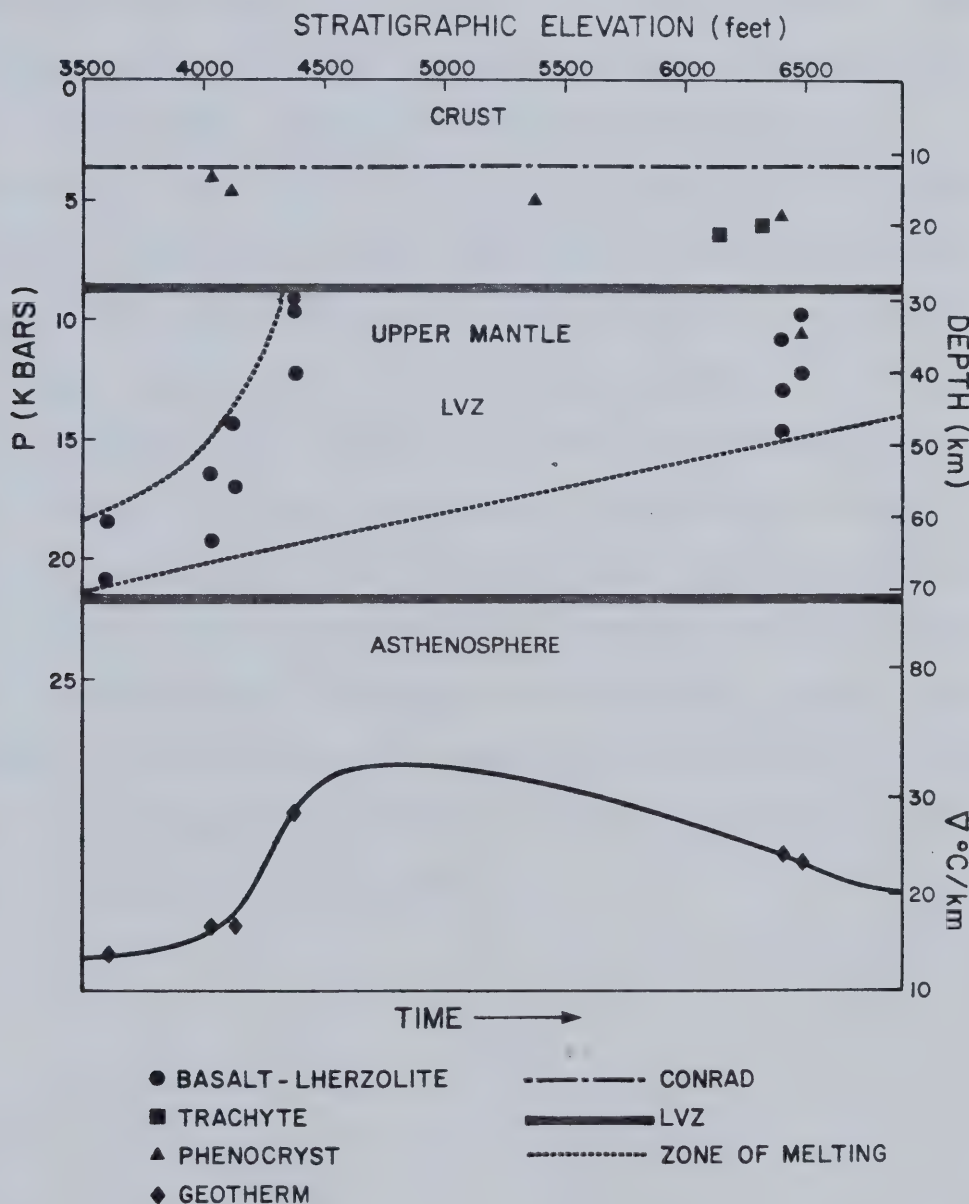
A summary of the geobarometry calculations for Level Mountain lavas is presented in Figure 10-4, with pressure

presented versus elevation (eruptive sequence) of the flows. The implication is that initial plateau volcanism originated at pressures from 18.5 to 21.0 kbar and subsequent lavas were derived from shallower depths. There is an indication of an upward migrating melting zone with time. This would be consistent with expectation from experimental studies on the spinel lherzolite system (Takahashi and Kushiro, 1981; Presnall, 1980; Ito and Kennedy, 1967). Following the reasoning of Presnall (1980), for a CO₂ bearing upper mantle, a rising geothermal gradient would intersect the lherzolite solidus cusp in the region of 20 kbar and remain there until one phase was exhausted (generally clinopyroxene). Subsequently the geotherm is constrained by the geometry of the spinel lherzolite solidus and a period of rising depth of melting could occur in a short time span, until the geotherm intersects the 10 kbar cusp on the lherzolite solidus. This sequence of events could have occurred at Level Mountain with the second cusp being reached by the time of extrusion for the basalts of the uppermost plateau (unit 4). The lavas of the stratocone could represent the further upward migration of the geotherm and melting zone into the base of the crust, or by generation of primary magmas at the 10 kbar cusp and further evolution in crustal level magma chambers.

Takahashi and Kushiro (1981) have found a partial melt of "phonolite" composition to exist in equilibrium with Fe- and K-rich spinel lherzolite (Salt Lake Crater, Oahu) at

Figure 10-4.

Geobarometry and geothermometry estimates for equilibration of Level Mountain basalts with spinel lherzolite using (Fo-En-SiO₂) and (Fo-En-Sp-Al₂O₃), imply a rising geothermal gradient and a rising zone of partial melting with time. Phenocryst equilibration conditions range from the shallow upper mantle to the lower crust. Trachyte estimates from (Fa-Mt-SiO₂) and (Q-SiO₂) imply equilibration in the lower crust.



temperatures as much as 200° below the apparent lherzolite solidus (anhydrous). These melts contain in excess of 9.0% by weight K₂O and are effectively peralkaline. This is reminiscent of the bimodal melting hypothesis of Yoder (1976). As the stratocone lavas from Level Mountain include phonolites and are dominantly peralkaline, the possibility still remains that they could be directly generated at mantle depths. Takahashi and Kushiro (1981) also performed a variety of "pyrolite" type experiments involving basaltic glass sandwiched between peridotites (spinel lherzolites). They found that plagioclase - pyroxene gabbros crystallized below the lherzolite solidus and were apparently stable in the PT field for spinel lherzolite. Should significant portions of such alkaline gabbros remain behind in the upper mantle they could contribute to the mantle differentiation and to compositional variation of subsequent partial melting episodes. The existence of gabbroic compositions at mantle depths could possibly account for the peralkaline salic lavas of the stratocone stage.

CHAPTER 11. A PALEOMAGNETIC STUDY OF THE LEVEL MOUNTAIN VOLCANICS

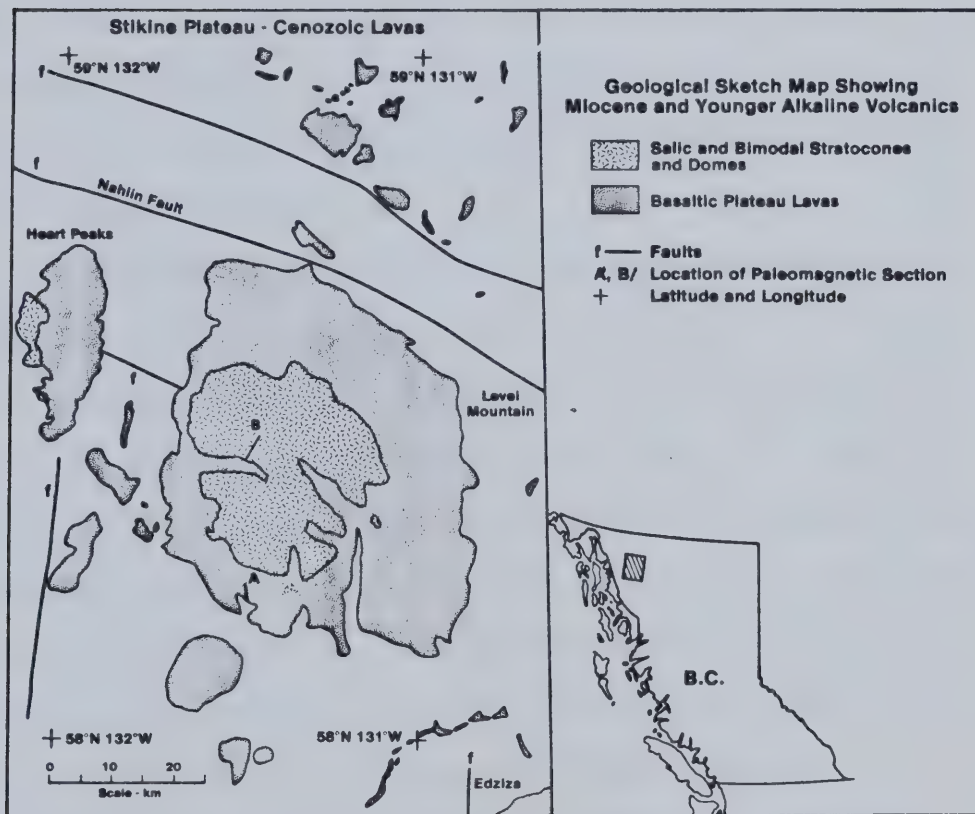
INTRODUCTION

Paleomagnetic studies have been conducted both on Mount Edziza (Souther and Symons, 1974) and on Level Mountain (Evans and Hamilton, 1980). At Level Mountain fifty cooling units were collected from two stratigraphic sections, Figure 11-1. The composite thickness of the proximal and distal sections is greater than 1000 meters. Fourteen magnetic polarity zones are found to be present as well as several low latitude virtual geomagnetic poles (VGP's) which probably represent transitions or excursions. A combination of magnetic data, stratigraphy and fission track dates indicates that the time span of Level Mountain volcanism extends from Epoch VII (greater than 6MY) to the Brunhes Epoch (less than 1MY). This will be shown to be similar to the results from Edziza.

Most sites carry a stable remanence (TRM), which can be determined with high precision. Fisher's precision parameter k generally exceeds 100. The two stratigraphic sections include several low latitude VGP's that probably represent polarity transitions or geomagnetic excursions. Filtering out the sites with low-latitude VGP's ($N=5$) and high internal scatter ($N=7$) leaves thirty-eight site means, twenty-four of which have normal polarity and fourteen of which are reversed. The average normal direction does not

Figure 11-1.

Location of the two paleomagnetic sections are shown on the geological sketch map of the Stikine Plateau: showing Level Mountain range and location of related Late Cenozoic volcanics.



differ significantly from the inverted reverse direction, and the overall mean yields a paleopole at 85°N lat. 256°E long., with an A_s , of 7°. The actual mean paleopole is slightly near-sided in terms of the common site longitude convention, which fails to support Wilson's eccentric dipole model (Wilson, 1972). Instead near-sidedness seems to be a persistent characteristic of paleopoles obtained from Western North America, suggesting the presence of a long term non-zonal anomaly.

The paleopole position for the best thirty-eight sites at Level Mountain includes the present spin axis as does the Edziza paleopole and the paleopole for the combined Stikine data sets. Since the circles of confidence for these paleopoles include the spin axis, any Late Cenozoic tectonic movements for the Stikine Terrane would appear to be small. The primary purpose of this study was to establish a magnetic stratigraphy for Level Mountain in hopes of correlating to the previously published magnetic stratigraphy of Edziza (Souther and Symons, 1974). An additional incentive was to seek information concerning the overall morphology of the geomagnetic field and its change with time. In this regard, the Late Cenozoic age and high latitude location of Level Mountain are particularly important. The rock magnetic properties of the samples were also investigated to document possible correlations between magnetic and petrological characteristics.

METHODOLOGY FOR THE PALEOMAGNETIC STUDY OF LEVEL MOUNTAIN

Field Procedures. Two stratigraphic sections of twenty-five flows each were collected. Five to seven cores were sampled, from each of the 50 flow-cooling units for a total of 252 cores. With three exceptions all of the flows were collected from contiguous stratigraphic sections. In these cases PBT, PBX, and PAF either exposure or access required that flows be projected "line of sight" back into the main section.

The PA section (distal and stratigraphically lower) was collected from the east facing canyon wall of the Little Tahltan River on the Southern Plateau margin at approximately 58.25°N 131.50°W , Plate 11-1. The section crosses 280 meters of vertical relief which spans the first four eruptive units (1-4) encompassing the plateau building stage at Level Mountain.

The PB section (proximal and stratigraphically higher) was collected from the South face of Meszah Peak and the south trending hanging valley which drains into the Kakuchuya Creek at approximately 58.49°N and 131.48°W , see plate 11-2. This section crosses 700m of vertical relief spanning the stratocone eruptive units 5 to 9. There is a 134m elevation gap between the two stratigraphic sections, which are separated by a lateral distance of 23km. According to field mapping there is no stratigraphic overlap between the two sections, but little or no section is inferred to be missing. The preferred interpretation is that the 134km elevation gap reflects the slope of the plateau surface

Plate 11-1.

The PA section through the basaltic flows of the Level Mountain was collected from the canyon wall of the Little Tahltan river, site PAA to upper right, site PAY lowest dark flow in stream notch above tree line. Map unit 1 extends from base of section to top of dark flows low on cliff. Map unit 2 is lighter coloured with thin flows. Map unit 3 comprises dark flows and tuffs to top of notch. Map unit 4 rests on a thick light coloured tuff unit that lies along the top of the cliff.

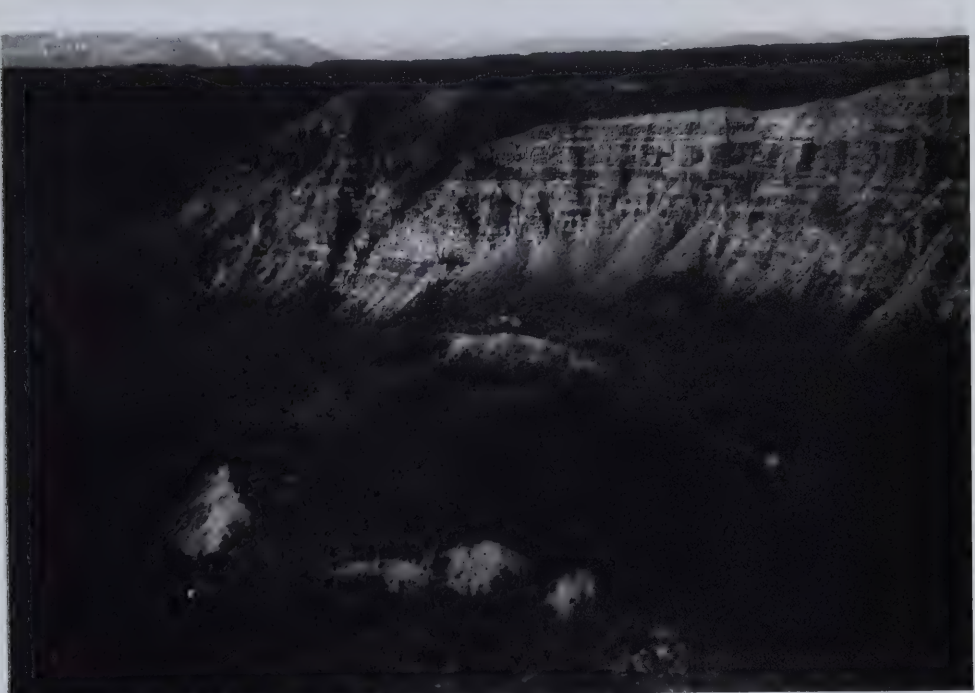




Plate 11-2.

View to SW along Hanging Valley from summit of Meszah Peak. The PB section through the stratocone followed the creek, down the hanging valley into the lower valley of Kakuchuya Creek.

(0.33°).

Laboratory Methods. The general measurement techniques to obtain the remanence vector for rock samples have been reviewed by McElhinny (1973) and Cox et al (1967). Pilot measurements of the magnetic vectors were made on a Princeton Applied Research Spinner magnetometer model SM-1 interfaced to a Wang 600 programmable calculator. The stability of one specimen from each flow was tested by routine alternating field (AF) techniques, mostly in peak fields of 2.5, 5, 10, 20, 40 and 80 mT. The results were used to identify regions of directional stability, and thus to select appropriate treatments for the remaining specimens. The bulk of a lab work was conducted using the Schonstedt SSM-1 interfaced to the Wang. The entire study involved about 1100 remanence measurements (presented in Appendix 3). Only one specimen from each core was measured as it has been demonstrated by Doell and Cox (1963, 1965) that very little additional accuracy is gained by multiple sampling. Each specimen was measured for natural remanent magnetization (NRM) and stepwise demagnetized to find a best estimate of D and I for each site. The stepwise demagnetization was performed in an alternating field (AF) apparatus designed and built by Murthy (1969). Due to the variation in rock types and rock magnetic properties a blanket treatment could not be prescribed for all sites. The minimum dispersion criterion (Irving et al, 1961) was applied to identify the best estimate of the mean remanence

direction at each site. Means were calculated in a hierachial fashion. The values of D and I corresponding to the lowest value of α_{ss} (highest Fisher k) were selected from among the sets of measurements at each site. In no case were fewer than three specimens from different cores finally selected to yield a D and I, and in most instances all cores could be used with no rejections. At nine sites one or two specimens exhibited anomalous behavior, either by systematically approaching the group formed by companion cores but never quite reaching this goal, or by stubbornly retaining a divergent direction. These specimens were excluded from further analysis, but it is noteworthy that they represent only 5% of the total data set. Although in part subjective, it is felt that this procedure yields the best available estimate of the true mean paleomagnetic vector at each site. A series of field and laboratory notes have been prepared site by site in descending stratigraphic order as a reference for this collection of data and to clarify any peculiarities at a given site. These notes are presented in Appendices 1 and 2.

The directional variance within each unit is generally small, with Fisher's precision parameter (Fisher, 1953) $k > 100$ in 34 out of 50 flows, and $k < 50$ in only 7 cases. Another convenient measure of the quality of the directional data is provided by the angular shift occurring at the demagnetization step used in the final analysis. When sites with poor internal grouping are excluded, as explained

below, these angular shifts are quite small. Sixty-seven percent of specimens undergo a shift of 3° or less, the corresponding values for $<5^\circ$ and $<10^\circ$ being 79% and 92% respectively. Thus a small fraction of the specimens have no direct evidence of end-points, and their inclusion rests on agreement with cores from the same site, as reflected by the appropriate site statistics.

MAGNETOSTRATIGRAPHY FOR LEVEL MOUNTAIN

The Stratocone Section, (PB)-Meszah Peak

The essential magnetostratigraphic information for Level Mountain is summarized in Table 11-1. The variation of VGP latitude as a function of elevation is presented as a magnetogram in Figure 11-2.

It is evident that the stratocone section (PB) spans at least three polarity zones. In order of increasing age these are normal, reversed, normal. The uppermost normal magnetozone, stratigraphically map unit 9, comprising hawaiite flows at the summit of Meszah Peak, can confidently be regarded as sampling the Brunhes (Epoch 1). These flows are the most recent on Level Mountain and field relations indicate that they postdate Quaternary continental glaciation (according to field mapping performed by the author and observations of Ostensoe, 1960).

Sites PBP down through PBL are clearly reversed. The most straightforward correlation with the established

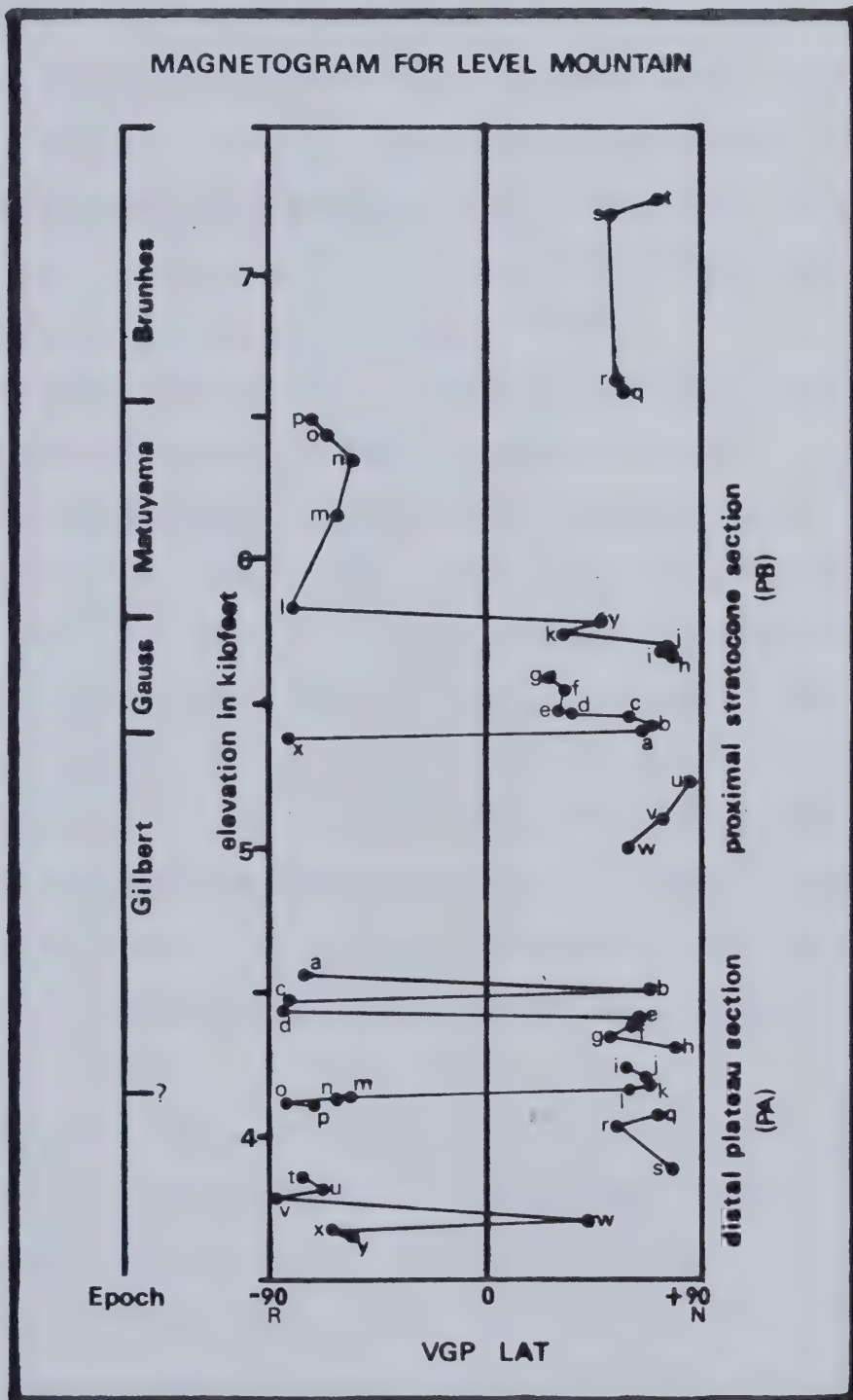
Table 11-1 Level Mountain Paleomagnetic Remanence Data by Sites

Unit	Site	Elev	Dens	% NRM	AF	n	R	k	α_{95}	D	I	LAT	LONG
9	PBT	7250	2.89	8.8	400	3(2)	2.9881	168	9.5	32.7	78.9	72.2	270.3
9	PBS	7200	2.96	0.5	800	3(2)	2.9932	294	7.2	45.5	55.1	52.7	336.7
9	PBR	6625	3.00	12.9	200	5	4.9378	64	9.6	51.7	61.9	55.0	322.1
9	PBQ	6580	2.94	4.1	400	3(2)	2.9886	175	9.3	30.4	54.0	59.0	355.9
8	PBP	6480	2.52	83.9	200	5	4.9656	116	7.1	216.0	-73.8	-71.6	119.0
8	PBO	6440	2.54	95.4	100	5	4.9387	65	9.5	184.0	-86.2	-65.5	51.3
7	PBN	6340	2.54	61.0	200	5	4.9983	2352	1.6	262.0	-78.3	-54.3	90.5
7	PBM	6160	2.60	101.0	50	5	4.9891	367	4.0	221.2	-62.3	-60.9	151.5
7	PBL	5835	2.62	79.1	200	5	4.9571	93	8.0	172.3	-65.6	-78.8	257.6
7	(PBY)	5780	2.58	16.4	100	5	4.7744	18	18.7	19.7	30.7	46.0	22.3
7	(PBK)	5745	2.54	100.0	0	5	4.7136	14	21.2	358.4	1.0	32.5	51.9
6b	PBJ	5690	2.80	35.0	100	5	4.9651	115	7.2	28.1	74.1	75.5	298.9
6b	PBI	5675	2.80	38.6	200	5	4.9709	138	6.6	20.2	80.8	73.7	252.3
6b	PBH	5655	2.75	51.8	50	5	4.9917	482	3.5	1.6	79.5	78.3	232.7
6a	PBG	5580	2.48	79.7	200	5	4.9867	301	4.4	19.2	-1.2	(29.4	27.8)
6a	PBF	5545	2.58	57.0	200	5	4.9621	106	7.5	12.4	5.1	(33.7	35.1)
6a	PBE	5475	2.50	78.3	200	5	4.9775	178	5.8	19.3	4.3	(32.1	27.0)
5b	PBD	5460	2.42	98.8	50	6	5.9849	331	3.7	18.7	14.5	(37.3	26.4)
5b	(PBC)	5450	2.78	98.8	100	5	4.8212	22	16.5	353.4	48.8	61.4	62.0
5b	PBB	5430	2.86	9.5	200	5	4.9167	48	11.2	331.8	66.0	70.7	122.1
5b	PBA	5420	2.80	76.2	50	4(1)	3.9968	937	3.0	4.3	53.9	66.3	41.2
5b	(PBX)	5385	2.87	35.8	50	5	4.6887	13	22.2	197.5	-76.8	-79.2	93.1
5a	PBU	5220	2.64	21.1	100	5	4.9351	62	9.8	348.9	72.6	84.1	144.0
5a	PBV	5100	2.26	100.0	0	4(1)	3.9908	326	5.1	8.9	61.8	74.0	25.8
5a	PBW	5000	2.34	46.7	100	5	4.9781	183	5.7	68.4	85.9	60.1	245.4
4	(PAA)	4560	2.87	11.5	400	5	3.9924	4	44.1	167.3	-64.0	-75.5	267.7
4	PAB	4505	2.64	235.4	100	5	4.9884	345	4.1	42.9	81.7	67.3	259.7
4	PAC	4465	2.66	70.4	200	5	4.9841	251	4.8	189.3	-67.3	-80.4	191.5
4	(PAD)	4440	2.63	9.8	400	2(2)	1.9869	76	29.0	169.5	-75.0	-83.5	0.4
4	PAE	4400	2.78	65.6	100	5	4.9978	1818	1.8	313.0	69.3	63.4	149.5
4	PAF	4370	2.58	25.5	100	5	4.9773	176	5.8	294.2	81.7	61.0	198.2
4	PAG	4340	2.66	54.9	100	5	4.9894	377	3.9	280.4	76.9	54.0	185.1
4	PAH	4300	2.56	42.2	100	5	4.9886	351	4.1	15.8	66.7	77.2	356.4
3	PAI	4230	2.70	39.1	200	5	4.9940	667	3.0	63.0	86.2	60.7	243.9
3	PAJ	4200	2.72	19.2	200	5	4.9878	328	4.2	310.1	80.0	66.0	191.3
3	PAK	4170	2.82	24.3	200	5	4.9346	61	9.9	330.7	83.6	68.2	213.2
3	PAL	4155	2.92	15.5	100	5	4.9804	204	5.4	308.6	70.1	61.7	154.6
3	PAM	4135	2.74	46.2	200	5	4.9744	156	6.1	163.2	-45.6	-56.9	258.1
3	PAN	4125	2.82	88.4	200	5	4.9294	57	10.3	169.4	-46.2	-58.6	248.3
3	PAO	4115	2.78	77.0	100	4(1)	3.9986	2141	2.0	167.0	-75.0	-82.5	355.8
3	PAP	4100	2.64	30.1	200	5	4.9317	59	10.1	173.4	-84.4	-69.0	46.5
2	PAQ	4065	2.70	33.1	200	5	4.9916	476	3.5	349.8	60.8	72.6	76.2
2	PAR	4030	2.88	47.1	100	4(1)	3.9957	698	3.5	44.7	57.8	55.3	334.5
2	PAS	3880	2.79	66.5	50	4(1)	3.9914	349	4.9	18.7	69.7	78.6	335.2
2	(PAT)	3860	2.40	108.1	200	4(1)	3.6531	9	33.1	156.6	-77.8	-76.2	8.3
2	PAU	3815	2.80	86.0	200	5	4.9910	444	3.6	154.6	-60.7	-67.2	285.6
2	PAV	3780	2.80	106.0	100	5	4.9259	54	10.5	178.8	-71.8	-88.5	256.5
1	PAW	3700	2.62	54.4	100	5	4.9698	133	6.7	0.0	21.3	(43.0	50.0)
1	PAX	3675	2.78	97.5	100	5	4.9955	889	2.6	147.5	-87.0	-62.9	42.9
1	PAY	3650	2.64	20.4	400	5	4.9770	174	5.8	65.5	-87.5	-55.7	41.9

Notes: Elev = elevation above sea level (feet)
 Dens = mean density in g/cc for cores from site
 % NRM = % of NRM intensity remaining upon reaching endpoint
 AF = field strength of last demag step upon reaching endpoint
 n = number of cores accepted (rejected)
 R = vector resultant of n unit vectors
 k = Fisher's precision parameter
 α_{95} = half-angle of cone of 95% confidence
 D = declination
 I = inclination
 LAT = latitude of equivalent VGP
 LONG = longitude of equivalent VGP

Figure 11-2.

Magnetogram for Level Mountain lavas showing polarity (VGP Lat) versus absolute stratigraphic elevation for the two Level Mountain sections. Lines are broken for erosional interval or other indicated time hiatus.



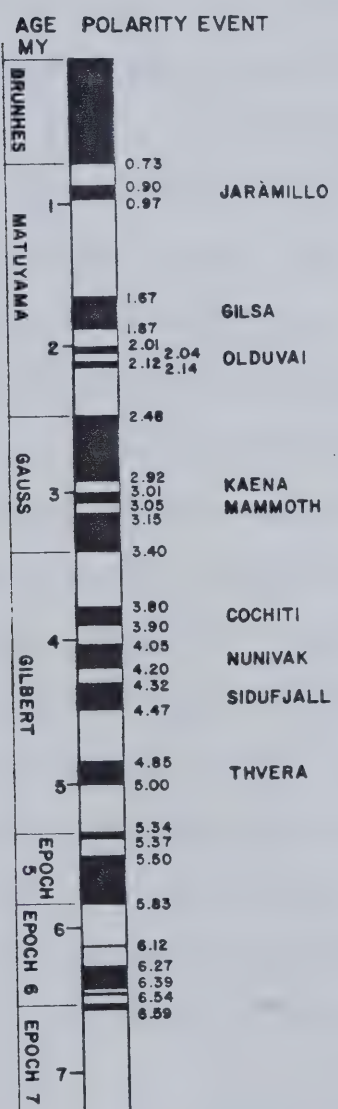
geomagnetic polarity time scale, Figure 11-3, is that these belong to the Matuyama (Epoch 2). It is uncertain whether this sequence of five reversed sites at Level Mountain lies above, below or misses the Jaramillo event entirely. It is not unreasonable to suppose that the short term normal events (Jaramillo, Gilsa, Olduvai) comprising less than 0.3MY (McDougall and Chamalaun, 1966; Cox, 1969) could be missed by a random sampling of only a few flows spread over the length of the Matuyama (some 1.75MY).

Sites PBY and PBK at the base of map unit 6 are normal, but of low precision, and have somewhat shallow inclinations, possibly representing a transition or excursion of the geomagnetic field. Flows at the base of map unit 6 have been dated (by fission track on pitchstones) at two locations on Level Mountain near the head of the Kakuchuya Valley. The dates are 2.61 ± 0.12 and 2.46 ± 0.12 MY (N. Briggs, pers. comm., 1978). These dates coincide within error to the Matuyama/Gauss boundary. It appears that the sequence of flows from PBL down through PBJ samples this transition, with sites PBY and PBK actually lying in the transition itself.

Sites PBJ, PBI and PBH most likely lie in the upper portion of the Gauss (Epoch 3). Below these basalts is a stratigraphic break and a lithological change to peralkaline trachytes. The next four flows have very shallow remanence directions, but the corresponding within- and between-site grouping is good. This group of flows (PBD, PBE, PBF, PBG)

Figure 11-3.

Reference geomagnetic polarity time scale adapted from Mankinen and Dalrymple (1979) down to the base of the Thvera, and from MacDougall et al (1977) down into Epoch 7.



represents either an excursion or a transition from an underlying normal to an unrecorded reversed polarity event lying between PBG and PBH. This could be the transition from the lower Gauss into the Mammoth event, the transition into the base of the Kaena, the transition out of the top of the Cochiti or the transition out of the top of the Nunivak. Without additional sampling or radiometric dating, this ambiguity cannot be resolved. The underlying three flows, PBC, PBB and PBA give normal directions, if somewhat shallow. Despite the shallow nature, the distribution of directions at PBA at least is very tight. Stratigraphically and petrochemically, site PBX belongs with map unit 5b and the sequence of basalts above, but is reversed. This site has no clear endpoint¹ but neither does it display random behavior to AF demagnetization. It is tentatively assigned to the top of the Gilbert (Epoch 4) implying that the base of map unit 5b samples the Gilbert to Gauss transition at 3.40MY (Mankinen and Dalrymple, 1979). The reason that this second interpretation is not favored is that the overlying sequence of seven flows would all have to fit into the 40,000 year normal interval between the Mammoth and the Kaena. These possibilities could be further assessed with

¹ On AF demagnetization as the softer (and usually random) components of remanence are progressively removed, the remanence direction changes systematically approaching the true TRM. Once the TRM has been reached, further demagnetization produces no change in direction until all of the remanence has been removed. Sister specimens and other cores from the same site also approach this common TRM direction, which is termed the endpoint.

another stratigraphic section. There is unsampled stratigraphy adjacent to PBX but it would have to be picked up laterally (westwards) along the northern Kakuchuya valley wall. The problem in the vicinity of the PB section is the morainal cover at this stratigraphic interval where the hanging valley enters the Kakuchuya.

The underlying map unit 5a is the basal unit of the stratocone. Sites PBU and PBV (phonolites) and site PBW (comendite) are all normal. This fact, and the foregoing discussion, would place the three flows in one of the short-lived normal events of the Gilbert reversed epoch. Another pitchstone fission track date of 4.51 ± 0.26 MY was obtained from this unit 5a further to the south across the Kakuchuya-Dudidontu ridge (N. Briggs, pers. comm.). Assuming this date to correspond to PBW, this site (within error) could correspond to the Sidufjall normal event between 4.47 and 4.32 MY (Mankinen and Dalrymple, 1979), or possibly the underlying Thvera. One other possibility is that the sequence of sites is not quite as old as unit 5a laterally, and that those flows of the PB section are younger than the date given, possibly placing them during either the Nunivak or the Cochiti event.

In summary, for the stratocone section, stratigraphic and map unit divisions correspond fairly well to magnetic breaks. There are many possible correlations between the PB section and the geomagnetic polarity time scale. The favored interpretation is that this sequence of twenty-five lavas

spans most of the recent four geomagnetic polarity epochs, commencing during the Gilbert at about 4.5MY and continuing up into the Brunhes, younger than 0.73MY. Alternatively, assuming that all of the normal and reversed polarity zones in the lower part of the stratocone have been sampled results in a minimum age estimate for the base of the stratocone between 3.40 and 3.15MY. In the favored interpretation, this sequence catches: the Gauss/Matuyama transition, the beginning of the transition into the Kaena or Mammoth event, and the transition from the Gilbert into the base of the Gauss. Eruptive activity appears to have been sparse and sporadic because the sampling indicates no evidence for the various events in the Brunhes and Matuyama Epochs.

The Plateau Section (PA)-Little Tahltan Canyon

The section of 25 flows sampled from the Little Tahltan Canyon crosses one of the best exposures of basalts which comprise the Level Mountain shield. This section is lower both in elevation and stratigraphic position than the stratocone section described above.

There is no radiometric data at all for the PA section and thus any correlation with the standard time-scale must be regarded as rather tentative. Furthermore, Mankinen and Dalrymple (1979) do not carry their polarity time scale beyond about 5MY. Taking the base of the PB section as representing the Sidufjall event, and simply matching the sequence of normal and reversed intervals determined by

McDougall et al (1977), see figure 11-3, leads to the conclusion that the lowest sites (PAX and PAY) fall near the middle of Epoch 6 (about 6MY). This is a minimum estimate for the onset of volcanism in the area. If "events" within the Gilbert epoch or Epochs 5 and 6 have been missed in this sampling, which seems probable, the base of the section will be correspondingly older. In this context it is reasonable to suppose that the eight flows (PAE to PAL) represent the lower part of Epoch 5 (5.50-5.83MY), not the very short normal interval at the top of Epoch 5 (5.34-5.37MY) which one-to-one matching implies. It also seems probable that the extremely short events at 6.12 and 6.39MY would not be recorded at Level Mountain. If this is so then sites PAQ to PAS may represent the normal interval 6.27 to 6.39MY, with sites PAX and PAY consequently having an age of about 6.6MY.

The frequency of volcanism during the plateau building is apparently greater than during the subsequent stratocone stage. For the minimum estimate of the onset of volcanism in the area of about 6MY, the duration of plateau building is about 1.5MY and possibly as long as 2.1MY for the case of missed events. This translates to an average time interval between eruptions of sixty to eighty thousand years, or about one order of magnitude more frequent activity than during the stratocone stage. However both the field relations and the remanence vectors indicate that eruptive activity during plateau time was more clustered. From this viewpoint, the four plateau units may have been short lived

intense periods of activity separated by quiescent periods of about half a million years in duration. For this second interpretation the quiescent periods during the plateau and stratocone stages are of about the same length, but the volumes of erupted material are more than an order of magnitude different.

A Comparison of the Paleomagnetic Sections from Level Mountain and Mount Edziza

Magnetograms for the three paleomagnetic sections from Mount Edziza (Souther and Symons, 1974) are shown in Figure 11-4. Tentative correlations of Level Mountain and Mount Edziza eruptive sequences to the geomagnetic polarity-time scale are given in Figure 11-5. The directions for sites PBS, PBR and PBQ agree with the uppermost flows of stratigraphic sections A and C on Edziza. The uppermost flows at both centres are basaltic in nature.

Sites PBP, PBO (map unit 8) and PBN (map unit 7) have steeper inclinations and more westerly declinations than most of the sites from map units 5, 7 and 9 of Edziza which are also interpreted to be of Matuyama age. While Souther and Symons (1974) have apparently caught the Jaramillo normal event at their site A6, no similar intervening normal event has been sampled at Level Mountain.

The directions for sites PBP, PBO and PBN are tentatively likened to the direction at Edziza's site A5 which is placed below the Jaramillo, while the intermediate chemistry of flows PBP and PBO (benmoreites) is similar to

Figure 11-4.

Magnetograms for the three Edziza stratigraphic sections. Data from Souther and Symons (1974). Elevation referenced to base of each section. Bar scale indicates map unit designation. Connecting lines are broken for time hiatus (or sampling gap) as inferred from stratigraphic notes.

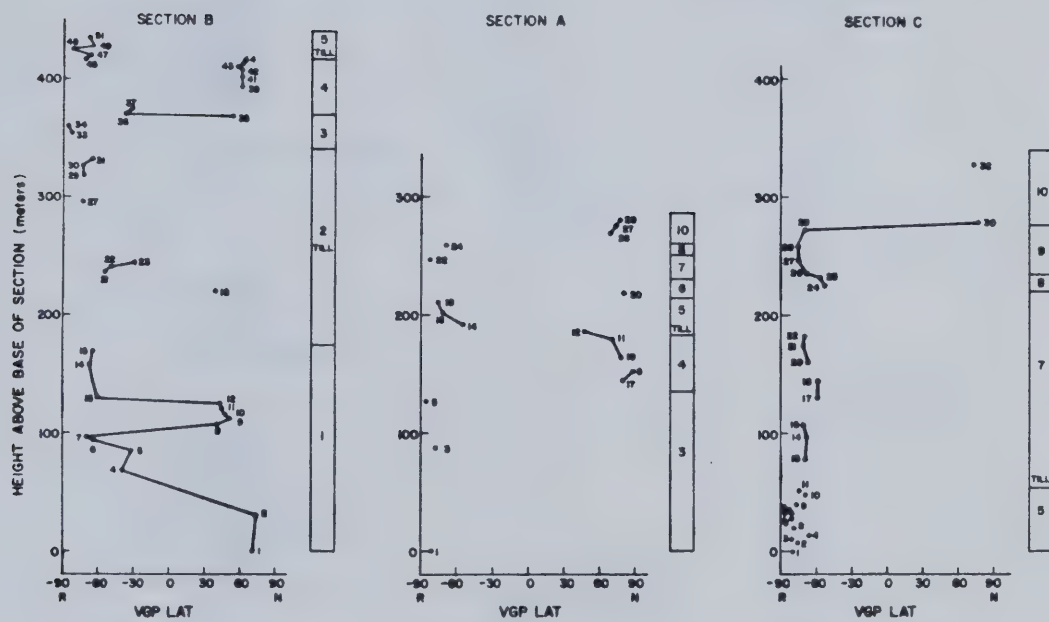
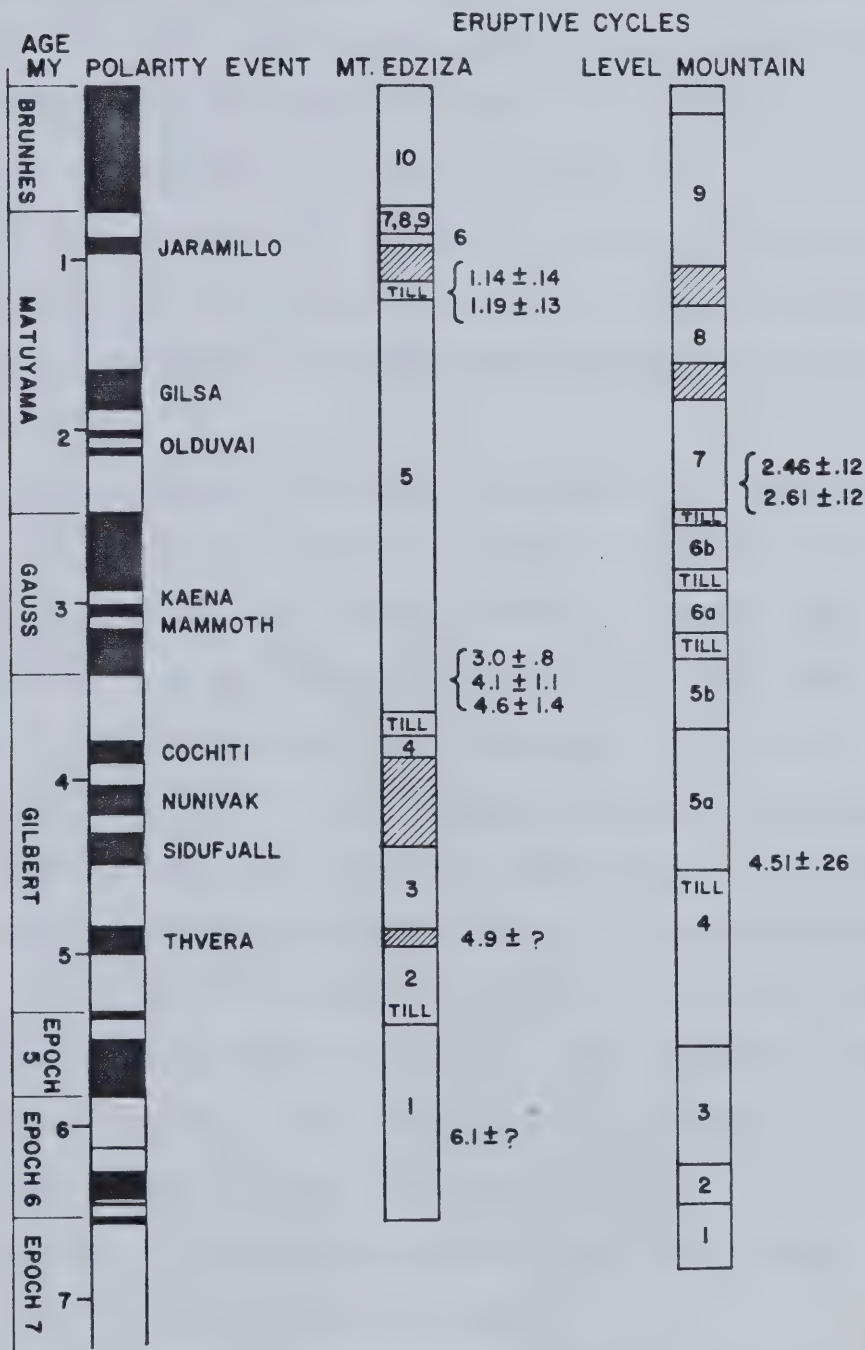


Figure 11-5.

Suggested correlation for volcanism at Level Mountain and Mount Edziza with the reference polarity time scale.



trachybasalts of unit 7 in sections A and C at Edziza.

The eruptive activity of map unit 6 (Level Mountain) appears to have been contemporaneous with glacial activity, as it is underlain by and includes tills, and is overlain by fluvioglacial sands and gravels. While the overlying unit could be Pleistocene, the underlying till implies a glaciation in the region at or prior to 2.5MY. The combination of information on glaciation at Level Mountain and Mount Edziza indicates that 3 or more episodes of continental glaciation occurred between the Pleistocene and about 5MY.

The stratigraphic interval including map units 5 and 6 at Level Mountain is lithologically most similar to the sequence from B16 to B32 (Edziza unit 2). These sections are both characterized by abundant peralkaline flows and tuffs. It appears that the bimodal volcanism and stratocone stage at Edziza may precede its equivalent at Level Mountain by as much as 0.5MY, with such activity beginning at Edziza during the reversed magnetozone of Epoch 5 or at the base of the Gilbert. It is also interesting to note that salic volcanics are included in the Edziza plateau, while at Level Mountain they are restricted to the Stratocone cap. There is a general age, magnetic and lithologic similarity for the stratocone section at Level Mountain and the younger portions of the 3 sections on Edziza.

The lower plateau section (B) at Edziza is bracketed by K-Ar dates as having been erupted between 6.1 and 4.9MY

(Souther and Symons, 1974). The best estimate from combined paleomagnetic and radiometric information is that the Edziza plateau building commences sometime during the lowest normal event of Epoch 6 sampling all three polarity zones of that epoch and the overlying reversed magnetozone of Epoch 5. The low latitude VGP site (PAW) could possibly represent a transition to the short normal zone at the top of Epoch 7. This indicates the possibility that the lowest sampled stratigraphy at Level Mountain is older by at least 0.4MY than the age cited for the base of the Edziza plateau.

CHAPTER 12. SUMMARY AND CONCLUSIONS REGARDING THE
PETROGENESIS OF THE LEVEL MOUNTAIN VOLCANICS AND THEIR
RELATIONSHIP TO THE TECTONICS OF THE INTERMONTANE BELT.

The most salient geological feature of the Stikine region of northwestern British Columbia is the Late Cenozoic volcanic activity. Since upper Miocene time more than 1700km³ of lavas have been erupted both as isolated flows and major volcanic edifices covering about 12% of the land area in the Stikine Volcanic Belt (Souther, 1977b). Within this region are eleven major volcanic centres of which Level Mountain and Mount Edziza are the largest. Most of the Stikine lavas belong to the sodic alkali basalt series and are of continental affinity. At level Mountain there are two volumetrically dominant lava types. Alkali basalt flows and related basic lavas (sub-alkaline basalt, hawaiite, ankaramite) comprise an oval shield approximately 50km in diameter with an average thickness of 600m. The shield-building stage lasted 2MY or more, ending during the Pliocene at about 4.5MY ago. At that time a fundamental change occurred both in the chemistry of the erupted lavas and their physiographic expression. This second stage of volcanism at level Mountain, with much greater variability in the eruptive style (including flows, pyroclastics, domes, cupolas, dykes and hypabyssal stocks), resulted in the construction of a complex centrally-placed stratocone cap approximately 25km in diameter with a thickness of about 750m. While the entire classic sodic alkali basalt

differentiation series is present, the dominant lavas of the stratocone stage were peralkaline trachytes. Other compositions in decreasing order of abundance are: comendites, rhyolites, hawaiites, benmoreites, phonolites and mugearites.

A variety of models for magma transport were calculated using one-atmosphere viscosity and liquidus determinations for the range of lava compositions. Basic magmas had very rapid ascent velocities in the range of 1 to 10 cm/sec with salic magmas being about two orders of magnitude slower. The volumes of typical flows and other single eruption features were on the order of 10^{-1} to 10^{-2} km³. That the Level Mountain range is comprised of many such low volume and low viscosity flows argues for low overall rates of volcanicity and the relatively efficient transport of small aliquots of magma directly from the upper mantle.

The isotopic and chemical evidence for the origin of the Level Mountain volcanics is straightforward. Basalts and inclusions with primitive $^{87}\text{Sr}/^{86}\text{Sr}$ values (0.7025 to 0.70440) and primitive Pb isotope ratios (in the range of typical values for MORB and oceanic islands) argue for an upper mantle derivation from a heterogeneous source. Oxygen isotope values for basalts and inclusions (5.5 to 5.9‰ $\delta^{18}\text{O}$ SMOW) confirm that the upper mantle beneath Level Mountain is normal with respect to oxygen. The shift to lighter isotopic compositions for the stratocone basalts, with respect to those on the shield stage,

indicates some heterogeneity for oxygen in the source region as well, and may indicate a shift in the depth of the melting zone as volcanism proceeded. Considering all of the Late Cenozoic lavas from the IMB, scatter in the O and Sr isotope signatures, along with the variation in major and trace element ratios for lavas of similar evolution, argues for a very local scale heterogeneity in their upper mantle source regions. Somewhat lower abundances of K, Rb, U, Th and light rare earths for lavas of the IMB, compared to those from the source regions of alkalic magmas in general (White et al, 1979), may indicate that the upper mantle beneath the Cordillera has been depleted by prior melting events. Such depletion might have occurred through volcanism and plutonism accompanying the Mesozoic emplacement of allochthonous Cordilleran terranes (Moninger and Price, 1979).

The major and trace element chemical variations for all of the Level Mountain lavas are inconsistent with the derivation of the volumetrically important peralkaline lavas of the Stratocone stage via the classical fractional crystallization processes from an alkali basalt primary magma. All of the chemical variation is typified by two clusters which are interpreted to indicate that there are two principle magma types, basalt and peralkaline trachyte. The peralkaline salic magmas have some equally primitive lead, strontium and oxygen isotope values to the basalts, but the range in oxygen and strontium extends to higher values indicating a combination of secondary processes

including crustal contamination and selective open system behavior. The peralkaline salic magmas are traditionally interpreted to be derived by substantial fractional crystallization of a wollastonite-normative intermediate or basaltic parent (the orthoclase effect of Bailey and Schairer, 1966). At Level Mountain the major element variation of these peralkaline lavas (principally Na and K) is inconsistent with a derivation via any extensive alkali feldspar fractionation. This interpretation is also born out in the normalized rare earth patterns which are totally lacking in europium anomalies. The distribution of salic lavas about the thermal minimum in the liquidus surface indicates that they may be a related series of partial melts. Geobarometry estimates for trachytes using silica activities give equilibration depths below 20km, in the lower crust. It is uncertain whether this reflects a depth of origin or rest point on the ascent path for the salic magmas. The high one-atmosphere temperatures determined in this study and the expected shape of the liquidus with increasing pressure (Bailey et al, 1974) suggest that the melting probably does not occur within the crust.

The source compositions and P, T conditions for the origin of the basaltic and peralkaline magmas are not very well constrained. Geothermometry and geobarometry calculations on lherzolite inclusions from the Stikine Volcanic Belt indicate equilibration depths in the range from 30 to 70 kilometers. Geobarometry estimates from silica

and alumina activities on Level Mountain lavas gives a similar depth range. This agrees with data for central B. C. reported by Fiesinger and Nicholls (1977) and Fujii et al., 1981. According to the recent synthesis of P and S wave residuals for the Cordillera, the upper mantle lacks a seismically resolvable high velocity lid, and these aforementioned depth estimates correspond to a range from the base of the crust down through the upper half of the low velocity zone (Wickens and Buchbinder, 1980). While the geobarometry estimates place the likely source region in the stability field for spinel lherzolite, the lherzolite compositions from the IMB are too geochemically depleted (Tatsumoto, 1978) to give rise to extractable quantities of basaltic partial melts. Matrix calculations give maximum partial melts of 4% but less than 1% is far more common. Similar calculations using Level Mountain basalts and a pyrolite source give partial melts in the range from 5% to 10% which is high enough for melt extraction. The salic lavas require either a more enriched source or a different derivation mechanism. Peralkaline partial melts can only be derived from peralkaline bulk compositions, which is an unlikely situation in the crust or the mantle. One possibility is that the upper mantle or portions of it become metasomatized by such processes as gaseous transfer of incompatible elements from deeper in the mantle or by a series of partial melting episodes with inefficient melt extraction (Boettcher and O'Neil, 1980). This differentiated

upper mantle could contain pods of compositions approaching granulite and gabbro, which is what the partial melting calculations for deriving salic melts require.

The cause of the Level Mountain and related Late Cenozoic volcanics of the IMB is an open question. Alkaline magmas are associated with extensional tectonics such as continental rift and oceanic fracture zones but they also occur on oceanic islands, seamount chains and in continental margin environments (MacDonald, 1974; Bailey, 1977). Some of the structural characteristics of the IMB, as deduced from regional geophysics, resemble a continental rift setting. This structural similarity and the presence of alkaline volcanism, led Souther (1977b) to hypothesize an incipient continental rift. A drawback to this model is the lack of active seismicity in the IMB (Milne et al, 1978) and that the magnitude and rates of volcanism for the SVB are lower than East Africa by two orders of magnitude. The related alkaline volcanism of the Anahim Volcanic Belt led Bevier et al (1979) to point out a possible association with a tear fault in the subducted Juan de Fuca plate. There has been no subduction activity in the vicinity of the northern Canadian Pacific margin since approximately 20MY ago (Grow and Atwater, 1970). This lack of a clear cut tectonic association led to a critical assessment the energy requirements for Level Mountain and the Stikine. Calculations on the amount of energy dissipated by volcanism indicate that the Late Cenozoic volcanism of the SVB could

be initiated and maintained by small changes (15%) in the total heat flux for the region. Changes of this magnitude could arise from the small tectonic stresses associated with the modern shear geometry of the adjacent continental margin (slip on the Queen Charlotte fault is about 6cm/yr) or from the re-equilibration of the thermal structure for the underlying upper mantle, with uplift and rebound of the geotherm following the completion of the subduction for the Kula plate in Mid-Tertiary time.

BIBLIOGRAPHY

Allegre, C. J., and Minster, J. F., 1978. Quantitative models of trace element behavior in magmatic processes. *Earth and Planetary Science Letters*, 38, pp.1-25.

Anderson, A. T. 1968. The oxygen fugacity of alkaline basalt and related magmas, Tristan de Cunha. *American Journal of Science*, 266, pp.704-727.

Anderson, A. T. 1974. Chlorine, sulfur and water in magmas and oceans. *Geological Society of America Bulletin*, 85, pp.1485-1492.

Anderson, A. T. 1976. Magma mixing: petrological process and volcanological tool. *Journal of Volcanology and Geothermal Research*, 1, pp.3-33.

Anderson, O. L., and Grew, P. C. 1977. Stress corrosion theory of crack propagation with applications to geophysics. *Reviews of Geophysics and Space Physics*, 15, pp.77-104.

Arculus, R. J. 1975. Melting behavior of two basalts in the range 10 to 35 kilobars. *Carnegie Institute of Washington Yearbook*, 74, pp.512-515.

Armstrong, R. L. 1968. A model for the evolution of strontium and lead isotopes in a dynamic earth. *Reviews of Geophysics*, 6, pp.175-200.

Armstrong, R. L., Green, N.L., and Watters, B.R. 1977. Strontium isotope study of Late Cenozoic volcanic rocks of the Canadian Cordillera. *Geological Association of Canada Programme with Abstracts*, 2, p.5.

Arth, J. G. 1976. Behavior of trace elements during processes and a summary of theoretical models and their applications. *U. S. G. S. Journal of Research*, 4, pp.41-47.

Ashby, M. E., and Verrall, R. A. 1978. Micromechanisms of flow and fracture and their relevance to the rheology of the upper mantle. *Philosophical Transactions of the Royal Society London Series A*, 288, pp.59-95.

Bacon, C. R., and Carmichael, I. S. E. 1973. Stages in the P-T Path of ascending basalt magma: an example from San Quintin, Baja California. *Contributions*

to Mineralogy and Petrology, 41, pp.1-22.

Bailey, D. K. 1969. The stability of acmite in the presence of H₂O. American Journal of Science, 267 A, (Schairer Volume) pp.1-16.

Bailey, D. K. 1974. Experimental petrology relating to oversaturated peralkaline volcanics. Bulletin Volcanologique, 38, pp.637-653.

Bailey, D. K. 1977. Continental rifting and mantle degassing. In Petrology and Geochemistry of Continental Rifts. Edited by E. R. Neuman and I. M. Ramberg. Reidel, Dordrecht.

Bailey, D. K., Cooper, J. P., and Knight, J. L. 1974. Anhydrous melting and crystallization of peralkaline obsidians. Bulletin Volcanologique, 38, pp.653-658.

Bailey, D. K., and Cooper, J. P. 1979. Comparison of the crystallization of pantelleritic obsidian under hydrous and anhydrous conditions. Fourth NERC Report, London. pp.230-233.

Bailey, D. K., and MacDonald, R. 1969. Alkali feldspar fractionation trends and the derivation of peralkaline liquids. American Journal of Science 267, pp.242-248.

Bailey, D. K., and MacDonald, R. 1970. Petrochemical variations among mildly peralkaline (comendite) obsidians from the oceans and continents. Contributions to Mineralogy and Petrology, 28, pp.340-5.

Bailey, D. K., and MacDonald, R. 1975. Fluorine and chlorine in peralkaline liquids and the need for magma generation in an open system. Mineralogical Magazine, 40, pp.405-414.

Bailey, D.K., and Schairer, J. F. 1964. Feldspar liquid equilibrium in peralkaline liquids - the orthoclase effect. American Journal of Science, 262, pp.1198-2006.

Bailey, D. K., and Schairer, J.F. 1966. The system Na₂O-Al₂O₃-Fe₂O₃-SiO₂, at one atmosphere and the petrogenesis of alkaline reactions. Journal of Petrology, 7, pp.114-170.

Baker, B. H., Goles, G. G., Leeman, W. P., and Lindstrom, M. M. 1977. Geochemistry and petrogenesis of a basalt-benmoreite-trachyte suite from the

southern part of the Gregory Rift, Kenya.
Contributions to Mineralogy and Petrology, 64,
pp.303-322.

Baker, I. 1969. Petrology of the volcanic rocks of St.
Helena Islands, South Atlantic. Bulletin of the
Geological Society of America, 80, pp.1283-1310.

Banks, R. J., and Ottey, P. 1974. Geomagnetic depth sounding
in and around the Kenya Rift valley. Geophysical
Journal of the Royal Astronomical Society, 36,
pp.321-335.

Basu, A. R. 1979. The mantle sample: inclusions in
kimberlites and other volcanics. In Geochemistry
of ultramafic xenoliths from San Quentin Baja
California, pp.391-400. edited by F. R. Boyd and
H. O. A. Meyer, publisher American Geophysical
Union.

Basu, A. R., and MacGregor, I. D. 1975. Chromite spinels
from ultramafic xenoliths. Geochimica et
Cosmochimica Acta, 39, pp.937-945.

Berry, M. J., and Forsyth, A. 1975. Structure of the
Canadian Cordillera from seismic refraction and
other data. Canadian Journal of Earth Sciences,
12, pp.187-208.

Bevier, M. L. 1977. Structure, petrology and geochemistry of
a peralkaline shield volcano. Rainbow range,
British Columbia. Abstracts, Geological Society
of America meeting, Seattle, p.897.

Bevier, M. L. 1978. Field relations and petrology of the
Rainbow Range shield volcano, West-Central
British Columbia. M.Sc. thesis, Department of
Geology, University of British Columbia,
Vancouver.

Bevier, M. L., Armstrong, R. L., and Souther, J. G. 1979.
Miocene peralkaline volcanism in West-Central
British Columbia - Its temporal and plate
tectonics setting. Geology, 7, pp.389-392.

Birch, F. 1966. Compressibility; elastic constants. In
Handbook of Physical Constants. Geological
Society of America Memoir No.97. edited by S. P.
Clark Jr.

Bird, R. B., Stewart, W. E., and Lightfoot, E. N. 1960.
Transport Phenomena. Wiley, New York.

Boettcher, A. L., and O'Neil, J. R. 1980. Stable isotope,

chemical and petrographic studies of high pressure amphiboles and micas: evidence for metasomatism in the mantle source regions of alkali basalts and comendites. American Journal of Science, 280 A, pp.594-621.

Bostock, H. S. 1948. Physiography of the Canadian Cordillera, with special reference to the area north of the fifty-fifth parallel. Geological Society of America Memoir 247.

Bottinga, Y., and Weill, D. F. 1970. Densities of liquid silicate systems calculated from partial molar volumes of oxide components. American Journal of Science, 269, pp.169-182.

Bowman, H. R., Asaro, F., and Perlman, J. 1973. On the uniformity of composition in obsidians and evidence for magmatic mixing. Journal of Geology, 81, pp.312-327.

Bowen, N. L. 1938. Lavas of the African rift valleys and their tectonic setting. American Journal of Science, Series 5, 35 A, pp.19-33.

Bowen, N. L., and Schairer, J. F. 1938. Crystallization equilibrium in nepheline-albite-silica mixtures with fayalite. Journal of Geology, 46, pp.397-411.

Boyd, F. R. 1973. A pyroxene geotherm. Geochimica et Cosmochimica Acta, 37, pp.2533-3576.

Brooks, C. K., and Printzlau, I. 1978. Magma mixing in mafic alkaline volcanic rocks: the evidence from relict phenocryst phases and other inclusions. Journal of Volcanology and Geothermal Research, 4, pp.315-331.

Brotzu, P., Morbidelli, L., Piccirillo, E. M., and Traversa, G. 1974. Petrological Features of the Boseti Mountains, a complex volcanic system in the axial portion of the main Ethiopian Rift. Bulletin Volcanologique, 38, pp.206-234.

Brousse, R., and Varet, J. 1966. Les trachytes du Mont-Dore et du Cantal septentrional et leurs enclaves. Bulletin Societe Geologique de France, 8, pp.246-262.

Brown, G. M., Holland, J. G., Sigurdsson, H., Tomblin, J. F., and Arculus, R. J. 1977. Geochemistry of the Lesser Antilles volcanic island arc. Geochimica et Cosmochimica Acta, 41, pp.785-802.

Bryan, W. B. 1964. Relative abundance of intermediate members of oceanic basalt - trachyte association: evidence from Clarion and Socorro Islands, Revillagigedo Islands, Mexico. *Journal of Geophysical Research*, 69, pp.3047-3049.

Bryan W. B. 1966. History and Mechanism of eruption of soda rhyolite and alkali basalt, Socorro Island, Mexico. *Bulletin Volcanologique*, 29, pp.453-480.

Bryan, W. B. 1976. A basalt-pantellerite association from Isla Socorro, Islas Revillagigedo, Mexico. In *Volcanoes and Tectonosphere*. Tokai U. Press.

Bryan, W. B., Finger, L. W., and Chayes, F. 1969. Estimating proportions in petrographic mixing equations by least squares approximation. *Science*, 163, pp.926-927.

Buchbinder, G., and Poupinet, G. 1977. P-wave residuals in Canada. *Canadian Journal of Earth Science*, 14, pp.1292-1304.

Buddington, A.F., and Lindsley, D. H. 1964. Iron titanium oxide minerals and synthetic equivalents. *Journal of Petrology*, 5, pp.310-357.

Bullard, E. C. 1949. Electromagnetic induction in a rotating sphere. *Proceedings of the Royal Society of London, Series A*, 199, p.413.

Bullard, E. C., Freedman, C., Gellman, H., and Nixon, J. 1950. The westward drift of the geomagnetic field. *Philosophical Transactions of the Royal Society of London, Series a*, 243, p.67.

Butterman, W. C., and Foster, W. R. 1967. Zircon stability and the ZrO_2 - SiO_2 phase diagram. *American Mineralogist*, 52, pp.880-885.

Campbell, R. B., 1961. Quesnel Lake map-area, west half, British Columbia. Geological Survey of Canada.

Campbell, R. B., and Tipper, H. W. 1971. Geology of the Bonaparte Lake map-area, Geological Survey of Canada, Memoir No. 363.

Caner, B. 1969. Long aeromagnetic profiles and crustal structure in Western Canada. *Earth and Planetary Science Letters*, 7, pp.3-11.

Caner, B. 1970. Electrical conductivity structure in Western Canada and petrological interpretation. *Journal of Geomagnetism and Geoelectricity*, 22,

pp.113-129.

Caner, B., Camfield, P. A., Anderson, F., and Niblett, E. R. 1969. A large scale magneto-telluric survey in Western Canada. Canadian Journal of Earth Science, 6, pp.1245-1261.

Carmichael, I. S. E., and MacKenzie, W. S. 1963. Feldspar - liquid equilibrium in pantellerites, an experimental study. American Journal of Science, 261, pp.382-396.

Carmichael, I. S. E., and Nicholls, J. 1967. Iron - titanium oxides and oxygen fugacities in volcanic rocks. Journal of Geophysical Research, 72, pp.4665-4687.

Carmichael, I. S. E., Nicholls, J., and Smith, A. E. 1970. Silica activity in igneous rocks. American Mineralogist, 55, pp.246-263.

Carmichael, I. S. E., Nicholls, J., Spera, F. J., Wood, B. J., and Nelson, S. A. 1977. High temperature properties of silicate liquids, applications to the equilibration and ascent of basaltic magma. Philosophical Transactions of the Royal Society, London, Series A, 286, pp.373-431.

Carmichael, I. S. E., Turner, F. J., Verhoogen, J. 1974. Igneous Petrology. McGraw-Hill, New York.

Carslaw, H. S., and Jaeger, J. C. 1973. Conduction of heat in solids. Oxford Clarendon, London.

Casey, J. 1980. Geology of the Heart Peaks Volcanic Centre. M.Sc. thesis, Department of Geology, University of Alberta, Edmonton.

Cathles, L. M. 1975. The Viscosity of the Earth's Mantle. Princeton University Press.

Cawthorn, R. G., and Collerson, K. D. 1974. The recalculation of pyroxene n-member parameters and the estimation of ferrous and ferric iron content from electron microprobe analysis. American Mineralogist, 59, pp.1203-1208.

Chayes, F. 1963. Relative abundance of intermediate members of the oceanic basalt - trachyte association. Journal of Geophysical Research, 68, pp.1519-1534.

Chayes, F. 1964. A petrographic distinction between Cenozoic volcanics in and around the open ocean. Journal

of Geophysical Research, 69, pp.1573-1588.

Church, S. E., and Tatsumoto, M. 1975. Lead isotope relations in oceanic basalts from the Juan de Fuca - Gorda Ridge area, N.E. Pacific ocean. Contributions to Mineralogy and Petrology, 53, p.253.

Clague, P. A. 1978. The oceanic basalt - trachyte association: an explanation of the Daly Gap. Journal of Geology, 86, pp.739-743.

Clark, S. P. 1966. Thermal Conductivity. Geological Society of America Memoir No. 97, pp.459-483.

Clayton, R. N., and Mayeda, T. K. 1963. The use of bromine pentafluoride in the extraction of oxygen from oxides and silicates for isotopic analysis. Geochimica et Cosmochimica Acta, 22, p.43.

Clowes, R. M. 1981. Geophysics and the Canadian Cordillera. Programme with abstracts, Geological Association of Canada, Vancouver.

Cockfield, W. E., 1925. Explorations between Atlin and Telegraph Creek, B.C. Geological Survey of Canada, Summer report, Part A, pp.37-74.

Cohen, L. H., Ito, K., and Kennedy, G. C. 1967. Melting and phase relations in an anhydrous basalt to 40 kilobar. American Journal of Science, 265, pp.475-518.

Cohn, S., and Ahrens, T. 1977. Dynamic tensile fracture of basic igneous rock. EOS Transactions of the American Geophysical Union, 58, p.1229.

Cooper, J. P., and Bailey, D. K. 1979. Oxidation state in anhydrous experiments of peralkaline obsidians. Fourth NERC Report (London), pp.234-241.

Cox, A. 1968. Lengths of geomagnetic polarity reversals. Journal of Geophysical Research, 73, pp.3247-3260.

Cox, A. 1969. Geomagnetic reversals. Science, 163, pp.237-245.

Cox, A., Dalrymple, G. B., and Doell, R. R. 1967. Reversals of the earth's magnetic field. Scientific American, 216, pp.44-54.

Cox, A., and Doell, R. R. 1960. Review of Paleomagnetism. Bulletin of the Geological Society of America,

71, pp.645-768.

Cox, K. G., Gass, I. G., and Mallick, D. I. J. 1969. The evolution of the volcanoes of Aden and Little Aden, South Arabia. Quarterly Journal of the Geological Society (London), 124, pp.283-308.

Cox, K. G., Glass, I. G., and Mallick, D. I. J. 1970. The peralkaline volcanic suite of Aden and Little Aden, S. Arabia. Journal of Petrology, 7, pp.433-461.

Craig, H. 1961. Standard for reporting the concentration of deuterium and ^{18}O in natural waters. Science, 133, p.1833.

Daly, R. A. 1933. Igneous Rocks and the Depths of the Earth. McGraw-Hill, New York.

Davis, B. T. C., and Boyd, F. R. 1966. The join $\text{Mg}_2\text{Si}_2\text{O}_5$ -CaMgSiO₄ at 30 kilobar pressure and its application to pyroxenes from kimberlites. Journal of Geophysical Research, 71, pp.3567-3576.

Deer, W. A., Howie, R. A., and Zussman, J. 1978. Rock Forming Minerals, Volume 2A: Single Chain Silicates. Longman, London.

Deines, P., Nafziger, R. H., Ulmer, G. C., and Woerman, E. 1974. Temperature-oxygen fugacity tables for selected gas mixtures in the system C-H-O at one atmosphere total pressure. Bulletin of the Earth and Mineral Sciences Experiment Station, No. 88, Pennsylvania State University.

DeLong, S. E., Fox, P. J., and McDowell, F. W. 1978. Subduction of the Kula Ridge at the Aleutian Trench. Geological Society of America Bulletin, 89, pp.83-95.

DePaolao, D. J. 1979. Estimate of the depth of origin of basic magmas: a modified thermodynamic approach and a comparison with experimental melting studies. Contributions to Mineralogy and Petrology, 69, pp.265-278.

Dey-Sarkar, S. K., and Wiggins, R. A. 1976. Upper mantle structure in western Canada. Journal of Geophysical Research, 81, pp.3619-3632.

Dickinson, D. R., Dodson, M. H., Gass, I. G., and Rex, D. C. 1969. Correlations of initial $^{87}\text{Sr}/^{86}\text{Sr}$ with Rb/Sr in some late tertiary rocks of S. Arabia.

Earth and Planetary Science Letters, 6,
pp.84-90.

Doell, R. R., and Cox, A. 1961. Paleomagnetism. Advances in Geophysics, 8, pp.221-313.

Doell, R. R., and Cox, A. 1963. The accuracy of the paleomagnetic method as evaluated from the historic Hawaiian lava flows. Journal of Geophysical Research, 68, pp.1997-2009.

Doell, R. R. and Cox, A. 1965. Paleomagnetism of Hawaiian lava flows. Journal of Geophysical Research, 70, pp.3377-3405.

Donaldson, D. H. 1976. An experimental investigation of olivine morphology. Contributions to Mineralogy and Petrology, 57, pp.187-213.

Donaldson, C. H., Williams, R. J., and Lofgren, G. 1975. A sample holding technique for study of crystal growth in silicate melts. American Mineralogist, 60, pp.324-326.

Duke, J. M. 1974. The effect of oxidation on the crystallization of an alkali basalt from the Azores. Journal of Geology, 82, pp.524-528.

Dupre and Allegre, 1980. Isotopic composition of lead and strontium and development of Azores Islands.

Eaton, J. P., and Murata, J. K. 1960. How volcanoes grow. Science, 132, pp.925-938.

Edgar, A. D., Parker, L. M. 1974. Comparison of melting relationships of some plutonic and volcanic peralkaline undersaturated rocks. Lithos, 7, pp.263-273.

Epstein, S. 1957. The variations of $^{18}\text{O}/^{16}\text{O}$ in nature and some geologic implications. In *Researches in Geochemistry*, Edited by Abelson, pp.217-240.

Ernst, W. G. 1962. Synthesis, stability relations and occurrence of riebeckite. Journal of Geology, 70, pp.689-736.

Evans, M. E., and Hamilton, T. S. 1980. Paleomagnetic results from a Late Tertiary-Quaternary volcano in northern British Columbia. EOS, Transactions of the American Geophysical Union, 61, p.218.

Fengor, M. 1981. Pedology, Fauna and Climate of the Level Mountain Range, northern British Columbia. In

preparation.

Ferrara, G., and Treuil, M. 1974. Petrological implications of trace element and strontium isotope distributions in basalt-pantellerite series. *Bulletin Volcanologique*, 88, pp.548-574.

Fiesinger, D. W. 1975. Petrology of the Quaternary volcanic centres in the Quesnel Highlands and Garibaldi provincial park areas, British Columbia. Ph.D. thesis, Department of Geology, University of Calgary, Calgary.

Fiesinger, D. W., and Nicholls, J. 1977. Petrography and Petrology of Quaternary volcanic rocks, Quesnel Lake region, east-central British Columbia. In *Volcanic Regimes in Canada*. Geological Association of Canada Special paper no.16 pp.25-38. Edited by W. R. A. Barager, L. C. Coleman and J. M. Hall.

Fisher, R. A. 1953. Dispersion on a sphere. *Proceedings of the Royal Society of London, Series A*, 217, pp.295-305.

Fitton, J. G., and Gill, R. C. O. 1970. The oxidation of ferrous iron in rocks during mechanical grinding. *Geochimica et Cosmochimica Acta*, 34, pp.518-524.

Flanagan, F. J. 1973. Values for international geochemical reference samples (1972). *Geochimica et Cosmochimica Acta*, 37, pp.1189-1200.

Fleet, M. E. 1974. Mg and Fe^{2+} site occupancies in coexisting pyroxenes. *Contributions to Mineralogy and Petrology*, 44, pp.207-214.

Fleet, M. E. 1974. Partition of Mg and Fe^{2+} in coexisting pyroxenes. *Contributions to Mineralogy and Petrology*, 44, pp.251-257.

French, W. J. 1971. The correlation between anhydrous crystallization temperatures and rock compositions. *Contributions to Mineralogy and Petrology*, 31, pp.154-158.

Frey, F. A. 1980. Evidence for heterogeneous primary MORB and mantle sources, NW Indian Ocean. *Contributions to Mineralogy and Petrology*, 74, pp.387-403.

Fudali, R. F. 1965. Oxygen fugacities of basaltic and andesite magmas. *Geochimica et Cosmochimica*

Acta, 29, pp.1063-1075.

Fujii, T., and Takahashi, E. 1978. On the solubility of alumina in orthopyroxene coexisting with olivine and spinel in the system MgO-Al₂O₃-SiO₂. Mineralogical Journal, 8, pp.122-128.

Fujii, T., and Scarfe, C. M. 1981. Petrology of ultramafic nodules from Boss Mountain, central British Columbia. Geological Association of Canada/Mineralogical Association of Canada, abstracts of Calgary meeting.

Fujii, T. Scarfe, C. M., and Hamilton, T. S. 1981. Geochemistry of ultramafic nodules from southern British Columbia: evidence for banding on the upper mantle. Geological Association of Canada/Mineralogical Association of Canada, abstracts of Calgary meeting.

Fulton, R. J. 1975. Quaternary geology and geomorphology, Nicola-Vernon area, British Columbia. Geological Survey of Canada, Memoir no.380.

Gabrielse, H., and Wheeler, J. O. 1961. Tectonic framework of southern Yukon and northwestern British Columbia. Geological Survey of Canada, paper no. 60-24.

Gabrielse, H., and Souther, J. G. 1962. Dease Lake, British Columbia map-area. Geological Survey of Canada Map 21-1962.

Garland, G. D., and Tanner, J. G. 1957. Investigations of gravity and isostasy in the southern Canadian Cordilleria. Publications of the Royal Dominion Observatory, 19, part5, pp.69-222.

Gass, I. G., and Mallick, D. I. J. 1968. Jebel Khariz: an upper Miocene strato volcano of comenditic affinity on the S. Arabian coast. Bulletin Volcanologique, 32, pp.33-38.

Ghent, E. D., Nicholls, J., Stout, M. Z., and Rotenfusser, B. 1977. Clinopyroxene amphibolite boudins from Three Valley Gap, B.C. Canadian Mineralogist, 15, pp.269-282.

Ghiorso, M.S., and Carmichael, I. S. E. 1980. A regular solution model for met-aluminous silicate liquids. Contributions to Mineralogy and Petrology, 71, pp.323-343.

Gibson, I. L. 1972. The chemistry and petrogenesis of a

suite of pantellerites from the Ethiopian Rift. Journal of Petrology, 13, pp.31-44.

Gibson, I. L. 1974. A review of the geology, petrology and geochemistry of the volcano Fant'ale. Bulletin Volcanologique, 38, pp.791-803.

Gilbert, M. C. 1969. High pressure stability of acmite. American Journal of Science (Schairer volume), 267 A, pp.145-159.

Goldich, S. S., Ingamells, C. O., Thaemletzd, p. 1959. The chemical composition of Minnesota Lake marl: a comparison of rapid and conventional chemical methods. Economic Geology, 54, pp.285-300.

Goldschmidt, V. M. 1937. The principle of distribution of chemical elements in minerals and rocks. Journal of the Chemical Society, pp.655-672.

Goles, G. G. 1976. Some constraints on the origin of the phonolites from the Gregory Rift, Kenya and inferences concerning basaltic magmas in the rift system. Lithos, 9, pp.1-8.

Gornostayev, V. P. 1972. On the deep geoelectric model of Pribaikalye. Geol. Geofiz., 6, pp.98-101.

Grant, F. S., and West, G. F. 1965. Interpretation Theory and Applied Geophysics. McGraw-Hill, New York.

Green, D. H., and Ringwood, E. A. 1967. The genesis of basaltic magmas. Contributions to Mineralogy and Petrology, 15, pp.103-190.

Green, H. W. 1976. Plasticity of olivine in peridotites. In Electron microscopy in mineralogy. Edited by H. R. Wenk, Springer-Verlag, New York.

Green, N. L. 1977. Multistage andesite genesis in the Garibaldi Lake area, southwestern B.C. Ph.D. thesis, Department of Geology, University of British Columbia, Vancouver.

Grow, J. A., and Atwater, T. 1970. Mid-Tertiary tectonic transition in the Aleutian ARC. Geological society of America Bulletin, 81, pp.3715-3722.

Hakli, T. A., and Wright, T. L. 1967. The fractionation of nickel between olivine and augite as a geothermometer. Geochimica et Cosmochimica Acta, 31, pp.877-884.

Halley, E. 1692. An account of the cause of the change of

the variation of the magnetic needle; with an hypothesis of the structure of the internal part of the earth. Philosophical Transactions of the Royal society, 17, pp.563-578.

Hamilton, D. L., and MacKenzie, W. S. 1965. Phase equilibration studies in the system Ne-Kal-Qtz-H₂O. Mineralogical Magazine, 34, pp.214-231.

Hamilton, T. S. 1979. The geology of claim blocks Fission 100-1000, Grizzly Hills Provincial forest. B.C. Department of Mines open file report for 1977.

Hamilton, T. S. 1981. The Level Mountain range and late Cenozoic volcanism in the Stikine. Abstract, February Geological Association of Canada Cordilleran Section Meeting, pp.22-23.

Hamilton, T. S., and Baadsgaard, H., and Scarfe, C. M. 1978. Petrogenesis of late Cenozoic volcanics, Level Mountain, northern British Columbia. Geological Association of Canada/Mineralogical Association of Canada/Geological Society of America programme abstracts, 10, pp.414-415.

Hamilton, T. S., and Muehlenbachs, K. 1977. The ¹⁸O geochemistry of Cenozoic lavas from the Level Mountain volcanic centre, British Columbia. EOS, America Geophysical Union Transactions, 58, p.1248.

Hamilton, T. S., and Scarfe, C. M. 1976. Cenozoic alkaline lavas from the Level Mountains volcanic centre. Abstracts, Geological Association of Canada/Mineralogical Association of Canada Annual Meeting, 1, p.47.

Hamilton, T. S., and Scarfe, C. M. 1977. Preliminary Report on the Petrology of the Level Mountain volcanic centre, northwestern British Columbia. Geological Survey of Canada, Paper no.77-1A, Report of activities, part A, pp.429-434.

Handin, J. 1966. Strength and Ductility. In Handbook of physical constants, Geological Society of America Memoir No.17, Edited by S. P. Clark.

Harris, N. B. W. 1981. The role of fluorine and chlorine in the petrogenesis of a peralkaline complex from Saudi Arabia. Chemical geology, 31, pp.303-311.

Heinricks, H., Schultz, B., Dobrick, J., and Wedepolil, K. H. 1980. Terrestrial geochemistry of Cd, Bi, Tl,

Pb, Zn, Rb. *Geochimica et Cosmochimica Acta*, 44, pp.1519-1535.

Hertogen, J., and Gijbels, R. 1976. Calculation of trace element fractionation during partial melting. *Geochimica et Cosmochimica Acta*, 40, pp.312,322.

Hervig, R. L. 1981. Dolomite-apatite inclusions in chrome diopside crystal, Bellsbrook kimberlite, South Africa. *American Mineralogist*, 66, pp.346-350.

Herzberg, C. T., and Chapman, N. A. 1976. Clinopyroxene geothermometry of spinel lherzolites. *American Mineralogist*, 61, pp.626,637.

Heirtzler, J. R., Dickson, G. D., Herron, E. M., Pitman, W. C., and LePichon, X. 1968. Marine magnetic anomalies, geomagnetic field reversals and motions of the ocean floor and continents. *Journal of Geophysical Research*, 73, pp.2119-2136.

Hibbard, M. J. 1981. The magma mixing origin of mantled feldspars. *Contributions to Mineralogy and Petrology*, 76, pp.158-170.

Hofmann, A. W., and Hart, S. R. 1978. An assessment of local and regional isotopic equilibrium in the mantle. *Earth and Planetary Science Letters*, 38, pp.44-62.

Hofmann, A. W., and Margaritz, M. 1977. Diffusion of Ca, Sr, Ba and Co in a basalt melt: implications for the geochemistry of the mantle. *Journal of Geophysical Research*, 82, pp.5432-5440.

Holland, H. D. 1972. Granites, solutions and base metal deposits. *Economic Geology*, 67, p.281.

Huebner, J. S. 1971. Research techniques for high pressure and high temperature. In *Solid Phase oxygen Buffers*. edited by G. C. Ulmer.

Hurley, P. M. 1977. Estimates of possible diffusional effects in trace element separations. *Earth and Planetary Science Letters*, 34, pp.225-230.

Irvine, T. N., and Baragar, W. R. A. 1971. A Guide to the Chemical Classification of the Common Volcanic Rocks. *Canadian Journal of Earth Science*, 8, pp.523-549.

Irving, E. 1964. Paleomagnetism and its applications to geological and geophysical problems. John Wiley,

New York.

Irving, E. 1966. The great paleozoic reversal of the geomagnetic field. EOS Transaction of the American Geophysical Union, 47, p.78.

Irving, E., Stott, P. M., and Ward M. A. 1961. Demagnetization of igneous rocks by alternating magnetic fields. Philosophical Magazine, 6 pp.225-241.

Ito, K., and Kennedy, G. C. 1967. Melting and phase relations in a natural peridotite to 40 kilobar. American Journal of Science, 265, pp.519-538.

Jacobs, J. A. 1975. The Earth's Core. Academic Press, New York.

Jackson, E. D. 1969. Chemical variation in coexisting chromite and olivine in the chromite zones of the stillwater complex. Economic Geology Monographs, 4, pp.41-71.

Jessop, A. 1971. The distribution of glacial perturbation of heat flow in Canada. Canadian Journal of Earth Science, 8, pp.162-166.

Jessop, A., and Judge, A. 1971. Five heat flow measurements from Southern Canada. Canadian Journal of Earth Science, 8, pp.711-716.

Jessop, A., and Souther, J. G. 1980. Geothermal measurements in northern B.C. and the southern Yukon. in preparation.

Johnson, S. H., Couch, R. W., Gemperle, M., and Banks, E. R. 1972. Seismic refraction measurements in southeast Alaska and western British Columbia. Canadian Journal of Earth Science, 9, pp.1756-1765.

Johnson, W. A. 1926. The Pleistocene of Cariboo and Cassiar districts, B. C. Royal Society of Canada, 3rd series, 20, pp.137-147.

Kanasewich, E. R. 1966. Deep crustal structure under the plains and Rocky Mountains. Canadian Journal of Earth Science, 3, pp.932-945.

Kawada, K. 1966. Studies of the thermal state of the earth: variation in the thermal conductivity of rocks. Bulletin of Earthquake Research Institute, Tokyo University, 44, pp.1071-1091.

Keen, C. E., and Hyndman, R. D. 1979. Geophysical review of the continental margins of eastern and western Canada. Canadian Journal of Earth Science, 16, pp.712-747.

Kelley, K. K., and King, E. G. 1961. Contributions to the data on theoretical metallurgy. XIV. Entropies of the elements and inorganic compounds. United States Bureau of Mines Bulletin, 592, 149pp.

Kelsey, C. H. and McKie, D. 1964. The unit cell of aenigmatite. Mineralogical Magazine, 33, pp.986-1001.

Kerr, F. A. 1936. The physiography of the Cordilleran region of northern B. C. Royal Society of Canada, 3rd series, 30.

Kiselev, A. I., Golovko, H. A., and Medvedev, M. E. 1978. Petrochemistry of Cenozoic basalts and associated rocks in the Baikal Rift zone. Tectonophysics, 45, pp.49-54.

Klein, C. 1968. Coexisting Amphiboles. Journal of Petrology, 9, pp.281-330.

Komar, P. D. 1972 (a). Mechanical interactions of phenocrysts and flow differentiation of igneous dykes and sills. Geological Society of America Bulletin, 83, pp.973-988.

Komar, P. D. 1972 (b). Flow differentiation in igneous dykes and sills: profiles of velocity and phenocryst concentration. Geological Society of America Bulletin, 83, pp.3443-3448.

Kuno, H., and Aoki, K. I. 1970. Chemistry of ultramafic nodules and their bearing on the origin of basaltic magmas. Physics of Earth and Planetary Interiors, 3, pp.273-301.

Kuno, M. 1973. Geomagnetic polarity changes and the duration of volcanism in successive lava flows. Journal of Geophysical Research, 78, pp.5972-5982.

Kushiro, I., Yono, Y. S., and Akimoto, S. 1968. Melting of a peridotite nodule at high pressures and high water pressures. Journal of Geophysical Research, 73, pp.6023-6029.

Lambert, A., and Caner, B. 1965. Geomagnetic depth-sounding and the coast effect in western Canada. Canadian Journal of Earth Science, 2, pp.485-509.

Langmuir, C. H., Bender, J. F., Bence, A. E., Hanson, G. N., and Taylor, S. R. 1977. Petrogenesis of basalts from the Famous area: Mid Atlantic ridge. *Earth and Planetary Science Letters*, 36, pp.133-156.

Lee, W. H. K., and Clark, S. P. 1966. Heat flow and volcanic temperatures. In *Handbook of Physical Constants*. Geological Society of America Memoir No. 97. pp.483-513.

Leeman, W. P., and Dasch, E. J. 1978. Strontium, lead and oxygen isotope investigation of the Skaergard Intrusion, E. Greenland. *Epsel*, 41, pp.47-59.

Leeman, W. P., Vitaliano, C. J., and Prinz, M. 1976. Evolved lavas from the Snake River Plain, Craters of the Moon National Monument, Idaho. *Contributions to Mineralogy and Petrology*, 56, pp.35-60.

LePichon, X., and Heirtzler, J. R. 1968. Magmatic anomalies in the Indian Ocean and sea floor spreading. *Journal of Geophysical Research*, 73, pp.2101-2117.

Lindsley, D. H. 1971. Synthesis and preliminary results on the stability of aenigmatite. *Carnegie Institute of Washington Yearbook*, 70, pp.188-190.

Lindsley, D. H., and Dixon, S. A. 1976. Diopside - enstatite equilibria at 850-1400°C, 5 to 35 kilobars. *American Journal of Science*, 276, pp.1285-1301.

Lindsley, D. H., and Haggerty, S. E. 1971. Phase relations of Fe-Ti oxides and aenigmatite; oxygen fugacity of the Pegmatoid zones. *Carnegie Institute of Washington Yearbook*, 70, pp.278-284.

Lloyd, F. E., and Bailey, D. K. 1975. Light element metasomatism of the continental mantle: The evidence and the consequences. *Physics and Chemistry of the Earth*, 9, pp.389-416.

Liotard, J. M., Verniers, J., and Dupuy, C. 1979. Variabilite des valeurs de coefficient de partage: influence de la structure des liquides magmatiques. *Chemical Geology*, 26, pp.237-247.

Littlejohn, A. L., and Greenwood, H. J. 1974. Lherzolite nodules in basalts from British Columbia, Canada. *Canadian Journal of Earth Science*, 11, pp.1288-1308.

Lovering, J. F. 1966. Electron microprobe analysis of chlorine in two pantellerites. *Journal of*

Petrology, 7, pp.65-67.

Lowry, R.K. 1981. Comment concerning experimental data on diffusion of major elements between glasses or liquids with basaltic rhyolitics and phenolitic compositions. Earth and Planetary Science Letters, 52, pp.221-222.

Maaloe, S. 1973. T-P relations of ascending primary magmas. Journal of Geophysical Research, 78, p.6877.

MacDonald, G. A., and Katsura, T. 1964. Chemical composition of Hawaiian lavas. Journal of Petrology, 5, pp.82-113.

MacDonald, R. 1974 (a). Tectonic settings and magma associations. Bulletin Volcanologique, 38, pp.575-594.

MacDonald, R. 1974 (b). Nomenclature and petrochemistry of the peralkaline oversaturated extrusive rocks. Bulletin Volcanologique, 38, pp.498-517.

MacDougall, K., Saemundsson, K., Johannesson, H., Watkins, N. D., and Kristjansson, L. 1977. Extension of the geomagnetic polarity time scale to 6.5MY. K-Ar dating, geological and paleomagnetic study of a 3,500m lava succession in W. Iceland. Geological Society of America Bulletin, 88, pp.1-15.

MacGregor, I. D. 1974. The system MgO-Al₂O₃-SiO₂: the solubility of Al₂O₃ in enstatite for spinel and garnet peridotite compositions. American Mineralogist, 59, pp.110-119.

Malkus, W. V. R. 1968. Precession of the earth as a cause of geomagnetism. Science, 160, pp.259-264.

Mankinen, E. A., and Dalrymple, B. G. 1979. Revised geomagnetic polarity time scale for the interval 0-5MYBP. Journal of Geophysical Research, 84, pp.615-626.

Manning, D. A. C. 1981. The effect of fluorine on liquidus phase relationships in the system Qz-Ab-Or with excess water at one kilobar. Contributions to Mineralogy and Petrology, 76, pp.206-215.

Manning, D. A. C., Hamilton, E. L., Henderson, C. M. B., and Dempsey, M. J. 1980. The probable occurrence of interstitial Al in hydrous fluorine bearing and fluorine free aluminosilicate melts. Contributions to Mineralogy and Petrology, 75,

pp.257-262.

Margaritz, M., Whitford, D. J., and James, D. E. 1978. Oxygen isotopes and the origin of high $^{87}\text{Sr}/^{86}\text{Sr}$ andesites. *Earth and Planetary Science Letters*, 40, pp.220-230.

Marsh, J. S. 1975. Aenigmatite stability in silica undersaturated rocks. *Contributions to Mineralogy and Petrology*, 50, pp.134-144.

Marsh, B. D., and Kantha, L. H. 1978. On heat and mass transfer from an ascending magma. *Earth and Planetary Science Letters*, 39, pp.435-443.

Mathez, E. A. 1973. Refinement of the Kudo-Weill plagioclase thermometer and its application to the basaltic rocks. *Contributions to Mineralogy and Petrology*, 41, pp.61-72.

Matsuhisa, Y. 1973. Oxygen isotope variation in magmatic differentiation processes of volcanic rocks of Japan. *Contributions to Mineralogy and Petrology*, 39, pp.277-288.

Matsuhisa, Y., Goldsmith, J. R., and Clayton, R. N. 1979. Oxygen isotope fractionation in the system Q-Ab-An-H₂O. *Geochimica et Cosmochimica Acta*, 43, pp.1131-1140.

Matsui, Y., Onuma, N., Nagasawa, H., Higuchi, H., and Banno, S. 1977. Crystal structure control in trace element partition among crystals and magma. *Bulletin of the Society of Mineralogy and Crystallography*

McBirney, A. R. 1963. Conductivity variations and terrestrial heat flow variation. *Journal of Geophysical Research*, 68, pp.6323-6329.

McBirney, A. R. 1969. Proceedings of the andesite conference. *Oregon Department of Mines Bulletin*, 65, pp.175-184.

McBirney, A. R., and Williams, H. 1969. Thermal aspects of the generation and rise of magmas. In *Geology of Galapagos Islands*. *Geological Society of America Memoir No. 118*, pp.180-194.

McDougall, I., and Chamalaun, F. H. 1966. Geomagnetic polarity scale of time. *Nature*, 5060, p.1415.

McDougall, I., Saemundsson, K., Johannesson, H., Watkins, N. D., and Kristjansson, L. 1977. Extension of the

geomagnetic polarity time scale to 6.5MY: K-Ar dating, geological and paleomagnetic study of a 3500m lava succession in W. Iceland. Geological Society of America Bulletin, 88, pp1-15.

McElhinney, M. W. 1973. Paleomagnetism and Plate Tectonics. Cambridge University Press.

McElhinney, M. W., and Merrill, R. T. 1975. Geomagnetic secular variation over the past 5MY. Reviews of Geophysics and Space Physics, 13, pp.687-708.

McIntire, W. L. 1963. Trace element partition coefficients, a review of theory and applications to geology. Geochimica et Cosmochimica Acta, 27, pp.1209-1264.

Mercier, J. C. C., and Nicolas, A. 1975. Textures and fabrics of upper mantle peridotites as illustrated by xenoliths from basalts. Journal of Petrology, 16, pp.454-487.

Millhollen, G. L. Irving, I. J., and Wyllie, P. J. 1974. Melting interval of peridotite with 5.7% H₂O to 30kilobars. Journal of Geology, 82, pp.575-587.

Milne, W. G. 1963. Seismicity of Western Canada. Boletin Bibliografico de Geofisica y Oceanographia Americanas, 3, pp.17-40.

Milne, W. G., Rogers, G. C., Riddihough, R. P., McMechan, G. A., and Hyndman, R. D. 1978. Seismicity of Western Canada. Canadian Journal of Earth Science, 15, pp.1170-1193.

Milne, W. G., Smith, W. E. T., and Rogers, G. C. 1970. Canadian seismicity and micro-earthquake research in Canada. Canadian Journal of Earth Science, 7, pp.591-601.

Minster, J. F., Minster, J. B., Allegre, C. J., and Treuil, M. 1977. Systematic use of trace elements in igneous processes. II. Inverse problem of the fractional crystallization process in volcanic suites. Contributions to Mineralogy and Petrology, 61, p.49.

Monger, J. W. H. 1968. Early Tertiary stratified rocks. Greenwood map area (82 E/2). Geological Survey of Canada paper no.67-42.

Monger, J. W. H., and Irving, E. 1980. Northward displacement of north-central British Columbia. Nature, 285, pp.289-293.

Monger, J. W. H., and Price, R. A. 1979. Geodynamic evolution of the Canadian Cordillera - progress and problems. *Canadian Journal of Earth Science*, 16, pp770-791.

Monger, J. W. H., Souther, J. G., and Gabrielse, H. 1972. Evolution of the Canadian Cordillera. *American Journal of Science*, 272, pp.577-602.

Mori, T. 1977. Geothermometry of spinel lherzolites. *Contributions to Mineralogy and Petrology*, 59, pp.261-279.

Mori, T., and Green, D. H. 1975. Pyroxenes in the system Mg_2SiO_4 - $CaMgSi_2O_6$ at high pressure. *Earth and Planetary Science Letters*, 26, pp.277-286.

Mori, T., and Green, D. H. 1976. Sub solidus equilibria between pyroxenes in the CaO - MgO - SiO_2 system at high pressures and temperatures. *American Mineralogist*, 61, pp.616-625.

Mori, T., and Green, D. H. 1978. Laboratory duplication of phase equilibria observed in natural garnet lherzolites. *Journal of Geology*, 86, pp.83-97.

Muehlenbachs, K., Anderson, A. T., and Sigvaldason, G. E. 1974. Low- ^{18}O basalts from Iceland. *Geochimica et Cosmochimica Acta*, 38, pp577-588.

Muehlenbachs, K., and Clayton, R. N. 1972. Oxygen isotope studies of fresh and weathered basalts. *Canadian Journal of Earth Science*, 9, pp.172-184.

Muehlenbachs, K., and Stone, G. T. 1973. Oxygen isotope compositions of some basaltic lavas from the Snake River plain. *Carnegie Institute of Washington Yearbook*, 72, pp.598-601.

Murase, T., and McBirney, A. R. M. 1973. Properties of some common igneous rocks and their melts at high temperatures. *Geological Society of America Bulletin*, 84, pp.3563-3592.

Murthy, G. S. Paleomagnetic studies in the Canadian shield. Ph.D. thesis, Department of Physics, University of Alberta, Edmonton.

Mysen, B. O. 1975. Partitioning of Fe and Mg between crystals and partial melts in a peridotite upper mantle. *Contributions to Mineralogy and Petrology*, 52, pp.69-76.

Mysen, B. O., and Boettcher, A. L. 1975. Melting of a

hydrous mantle I and II. *Journal of Petrology*, 16, pp.520-593.

Mysen, B. O., and Kushiro, I. 1979. Pressure dependance of Ni partitioning between forsterite and aluminous silicate melts. *Earth and Planetary Science Letters*, 42, pp.383-388.

Mysen, B. O., Virgo, D., and Scarfe, C. M. 1980. Relations between the anionic structure and viscosity of silicate melts - a raman spectroscopic study. *American Mineralogist*, 65, pp.690-710.

Nagata. T. 1961. Rock Magnetism. Mazuren press, Tokyo.

Naney, M. T., and Swanson, S. E. 1980. The effect of Fe and Mg on crystallization in granitic systems. *American Mineralogist*, 65, pp.639-654.

Nash, W. P., Carmichael, I. S. E., and Johnson, R. W. 1969. The mineralogy and petrology of Mount Suswa, Kenya. *Journal of Petrology*, 10, pp.409-439.

Nash, W. P., and Evans, J. H. 1977. Natural silicic liquids, fugacities and flow. *Abstracts, Geological Association of America meeting*, Seattle, p.110.

Neir, A. O. 1947. A mass spectrometer for isotope and gas analyses. *Review of Scientific Instruments*, 18, pp.398-411.

Neumann, H., Mead, J., and Vitaliano, C. J. 1954. Trace element variation during fractional crystallization as calculated from the distribution law. *Geochimica et Cosmochimica Acta*, 6, pp.90-00.

Nicholls, J. 1980. A simple thermodynamic model for estimating the solubility of H_2O in magmas. *Annales de Geophysique*, 36, p.211.

Nicholls, J., and Carmichael, I. S. E. 1969. Peralkaline acid liquids: a petrologic study. *Contributions to Mineralogy and Petrology*, 20, pp.268-294.

Nicholls, J., and Carmichael, I. S. E. 1972. The equilibration temperature and pressure of various lava types with spinel and garnet peridotite. *American Mineralogist*, 57, pp.941-959.

Nicholls, J., Carmichael, I. S. E., and Stormer, J. C. 1971. Silica Activity and P(total) in igneous rocks. *Contributions to Mineralogy and Petrology*, 33,

pp.1-20.

Nicholls, J., Stout, M. Z., and Fiesinger, D. W. 1981. Petrologic variations in Quaternary volcanic rocks, British Columbia, and the underlying upper mantle. In press.

Nicholls, J., Stout, M. Z., and Ghent, E. D. 1976. Petrology and basanite and trachy basalt lavas, western British Columbia. EOS American Geophysical Union Transactions, 57, p.1018.

Nixon, P. H., Rogers, N. W., Gibson, I. L., and Grey, A. 1981. Depleted and fertile mantle xenoliths from South African kimberlites. Annual Reviews of Earth and Planetary Science, 9, pp.285-309.

Noble, D. C. 1965. Gold Flat member of Thirsty Canyon Tuff - a pantellerite ash flow sheet in southern Nevada. U.S.G.S. Professional paper 525-B, pp.85-90.

Noble, D. C. 1967. Sodium, potassium and ferrous iron contents of some secondarily hydrated natural silicic glasses. American Mineralogist, 52, pp.280-286.

Noble, D. C. 1968. Systematic variation of major elements in comendite and pantellerite glass. Earth and Planetary Science Letters, 4, pp.167-172.

Noble, D. C., and Haffty, J. 1969. Minor element and some revised major element content of some Mediterranean pantellerites and comendites. Journal of Petrology, 10, pp.502-509.

Noble, D. C., and Parker, D. F. 1974. Peralkaline silicic volcanic rocks of the western United States. Bulletin Volcanologique, 38, pp.803-828.

Obata, M. 1976. The solubility of Al_2O_3 in orthopyroxenes in spinel and plagioclase peridotites and spinel pyroxenite. American Mineralogist, 61, pp.804-816.

O'Neill, J. R. 1977. Stable isotopes in mineralogy. Physics and Chemistry of Minerals, 2, pp.105-123.

O'Neill, J. R., and Taylor, H. P. 1967. Oxygen isotope and cation exchange chemistry of feldspars. American Mineralogist, 52, pp.1414-1437.

Onuma, N., Higuchi, H., Wakita, H., and Nagasawa, H. 1968. Trace element partition between two pyroxenes

and the host lava. *Earth and Planetary Science Letters*, 5, pp.47-51.

Osborn, E. F. 1942. The system CaSiO₃-diopside-anorthite. *American Journal of Science*, 240, pp.751-788.

Ostensoe, E. 1960. Level Mountain, northwestern British Columbia. B.Sc. thesis, Department of Geology, University of British Columbia, Vancouver.

Parrish, R. 1981. Cenozoic uplift history of the coast mountains of British Columbia. Abstract, Geological Association of Canada, Cordilleran section meeting, Vancouver, p.30.

Pearce, J. A., and Cann, J. R. 1973. Tectonic setting of basic volcanic rocks determined using trace element analyses. *Earth and Planetary Science Letters*, 19, pp.290-300.

Pearce, J. A., and Norry, M. J. 1979. Petrogenetic implications of Ti, Zr, Y, and Yb variations. *Contributions to Mineralogy and Petrology*, 69, pp.33-47.

Peters, L. J. 1949. The direct approach to magnetic interpretation and its practical implications. *Geophysics*, 14, pp.290-320.

Philpotts, J. A., and Schnetzler, C. C. 1970. Phenocryst-matrix partition coefficients for K, Rb, Sr and Ba with applications to anorthosite and basalt genesis. *Geochimica et Cosmochimica Acta*, 34, pp.307-322.

Philpotts, J. A. 1978. The law of constant rejection. *Geochimica et Cosmochimica Acta*, 42, pp.909-920.

Pinson, R. H., and Smith, D. G. W. 1975. The development of carbonate bearing biotite isograd assemblages from Tete Jaune Cache, B.C. *Canadian Mineralogy*, 13, pp.151-161.

Piotrowski, J. M., and Edgar, A. D. 1970. Melting relations on undersaturated alkaline rocks from Greenland, Africa, and Canada. *Medd. om. Gronland*, 181, p.66.

Piwnski, A. J. 1973. Experimental studies of igneous rock series central Sierra Nevada batholith, California, Part II. N. Jb. Miner. Mh. pp.193-215.

Pollack, H. N., and Chapman, D. S. 1977. Mantle heat flow.

Earth and Planetary Science Letters, 34,
pp.174-184.

Presnall, D. C. 1976. Alumina content of enstatite as a
geobarometer for plagioclase and spinel
lherzolites. American Mineralogist, 61,
pp.582-588.

Presnall, D. C. 1980. A double partial melt zone in the
mantle beneath Mid ocean Ridge. Physics of Earth
and Planetary Interiors, 23, pp.103-111.

Price, R. C., and Chappell, B. W. 1975. Fractional
crystallization and the petrology of Dunedin
volcano. Contributions to Mineralogy and
Petrology, 53, pp.157-182.

Ranalli, G. 1980. Rheological properties of the upper mantle
in Canada from olivine microrheology. Canadian
Journal of Earth Sciences, 17, pp.1499-1505.

Reed, S. J. B., and Ware, N. G. 1975. Quantitative electron
microprobe analysis of silicates using energy
dispersive X-Ray spectrometry. Journal of
Petrology, 16, pp.499-519.

Reitmayr, G. 1975. An anomaly of the upper mantle below the
Rhinegraben studied by the inductive response of
natural electromagnetic fields. Journal of the
Royal Astronomical Society, 41, pp.651-658.

Riddihough, R. P. 1977 A model for recent plate interactions
off Canada's west coast. Canadian Journal of
Earth Science, 14, pp.384-396.

Riddihough, R. P. 1981. Major plate interactions affecting
the Canadian Cordillera over the last 100 Ma:
constraints and uncertainties. Abstracts,
Geological Association of Canada, Cordilleran
section meeting, Vancouver, p.33.

Ridley, K. J. 1975. The non-reproducibility of chemical
analyses on reference rock standards and an
evaluation of the cause of the problem. M.Sc.
thesis, Department of Geology, University of
Windsor, Windsor, Ontario.

Ridley, W. I. 1970. The petrology of Las Canadas volcanoes,
Tenerife, Canary Islands. Contributions to
Mineralogy and Petrology, 26, pp.124-160.

Robie, R. A., Hemmingway, B. S., and Fisher, J. R. 1978.
Thermodynamic properties of minerals and related
substances at 298.15°K and 1Bar (10^5 pascals)

pressure and at higher temperatures. Geological Survey Bulletin 1452.

Roebroeck, E. J., and Nyland, E. 1975. P-Wave residuals in western Canada. Canadian Journal of Earth Science, 12, pp.174-181.

Roedder, E. 1965. Liquid CO₂ inclusions in olivine bearing nodules and phenocrysts from basalts. American Mineralogist, 50, pp.1746-1782.

Roy, R. F., Blackwell, D. D., and Birch, F. 1968. Heat generation of plutonic rocks and continental heat flow provinces. Earth and Planetary Science Letters, 5, pp.1-12.

Rucklidge, J. C., Gibb, F. G., Fawcett, J. J., and Gasparini, E. L. 1970. Rapid rock analysis by microprobe. Geochimica et Cosmochimica Acta, 34, pp.245-247.

Russell, R. D. 1972. Evolutionary model for lead isotopes in conformable ores and in ocean volcanics. Reviews of Geophysics and Space Physics, 10, p.529.

Scarf, C. M. 1973. Viscosity of basic magmas at varying pressure. Nature, 241, pp.101-102.

Scarf, C. M. 1977. Viscosity of a pantellerite melt at one atmosphere. Canadian Mineralogist, 15, pp.185-189.

Scarf, C. M., and Hamilton, T. S. 1980. Viscosity of lavas from the Level Mountain volcanic centre, northern British Columbia. Carnegie Institute of Washington Institute Yearbook, 79, pp.318-320.

Scarf, C. M., Mysen, B. O., and Rai, C. S. 1979. Invariant melting behavior of mantle material: partial melting of two lherzolite nodules. Carnegie Institute of Washington Yearbook, 78, pp.498-501.

Scarf, C. M., Paul, D. K., and Harris, P. G. 1972. Melting experiments at one atmosphere on two ultramafic nodules. N. Jb. Min. Mb., 10, pp.469-476.

Schairer, J. F., and Bowen, N. L. 1955. The system K₂O-Al₂O₃-SiO₂. American Journal of Science, 253, pp.681-746.

Schairer, J. F., and Bowen, N. L. 1956. The system Na₂O-Al₂O₃-SiO₂. American Journal of Science, 254, pp.129-195.

Schilling, J. G. 1973. Iceland mantle plume: geochemical study of Reykjanes Ridge. *Nature*, 242, pp.565-575.

Schimann, K., and Smith, D. G. W. 1980. The optical fusion of whole rock powder and their analysis by an electron microprobe technique. *Canadian Mineralogist*, 18, pp.131-143.

Schmincke, H. U. 1974. Volcanological aspects of peralkaline silicic welded ash flow tuffs. *Bulletin Volcanologique*, 38, pp.594-637.

Seitz, M. G. 1973. U and Th partitioning in diopside-melt and whitlockite- melt systems. *Carnegie Institute of Washington Yearbook*, 72, p.581.

Self, S., and Gunn, B. M. 1976. Petrology, volume and age relations of alkaline and saturated peralkaline volcanics from Terceria, Azores. *Contributions to Mineralogy and Petrology*, 54, pp.293-313.

Shand, S. J. 1927. *The Eruptive Rocks*. Wiley, New York.

Shandley, P. D., and Bacon, L. O. 1963. Abstracts, Society of Exploration Geophysicists New Orleans meeting.

Shaw, D. M. 1961. Element distribution laws in geochemistry. *Geochimica et Cosmochimica Acta*, 23, p.116.

Shaw, H.R. 1963. Obsidian - H₂O viscosities at 1000 and 2000 bars in the temperature range 700 to 900°C. *Journal of Geophysical Research*, 68, pp.6337-6343.

Shaw, H. R. 1965. Comments on viscosity, crystal settling and convection in granitic magmas. *American Journal of Science*, 263, pp.120-152.

Shaw, H. R. Rheology of basalt in the melting range. *Journal of Petrology*, 10, pp.510-535.

Shaw, H. R. 1972. Viscosity of magmatic silicate liquids. *American Journal of Science*, 272, pp.870-893.

Sinclair, P. D., Templeman-Kluit, D. J., and Medaris, L. G. 1977. Lherzolite nodules from a Pleistocene cinder cone in central Yukon. *Canadian Journal of Earth Science*, 15, pp.220-226.

Skiles, D. D. 1972. The laws of reflection and refraction of incompressible magnetohydrodynamic waves in a fluid-solid interface. *Physics and Chemistry of*

Planetary Interiors, 5 p.90.

Skinner, B. J. 1962. Thermal expansion of ten minerals. U. S. G. S. Professional paper 450D, pp.109-112.

Skinner, B. J. 1966. Thermal expansion. In *Handbook of Physical Constants*. Geological Society of America Memoir No.97, pp.75-97.

Sleep, N. H. 1974. Separation of magma from a mostly crystalline mush. *Bulletin of the Geological Association of America*, 85, pp.1225-1232.

Smith, D. G. W. 1976. Mineralogical Association of Canada Short Course in Microbeam Techniques.

Smith, D. G. W., and Gold, C. M. 1979. EDATA2: A Fortran IV computer program for processing wavelength and/or energy dispersive electron microprobe analyses. In *Microbeam Analyses*. Edited by D. E. Newbury, San Francisco Press.

Smith, P. J., and Needham, J. 1967. Magnetic declination in medieval China. *Nature*, 214, p.1213.

Sobolev, N. V. 1977. Deep-seated inclusions in kimberlites and the problem of the compositions of the upper mantle.

Soga, N. 1967. Elastic constants of garnet under pressure and temperature. *Journal of Geophysical Research*, 72, pp.4227-4234.

Sorenson, H. 1970. Internal structures and geological setting of three agpaitic intrusions: Khibina and Lovozero of the Kola Peninsula and Ilimaussaq, S. Greenland. *Canadian Mineralogist*, 10, pp.299-334.

Souther, J. G. 1967. Acid volcanism and its relationship to recent crustal movements in the Canadian Cordillera. *Bulletin Volcanologique*, 40, pp.161-176.

Souther, J. G. 1970. Volcanism and its relationship to recent crustal movements in the Canadian Cordillera. *Canadian Journal of Earth Science*, 7, pp.553-568.

Souther, J. G. 1971. Geology and mineral deposits of Tulsequah map-area, British Columbia, Geological Survey of Canada, Memoir no.362.

Souther, J. G. 1977 (a). Volcanism and tectonic environments

in the Canadian Cordillera - a second look. In Volcanic regimes in Canada. Geological Association of Canada Special Paper, volume 16, pp.3-24.

Souther, J. G. 1977 (b). Late Cenozoic volcanism and tectonics of the west central Cordillera of North America. Abstracts, Geological Association of America, Seattle meeting, p.1185.

Souther, J. G., and Armstrong, J. E. 1966. North-central belt of the Cordillera of British Columbia. Canadian Institute of Mining Special, 8, pp.171-184.

Souther, J. G., and Symons, D. T. A. 1974. Stratigraphy and paleomagnetism of Mount Edziza volcanic complex, northwestern British Columbia. Geological Survey of Canada Paper 73-32.

Sparks, R. S. J., and Pinkerton, H. 1978. Effect of degassing on rheology of basaltic lava. Nature, 276, pp.385-386.

Sparks, R. S. J., Pinkerton, H., and MacDonald, R. 1977. The transport of xenoliths in magmas. Earth and Planetary Science Letters, 35, pp.234-238.

St.Armand, P. 1957. Geological and geophysical synthesis of the tectonics of portions of British Columbia, the Yukon and Alaska. Bulletin of Geological Society of America, 68, pp.1343-1370.

Stacey, R. A. 1973. Gravity anomalies, crustal structure and plate tectonics in the Canadian Cordillera. Canadian Journal of Earth Science, 10, pp.615-628.

Stacey, R. A. 1974. Plate tectonics, volcanism and the lithosphere in British Columbia. Nature, 250, pp.133-134.

Stanton, R. L., and Bell, J. D. 1969. Volcanic and associated rocks of the New Georgia group, British Islands Protectorate. Overseas Geological and Mineralogical Research, 10, pp.113-145.

Stocker, R. L., and Gordon, R. B. 1975. Velocity and internal friction in partial melts. Journal of Geophysical Research, 80, pp.4828-4836.

Stroh, J. M. 1975. Late Cenozoic volcanism, Baja California Norte, Mexico. Ph.D. thesis, Geology Department,

University of Washington, Seattle.

Stroh, J. M. Solubility of alumina in orthopyroxene plus spinel as a geobarometer in complex systems: applications to spinel bearing alpine type peridotites. Contributions to Mineralogy and Petrology, 54, pp.173-188.

Stull, D. R., and Prophet, H. 1971. JANAF thermochemical tables. National Standard Reference Data Service, U. S. National Bureau of Standards, 37, p.1141.

Sun, S. S. 1973. Lead isotope studies of young volcanic rocks from Oceanic islands, Mid Ocean Ridges and Island Areas. Ph.D. thesis, Department of Geology, Columbia University, New York.

Sun, S. S., and Hanson, G. N. 1976. Rare earth element evidence for differentiation of McMurdo volcanics, Ross Island, Antarctica. Contributions to Mineralogy and Petrology, 54, pp.139-155.

Sun, S. S., Tatsumoto, M., and Schilling, J. G. 1975. Mantle mixing along the Reykjanes Ridge axis: Pb isotope evidence. Science, 190, p.143.

Sutherland, D. S. 1974. Petrography and mineralogy of peralkaline silicic rocks. Bulletin Volcanologique, 38, pp.517-548.

Symons, D. T. A. 1978. Paleomagnetism of Mesozoic plutons in the western most complex of British Columbia. Canadian Journal of Earth Science, 14, pp.2127-2139.

Takahashi, E., and Kushiro, I. 1981. Melting of a dry peridotite at high pressures and basalt magma genesis. In press.

Takeuchi, H., Fujii, N., and Kikuchi, M. 1972. Mechanism of magma ascent. Zishim. Ser.2 25, pp.266-268.

Tatsumoto, M. 1978. Isotopic composition of lead in Oceanic basalt and its implication to mantle evolution. Earth and Planetary Science Letters, 78, pp.63-87.

Taylor, H. P. 1968. The oxygen isotope geochemistry of igneous rocks. Contributions to Mineralogy and Petrology, 19, pp.1-71.

Thompson, R. N. 1972. Melting behavior of two Snake River

lavas at pressures up to 35kbar. Carnegie Institute of Washington Yearbook, 71, pp.406-410.

Thompson, R. N., and Chisholm, J. E. 1969. Synthesis of Aenigmatite. Mineralogical magazine, 37, pp.253-255.

Thompson, R. N., and Flower, M. F. J. 1971. One atmosphere melting and crystallization relations of lavas from Anjouan, Comores Archipelago, Western Indian Ocean. Earth and Planetary Science Letters, 12, pp.97-107.

Thompson, R. N., and MacKenzie, W. S. 1967. Feldspar-liquid equilibria in peralkaline acid liquids, an experimental study. American Journal of Science, 265, pp.714-734.

Tilley, C. E., Yoder, H. S., and Schairer, J. F. 1964. New relations on melting of basalts. Carnegie Institute of Washington Yearbook, 63, pp.92-97.

Tuma, J. J. 1976. Handbook of Physical Calculations. McGraw-Hill, New York.

Tuttle, O. F. 1958. Origin of granite in the light of experimental studies in the system $\text{NaAlSi}_3\text{O}_8$ - $\text{KAISiO}_3\text{O}_8$ - SiO_2 - H_2O . Geological Society of America memoir No.74.

Urey, H. C. 1947. The thermodynamics of Isotopic Substances. Journal of the Chemical Society, London, pp.562-581.

Vacquier, V., Steenland, N., Henderson, R., and Zeitz, I. 1951. Interpretation of Aeromagnetic maps. Geological Society of America Memoir No. 47.

Varet, J. 1969. Les phonolites agpaitiques et miaskitiques du Cantal septentrional (Auvergne France). Bulletin Volcanologique, 33, pp.621-656.

Varne, R. 1970 Hornblende lherzolite and the upper mantle. Contributions to Mineralogy and Petrology, 27, pp.45-51.

Vestine, E. H. 1967. Main Geomagnetic Field. In *Physics of Geomagnetic Phenomena*. Edited by S. Matsushita and W. H. Campbell. Academic Press, New York.

Vine, F. J., and Hess, H. H. 1970. Sea floor spreading. In *The Sea*. Edited by A. E. Maxwell. Volume 4, pp.587-622.

Vine, F. J., and Mathews, D. H. 1963. Magnetic anomalies over Oceanic Ridges. *Nature*, **199**, p.947.

Virgo, D., Mysen, B. O., Scarfe, C. M., and Sharma, S. K. 1979. Contrasting pressure dependence of the viscosity of silicate melts. *EOS Transactions of the American Geophysical Union*, Spring meeting.

Wolfinger, M., and Robert, J. L. 1980. Structural control of the distribution of trace elements between silicates and hydrothermal solutions. *Geochimica et Cosmochimica Acta*, **44**, pp.1455-1463.

Waff, H. S., and Bulau, J. R. 1979. Equilibrium fluid distribution in an ultramafic partial melt under hydrostatic conditions. *Journal of Geophysical Research*, **84**, pp.6109-6114.

Waff, H. S., and Holdren, G. R. 1980. The nature of grain boundaries in Dunite and lherzolite xenoliths: implications for magma transport in refractory upper mantle material. *EOS Transactions of the American Geophysical Union*, **61**, p.1239.

Waldbaum, D. R. 1971. Temperature changes associated with adiabatic decompression in geological processes. *Nature*, **232**, pp.545-547.

Washington, H. S. 1896. Volcanic rocks of central Italy. *Journal of Geology*, **4**, pp.547-554.

Washington, H. S. 1913. The volcanoes and rocks of Pantelleria. *Journal of Geology*, **21**, pp.653-713.

Washington, H. S. 1914. The volcanoes and rocks of Pantelleria. Part III. Petrology. *Journal of Geology*, **22**, pp.16-27.

Wass, S. Y., and Rogers, N. W. 1980. Mantle metasomatism - precursor to continental alkaline volcanism. *Geochimica et Cosmochimica Acta*, **44**, pp.1811-1823.

Watkins, N. D. 1973. Brunhes epoch geomagnetic secular variation on Reunion Island. *Journal of Geophysical Research*, **78**, p.7763.

Watson, K. D., and Mathews, W. H. 1944. The Tuya-Teslin area, northern British Columbia. *British Columbia Department of Mines, bulletin No. 19*.

Weaver, S. D., Scleal, J. S. C., and Gibson, J. L. 1972. Trace element data relevant to the origin of trachytic and pantelleritic lavas in the East

African Rift system. Contributions to Mineralogy and Petrology, 36, pp.181-194.

Wells, P. R. A. 1977. Pyroxene geothermometry in simple and complex systems. Contributions to Mineralogy and Petrology, 62, pp.129-139.

Wheeler, J. O., and Gabrielse, H. 1972. The Cordilleran structural province. In Variations in Tectonic Styles in Canada. Edited by R. A. Price and R. J. W. Douglas, Geological Association of Canada, special paper no.11, pp.1-81.

White, W. M. 1979. The petrology and geochemistry of the Azores Islands. Contributions to Mineralogy and Petrology, 69, pp.201-214.

White, W. M., Hart, S. R., and Schilling, J. G. 1975. Geochemistry of the Azores and the Mid Atlantic Ridge. Carnegie Institute of Washington Yearbook, 74, pp.224-234.

White, W. M., Tappin, M. D., and Schilling, J. G. 1979. The petrology and geochemistry of the Azores Islands. Contributions to Mineralogy and Petrology, 69, pp.201-213.

White, W. H. 1959. Cordilleran tectonics in British Columbia. Bulletin of the American Association of Petroleum Geologists, 43, pp.60-100.

White, W. H., Bone, M. N., and Milne, W. G. 1968. Seismic refraction surveys in British Columbia, a preliminary interpretation. In The crust and the upper mantle under the Pacific area. American Geophysical Union Monograph no.12, pp.81-93.

White, W. H., and Savage, J. C. 1965. A seismic refraction and gravity study of the earth's crust in British Columbia. Bulletin of the Seismological Society of America, 55, pp.463-486.

Wickens, A. J. 1971. Variations in lithosphere thickness in Canada. Canadian Journal of Earth Science, 8, pp.1154-1162.

Wickens, A. J. 1977. The upper mantle of southern British Columbia. Canadian Journal of Earth Science, 14, pp.1100-1115.

Wickens, A. J., and Buchbinder, G. G. R. 1980. S-wave residuals in Canada. Bulletin of the Seismological Society of America, 70, pp.809-822.

Wilshire, H. G., and Jackson, E.D. 1975. Problems in determining mantle geotherms from pyroxene compositions. *Journal of geology*, 83, pp.313-329.

Wilshire, H. G., and Shervais, J. W. 1974. Al-augite and Cr-diopside ultramafic xenoliths in basaltic rocks from western U. S.: structural and tectonic relationships. *Physics and Chemistry of the Earth*, 9, pp.257-272.

Wilshire, H. G., and Trask, N. J. 1971. Structural and textural relationships of amphiboles and phlogopite in peridotite inclusions, Dish Hill, California. *American Mineralogist*, 56, pp.240-255.

Wilson, R. L. 1970. Permanent aspects of the earth's non-dipole magnetic field over upper Tertiary times. *Geophysical Journal of the Royal Astronomical Society*, 19, pp.417-438.

Wilson, R. L. 1970. Paleomagnetic stratigraphy of Tertiary lavas from northern Ireland. *Geophysical Journal of the Royal Astronomical Society*, 20, p.1

Wilson, R. L. 1971. Dipole offset- the time average paleomagnetic field over the past 25MY. *Geophysical Journal of the Royal Astronomical Society*, 22, pp.491-504.

Wilson, R. L. 1972. Paleomagnetic differences between normal and reversed field sources, and the problem of far sided and right handed pole positions. *Geophysical Journal of the Royal Astronomical Society*, 28, pp.295-304.

Wilson, R. L., Dagley, P., and McCormack, A. G. 1972. Paleomagnetic evidence about the source of the geomagnetic field. *Geophysical Journal of the Royal Astronomical Society*, 28, p. 213.

Wones, D. R., and Gilbert, M. E. 1969. The fayalite - magnetite - quartz assemblage between 600°C and 800°C. *American Journal of Science (Schairer volume)*, 267A, pp.480-488.

Wright, J. B. 1971. The phonolite - trachyte spectrum. *Lithos*, 4, pp.1-5.

Wright, T. L., and Doherty, P. C. 1970. A linear programming and least squares computer method for solving petrologic mixing problems. *Bulletin of the Geological Society of America*, 81, pp.1995-2008.

Wyllie, P. J. 1971. The Dynamic Earth, a textbook in Geosciences. John Wiley and Sons, New York.

Yagi, K. 1966. The system acmite - diopside - and its bearing on the stability relation of natural pyroxenes of the acmite - hedenbergite diopside series. American Mineralogist, 51, pp.976-1000.

Yagi, K., and Souther, J. G. 1974. Aenigmatite from Mount Edziza, British Columbia. American Mineralogist, 59.

Yoder, H. S. 1965. Diopside - anorthite - water at 5 and 10 kilobars and its bearing on explosive volcanism. Carnegie Institute of Washington Yearbook, 64, pp.82-89.

Yoder, H. S. 1973. Contemporaneous basaltic and rhyolitic magmas. American Mineralogist, 58, pp.153-171.

Yoder, H. S. 1976. Generation of basaltic magma. Publication of the National Academy of Science, Washington.

Yoder, H. S., and Tilley, C. E. 1962. Origin of basaltic magmas: an experimental study of natural and synthetic rock systems. Journal of Petrology, 3, pp.342-532.

Yorath, C. J., and Chase, R. L. 1981. Tectonic history of allochthonous terranes: northern Canadian Pacific continental margin. Abstracts, Geological Association of Canada, Cordilleran section meeting, Vancouver.

Zimmerman, C., and Kudo, A. M. 1979. Geochemistry of andesites and related rocks, Rio Grande Rift, New Mexico. In Rio Grande Rift: Tectonics and Magmatism. Edited by R. E. Riecker, American Geophysical Union Publication, pp.355-382.

APPENDIX 1. FIELD AND REMANENCE NOTES ON LEVEL MOUNTAIN
STRATOCONE SECTION

SITE COMMENTS (PB section decreases in elevation to south)

PBT Hawaiite summit of Meszah Peak, map unit 9. Magnetic declination very erratic in site vicinity, possibility of lightening strikes, directions approach selected at different rates from different directions, inhomogeneous magnetization between cores, sister specimens often disagree until cleaned to >800 oersteds. The chosen direction is not a stable endpoint for all cores. The rejected ones were still coming in. Cores 2 through 5 topographically oriented on Nuttlitude cone.

PBS Hawaiite next to highest flow on west shoulder of Meszah Peak between crater and dyke, map unit 9. While three cores approach a common endpoint, cores 4 and 5 do not, indicating the site to be inhomogeneously magnetized.

PBR Hawaiite highest prominent cliff outcrop on West shoulder of Meszah Peak as seen from south side, map unit 9. Abundant xenoliths, all cores approach a common endpoint in 200 to 400 oersted range. Restricting choice to cores 1,2 and 5 at 400 oersteds would improve statistics without changing direction.

PBQ Hawaiite cliff former below PBR map unit 9, abundant xenoliths, all cores approach common endpoint at 200 to 400 oersteds. Restricting choice to cores 1,2 and 5 improves statistics without changing direction. Below this elevation steep slopes, talus and scoria limit available outcrop. Additional section between Q and P could be collected on East face of Meszah Peak with aid of rope work.

PBP Benmoreite map unit 8. Narrow outcrop <3m wide in creek-snow chute on South face of Meszah Peak. Flows at this level are all thin and aside from a few blocky outcrops like this are scoriaceous, many thin trachytes interspersed, frequency decreasing upsection. All cores approach a common endpoint and stay there between 25 and 400 oersteds.

Appendix 1. continued.

PBO Benmoreite map unit 8, lowest blocky outcrop in snow chute, abundant mafic inclusions, below this point talus and scree cover resumes, all cores are stable at a common endpoint from NRM to 800 oersteds. Restricting choice to cores 1,2 and 3 improves statistics without changing direction.

PBN Trachyte lava tube low on south face of Meszah Peak, map unit 7A. All specimens are stable and coincident from NRM to 400 oersteds.

PBM Trachyte ledge, unit 7A at break in slope between lava tubes and tarn, all cores coincident from NRM to 400 oersteds.

PBL Trachyte ledge unit 7A. Site inhomogeneously magnetized probably due to low and variable magnetic mineral content. Cores come in from different directions at different rates. Endpoint somewhat scattered. statistics can be improved without affecting direction by restricting choice to cores 1,2,3 and 4 at 400 oersteds.

PBY Trachyte flow massive columnar jointing, flow 46m thick, unit 7A, cores sampled from separate columns 2/3 of the way up the flow, site is transitional and scattered. No obvious stable endpoint is achieved. Intensity is low and remnance is soft. Statistics can't be much improved unless sample is dropped to 2 cores.

PBK Basal trachyte flow of unit 7A, near base of cliff outcrop formed by PBY. Laterally unit 6 is overlain by fluvioglacial/volcanofluvioglacial sands and gravels. Site is scattered and transitional. Some of scatter could be due to poor coring as all specimens were either in three pieces, short, or hole oriented.

PBJ Basalt, unit 6B. Columnar jointed outcrop forms waterfall, good agreement of all specimens from NRM to 400 oersteds.

PBI Hawaite, unit 6B. Weathering light grey very abundant phenocrysts of plagioclase and black augite, good agreement of all specimens from NRM to 400 oersteds.

PBH Hawaite, unit 6B, with very abundant plagioclase and black augite. Direction chosen as stable endpoint, statistics can be markedly improved without changing direction by eliminating core 3, which comes in more slowly than the others and shows some disagreement between sister specimens, possible hematite and CRM component in core 3.

Appendix 1. continued.

PBG Peralkaline trachyte, unit 6A. Uppermost of three similar flows, all cores agree with good statistics but inclination is very shallow, transitional site.

PBF Peralkaline trachyte, unit 6A. Forms ledge and holds up flat profile in stream valley, phenocrysts of anorthoclase, fayalite and green pyroxene, all specimens agree from NRM to 800 oersteds with shallow inclination, transitional direction.

PBE Peralkaline trachyte flow, unit 6A. Holds up prominent waterfall, peculiar exfoliation textures, good agreement of all specimens but shallow inclination, transitional direction. From this point down only the prominent resistant flows are sampled, tuffs and agglomerates are omitted. Laterally in several places a till is present at this stratigraphic level.

PBD Vesicular brown weathered hawaiite, unit 5B, with plagioclase and augite phenocrysts. All specimens coincide at a shallow inclination transitional direction. These cores all contain appreciable maghemite both as phenocryst alteration and as veins and amygdules.

PBC Amygdaloidal alkali basalt flow, unit 5B. All cores achieve stable endpoints but site is somewhat scattered. Statistics can be improved without affecting direction by eliminating core 3 which was hole oriented.

PBB Alkali basalt with plagioclase and black pyroxene phenocrysts, unit 5B. Site somewhat scattered. Core 2 was eliminated due to inhomogeneity inferred from disagreement between sister specimens.

PBA Hawaite flow, unit 5B, stable endpoint for four specimens

PBX Hawaite rubbly outcrop west of stream cut, unit 5B. No exposure in creek at this point due to lateral moraine of Kakuchuya valley, site is definitely reversed. Eliminating core 2 improves statistics but does not affect direction.

PBU Phonolite flows cooled as a single unit. Slight primary (?) dip down 11° to N 230° E, unit 5A, site is somewhat scattered.

Appendix 1. continued

PBV Phonolite flows, unit 5A. Weak site, all specimens but one have common NRM direction but scatter away randomly by 100 oersteds indicating a soft remnance.

PBW Crystalline comendite flow, unit 5A. Stable direction for all cores from NRM to 100 oersteds.

APPENDIX 2. FIELD AND REMANENCE NOTES ON LEVEL MOUNTAIN PLATEAU SECTION

SITE COMMENTS (Little Tahltan section decreases in elevation to south along E facing cliff)

PAA Alkali basalt flow, map unit 4. Columnar outcrop, local topographic high back from cliff edge, possible lightening strikes, inhomogeneous site all cores approach the chosen endpoint but at different rates. Cores 3 and 5 were rejected as they were still coming in at 400 oersteds but became random by 600.

PAB Alkali basalt flow, map unit 4, 3m thick columnar flow sampled 1m up from base. This was the next prominent outcrop 150m south of PAA, very coherent site, stable from NRM to 400 oersteds.

PAC Hawaite flow, map unit 4, abundant phenocrysts of plagioclase and black clinopyroxene, good site, all cores agree from NRM to 200 oersteds.

PAD Alkali basalt, map unit 4. Site is reversed but scattered, while individual cores attain stable endpoints (1 and 4), there is no common direction. Each core came from a different column and the flow was sampled over a distance of 15m laterally but this is not atypical.

PAE Hawaite map unit 4, very tight site. All cores agree from NRM to 400 oersteds.

PAF Hawaite, map unit 4. No safe access at this point in section so PAF was sampled 300m line of site to the south, good endpoint for all cores 100 to 200 oersteds.

PAG Hawaite, map unit 4. Good endpoint. All specimens stable and coincident from 50 to 400 oersteds.

PAH Hawaite basal columnar flow of map unit 4 rests on yellowish green tuff horizon that delimits units 3 and 4 over much of the southern plateau, stable direction, all cores agree from NRM to 200 oersteds.

PAI Basalt highest major cooling unit of continuous exposure and thickness of unit 3, spheriodially weathering coarse ophitic texture. The five cores here were sampled from only two columns, good site, all cores agree in 100 to 200 oersted range.

APPENDIX 2. continued.

PAJ Alkali basalt, map unit 3, good site, all specimens agree in 100 to 200 oersted range.

PAK Alkali basalt, map unit 3, calcite and zeolites present, rejecting core 5 improves statistics without significantly changing direction.

PAL Alkali basalt, basal flow of 3 that comprises a single columnar cooling unit, forms promontory north of stream notch in cliff. While the overlying section was sampled along 2km of cliff margin, the underlying section follows the stream notch in this cliff and is nearly vertical. All cores for this suite attain a good common endpoint between 100 and 200 oersteds.

PAM Basalt flow with thompsonite and chabazite in fractures. This is third flow down from PAL due to poor access, map unit 3. The intervening flows may contain the transition from the reverse polarity of PAL. The stable endpoint is achieved by all cores at 200 oersteds, the direction is a little shallow making this a transitional site.

PAN Alkali basalt unit 3, lower flow of pair that comprises a single columnar cooling unit immediately below PAM, site somewhat scattered similar shallow reversed direction to PAM, statistics can be improved by restricting choice to cores 2,3 and 5 but direction does not change.

PAO Basalt unit 3, xenocrysts of forsterite and brown spinel, , good site tight distribution for 25 to 400 oersteds on all but core 4, which is consequently rejected.

PAP Basalt columnar outcrop, unit 3, overlies carbonized wood and peat, site reversed and somewhat scattered best agreement in direction at 200 oersteds but core 4 still coming in.

PAQ Alkali basalt, lowest flow in unit 3, upwards to PAP there are two flows and a rubbly Lahar which were not sampled due to poor access on cliff face, this sampling gap coincides with a polarity change, this site is normal with good agreement for all cores above 200 oersteds despite the fact that PAQ is mapped in unit 3 and seems to belong there chemically as well, its magnetic orientation appears to go better with underlying PAR and PAS. The time interval between units 2 and 3 is probably small.

APPENDIX 2. continued

PAR Alkali basalt separated from PAQ by an orange-buff tuff horizon mapped as the unit 2-3 boundary. There is good agreement for all cores by 200 oersteds except #2 which did not have a sun bearing and the two topographic sitings disagreed. This core also did not achieve an endpoint so it should be rejected.

PAS Transitional hawaiite-basalt map unit 2, Two flows between here and PAR were omitted due to cover inside the notch and no access on the cliff face, core 5 had to be rejected because it disagreed with all other cores and was more intensely magnetized by 2 to 3 orders of magnitude, otherwise this is a good site.

PAT Vesicular altered hawaiite (?) flow map unit 2, two flows omitted between here and PAS. From here down cliff exposure required that safety ropes be used during drilling and orientation. This site is quite scattered, all cores achieve endpoints but only 1 and 2 coincide, the site is reversed but probably has a later CRM component related to maghemite alteration as seen petrographically, and in failure of core to saturate even by 5 kilogauss in IRM test.

PAU Basalt, map unit 2, massive columnar flow >5m thick, one flow between here and PAT not sampled, most cores coincide from NRM to 400 oersteds.

PAV Basalt lowest massive flow in map unit 2. This columnar cooling unit is comprised of four individual flows, one cooling unit between here and PAU not sampled. Cores 2 and 3 were drilled through fractures and became broken in several pieces and had to be hole oriented. They scatter somewhat from other 3 cores which show good agreement by 200 oersteds.

PAW Alkali basalt highest cooling unit in map unit 1, the 1 to 2 boundary, mapped at the top of PAW because of distinctive colour and massive appearance of underlying flows. However there is no tuff horizon, paleosol or other obvious time break here. This site has an unusual shallow inclination but is normal compared to adjacent flows above and below. It is also low intensity for basalts, probably represents an excursion since long time break is not inferred.

APPENDIX 2. continued.

PAX Transitional basalt massive cooling unit typical of map unit 1, good agreement for all cores from NRM to 200 oersteds.

PAY Basalt massive basal flow of map unit 1. Below this level there is no further outcrop nearby, only several hundred feet of rubbly cold agglomerates (volcano-fluviatile). The Little Tahltan River here appears to be resequent to a Tertiary stream valley of moderate proportions. Bedrock is porphyry similar to outcrop on Kaketsa Mtn. and of the Sloko volcanics. Although all cores agree with high Fisher k the best direction is probably given by cores 1 and 4 at 100 to 400 oersteds as other cores approach and pass through this region.

APPENDIX 3. REMANENCE DATA FOR LEVEL MOUNTAIN LAVAS

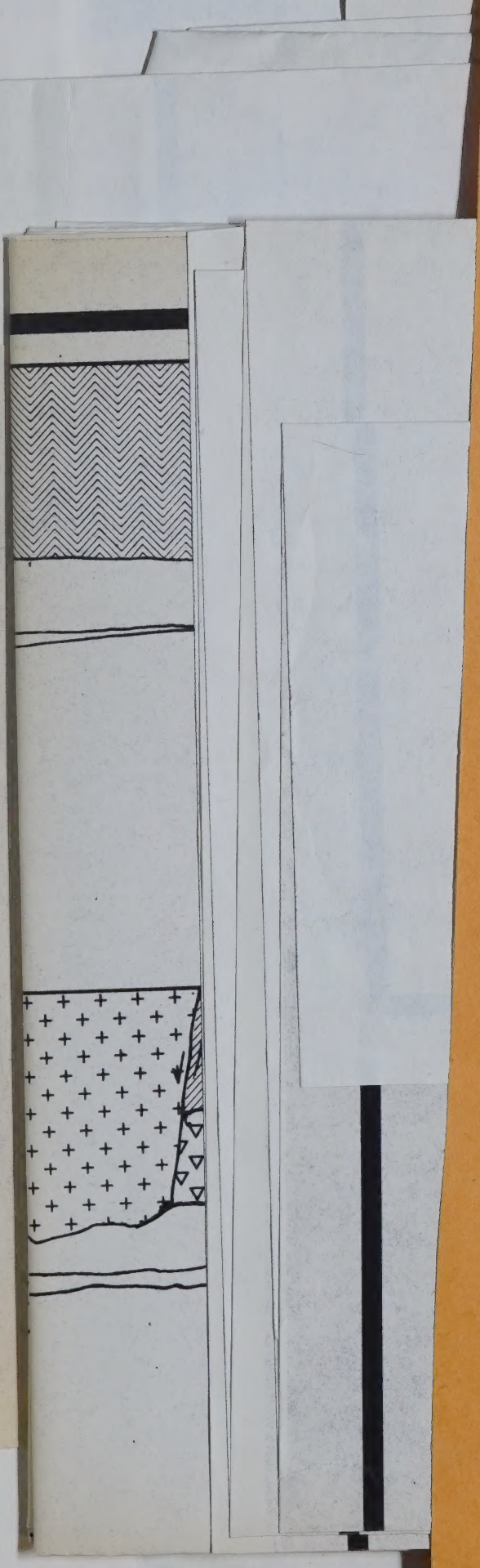
SITE	DENS	ELEV	TREAT	EMU	INC	DEC	SITE	DENS	ELEV	TREAT	EMU	INC	DEC	SITE	DENS	ELEV	TREAT	EMU	INC	DEC
PBT01A	3.1	7250	0	3.52E-03	62.6	-5.1	PBT05B	2.9	7250	400	4.95E-03	36.9	78.4	PBQ01A	3.0	6580	100	3.75E-03	26.5	58.8
PBT01A	3.1	7250	25	3.08E-03	61.6	-17.0	PBT05B	2.9	7250	800	1.97E-03	43.3	68.4	PBQ01A	3.0	6580	200	1.11E-03	29.4	55.3
PBT01A	3.1	7250	50	2.40E-03	59.1	-1.9	PBT05B	2.9	7250	1000	1.29E-03	40.5	72.3	PBQ01A	3.0	6580	400	5.14E-04	37.1	55.2
PBT01A	3.1	7250	100	1.04E-03	56.2	8.4	PBS01C	3.0	7200	0	5.16E-03	11.8	51.7	PBQ02B	3.0	6580	0	9.08E-03	35.3	55.2
PBT01A	3.1	7250	200	9.32E-03	69.1	19.1	PBS01C	3.0	7200	100	5.16E-03	22.0	49.9	PBQ02B	3.0	6580	100	3.88E-03	36.3	54.1
PBT01A	3.1	7250	400	8.06E-03	50.0	42.4	PBS01C	3.0	7200	200	1.92E-03	21.0	52.6	PBQ02B	3.0	6580	200	1.21E-03	41.0	54.8
PBT01A	3.1	7250	800	3.71E-03	60.0	50.0	PBS01C	3.0	7200	400	5.59E-04	15.6	56.5	PBQ02B	3.0	6580	400	5.14E-04	38.6	46.6
PBT01A	3.1	7250	1000	2.77E-03	62.1	51.1	PBS01C	3.0	7200	800	1.84E-02	50.0	57.0	PBQ03B	3.0	6580	0	2.68E-02	143.8	12.4
PBT02B	2.9	7250	0	4.46E-03	196.5	13.4	PBS02A	2.9	7200	0	1.06E-02	54.5	8.6	PBQ03B	3.0	6580	25	2.09E-02	142.8	13.2
PBT02B	2.9	7250	25	4.39E-03	197.5	14.7	PBS02A	2.9	7200	100	5.53E-02	22.9	26.8	PBQ03B	3.0	6580	50	1.07E-02	135.2	21.9
PBT02B	2.9	7250	50	3.99E-03	207.1	20.1	PBS02A	2.9	7200	200	1.94E-03	25.5	35.7	PBQ03B	3.0	6580	100	3.27E-03	117.4	40.8
PBT02B	2.9	7250	100	2.76E-03	195.0	63.1	PBS02A	2.9	7200	400	7.67E-04	33.6	41.7	PBQ03B	3.0	6580	200	7.79E-04	79.0	61.4
PBT02B	2.9	7250	200	1.16E-03	59.7	86.8	PBS02A	2.9	7200	800	2.62E-04	40.3	50.8	PBQ03B	3.0	6580	400	3.75E-04	54.6	57.5
PBT02B	2.9	7250	400	5.66E-04	3.0	84.1	PBS02C	3.0	7200	0	1.26E-02	52.4	18.8	PBQ03B	3.0	6580	800	1.46E-04	66.7	54.5
PBT02B	2.9	7250	800	1.59E-04	70.0	44.5	PBS02C	3.0	7200	25	1.13E-02	43.2	-10.1	PBQ04B	2.9	6580	0	2.67E-02	104.2	17.5
PBT03A	3.0	7250	0	4.24E-03	321.9	59.5	PBS03C	3.0	7200	50	8.79E-03	32.5	2.1	PBQ04B	2.9	6580	100	6.16E-03	89.9	28.6
PBT03A	3.0	7250	25	4.09E-03	333.8	59.5	PBS03C	3.0	7200	100	5.19E-03	26.0	14.2	PBQ04B	2.9	6580	200	1.68E-03	78.6	37.7
PBT03A	3.0	7250	50	4.35E-03	333.9	56.9	PBS03C	3.0	7200	200	1.42E-03	24.9	26.8	PBQ04B	2.9	6580	400	5.84E-04	79.9	38.9
PBT03A	3.0	7250	100	4.26E-03	332.9	58.9	PBS03C	3.0	7200	400	5.66E-04	21.6	35.2	PBQ04B	2.9	6580	800	1.56E-04	68.3	46.1
PBT03A	3.0	7250	200	3.38E-03	337.0	73.4	PBS03C	3.0	7200	800	1.76E-02	47.3	57.4	PBQ04B	2.8	6580	0	7.61E-03	18.6	32.6
PBT03A	3.0	7250	400	1.56E-03	9.8	73.7	PBS03A	2.9	7200	0	5.55E-01	354.4	6.2	PBQ05B	2.8	6580	100	2.79E-03	21.1	48.0
PBT03A	3.0	7250	800	4.53E-03	19.4	77.8	PBS03A	2.9	7200	100	5.54E-02	7.6	17.9	PBQ05B	2.8	6580	200	1.47E-02	21.8	51.3
PBT03C	3.0	7250	0	3.33E-03	334.9	55.7	PBS04A	2.9	7200	200	5.29E-03	8.1	11.3	PBQ05B	2.8	6580	400	8.80E-04	20.9	51.5
PBT03C	3.0	7250	25	3.52E-03	334.8	55.8	PBS04A	2.9	7200	400	1.22E-03	6.7	4.4	PBP01B	2.6	6480	0	8.72E-04	224.5	-58.6
PBT03C	3.0	7250	50	3.22E-03	325.1	65.1	PBS04A	2.9	7200	0	4.12E-02	58.6	-7.1	PBP01B	2.6	6480	100	9.47E-04	225.5	-66.9
PBT03C	3.0	7250	100	3.38E-03	334.9	55.7	PBS03B	3.0	7200	100	8.98E-02	50.5	-9.9	PBP01B	2.6	6480	200	7.18E-04	225.4	-66.4
PBT03C	3.0	7250	200	2.47E-03	19.1	63.6	PBS03B	3.0	7200	200	2.19E-02	51.4	-B.7	PBP02A	2.5	6480	0	8.41E-04	146.9	-71.6
PBT03C	3.0	7250	400	1.51E-03	34.9	65.9	PBS03B	3.0	7200	400	1.00E-02	51.1	-5.9	PBP02A	2.5	6480	100	2.18E-04	182.2	-76.2
PBT03C	3.0	7250	800	4.53E-03	68.6	74.2	PBT02B	3.0	6625	0	8.73E-03	130.0	62.8	PBP02A	2.5	6480	200	6.79E-04	188.5	-76.0
PBT03T	3.1	7250	0	3.33E-03	334.9	55.7	PBT02B	3.0	6625	100	3.16E-03	50.6	63.7	PBP02A	2.5	6480	400	8.06E-04	224.2	-86.2
PBT03T	3.1	7250	25	3.52E-03	334.8	55.8	PBT02B	3.0	6625	200	1.12E-03	51.8	60.8	PBP02A	2.5	6480	100	9.47E-04	223.8	-87.8
PBT03T	3.1	7250	50	3.22E-03	325.1	65.1	PBT02B	3.0	6625	400	5.38E-04	37.7	58.7	PBP02A	2.5	6480	200	6.76E-04	202.0	-75.8
PBT03T	3.1	7250	100	2.41E-03	63.5	78.7	PBT02B	3.0	6625	800	4.82E-02	105.2	21.5	PBP02A	2.5	6480	0	7.06E-04	295.7	-71.2
PBT03T	3.1	7250	200	9.81E-03	53.1	74.6	PBT02B	3.0	6625	0	8.72E-03	41.1	54.1	PBP02A	2.5	6480	25	9.30E-04	260.7	-79.1
PBT03T	3.1	7250	400	4.53E-03	68.6	74.2	PBT02B	3.0	6625	100	4.37E-03	29.2	61.3	PBP03A	2.5	6480	100	6.79E-04	188.5	-76.0
PBT03T	3.1	7250	800	1.55E-03	42.8	87.1	PBT02B	3.0	6625	200	9.06E-04	28.7	62.5	PBP03A	2.5	6480	200	6.24E-04	233.8	-87.2
PBT04B	2.4	7250	0	3.22E-03	63.7	83.0	PBT02B	3.0	6625	400	1.42E-04	18.2	60.2	PBP03A	2.5	6480	400	3.44E-04	235.6	-76.0
PBT04B	2.4	7250	25	1.87E-03	253.9	61.5	PBT02B	3.0	6625	800	4.10E-02	68.7	39.2	PBP03A	2.5	6480	0	8.55E-05	343.1	-68.7
PBT04B	2.4	7250	50	1.12E-03	260.2	35.3	PBT02B	3.0	6625	100	5.55E-03	80.7	47.0	PBP04A	2.5	6480	25	9.30E-04	235.7	-49.9
PBT04B	2.4	7250	100	1.55E-05	40.1	73.4	PBT02B	3.0	6625	200	2.24E-03	69.7	53.8	PBP04A	2.5	6480	50	1.01E-03	244.9	-80.8
PBT04B	2.4	7250	200	1.05E-06	44.0	76.6	PBT02B	3.0	6625	400	7.98E-04	29.1	62.3	PBP05A	2.5	6480	200	8.70E-04	222.0	-78.2
PBT04B	2.4	7250	400	1.62E-06	72.6	76.7	PBT02B	3.0	6625	800	9.06E-04	70.7	50.7	PBP05A	2.5	6480	400	8.06E-04	223.8	-68.2
PBT04B	2.4	7250	800	1.87E-03	223.1	71.0	PBT02B	3.0	6625	0	2.01E-02	112.1	39.2	PBP05A	2.5	6480	0	2.24E-03	202.7	-85.0
PBT04B	2.4	7250	1000	2.06E-03	276.0	68.2	PBT02B	3.0	6625	100	4.10E-03	68.7	65.1	PBP05A	2.5	6480	50	2.33E-03	222.0	-85.0
PBT05B	2.9	7250	0	1.57E-01	72.9	40.9	PBT02B	3.0	6625	200	1.61E-03	70.0	64.5	PBP05A	2.5	6480	0	1.74E-03	228.6	-75.6
PBT05B	2.9	7250	200	1.36E-02	11.6	83.0	PBT02B	3.0	6625	400	3.85E-04	99.8	69.6	PBP05A	2.5	6480	25	1.73E-03	228.3	-76.0
PBT05B	2.9	7250	800	1.05E-03	224.5	31.3	PBT02B	3.0	6625	800	7.98E-04	134.4	52.2	PBP05A	2.5	6480	50	1.05E-03	227.7	-76.6
PBT05B	2.9	7250	1000	1.05E-03	274.5	54.3	PBT02B	3.0	6625	0	8.63E-03	38.2	52.9	PBP05A	2.5	6480	100	1.72E-03	226.2	-77.5
PBT05B	2.9	7250	1200	1.05E-03	223.1	71.0	PBT02B	3.0	6625	100	4.87E-03	32.7	61.2	PBP05A	2.5	6480	200	1.76E-04	210.3	-83.4
PBT05B	2.9	7250	1400	1.05E-03	276.0	68.2	PBT02B	3.0	6625	200	2.42E-03	34.0	62.4	PBP05A	2.5	6480	400	8.45E-04	174.6	-86.2
PBT05B	2.9	7250	1600	1.36E-02	11.6	83.0	PBT02B	3.0	6625	400	1.03E-03	35.2	63.0	PBP05A	2.5	6480	0	8.57E-04	223.3	-79.3
PBT05B	2.9	7250	2000	1.36E-02	11.6	83.0	PBT02B	3.0	6580	0	9.35E-03	39.9	56.1	PBP05A	2.4	6440	100	4.28E-03	50.8	-87.7
PBQ01A							PBQ01A						PBQ01A							

SITE	DENS	ELEV	TREAT	END	INC	DEC	SITE	DENS	ELEV	TREAT	END	INC	DEC
PB003C	2.4	6440	200	3.35E-03	45.1	-86.4	PBL03C	2.6	5835	100	1.38E-04	190.0	-54.8
PB004A	2.6	6440	0	1.74E-03	80.4	-73.1	PBL03C	2.6	5835	200	1.60E-04	189.2	-61.9
PB004A	2.6	6440	50	1.80E-03	68.8	-79.4	PBL03C	2.6	5835	400	1.27E-04	193.6	-65.6
PB004A	2.6	6440	100	1.65E-03	63.6	-79.3	PBL03C	2.6	5835	800	7.06E-05	182.5	-67.2
PB004A	2.6	6440	0	1.20E-02	178.3	-76.7	PBL04A	2.6	5835	0	1.33E-04	148.0	-66.9
PB005A	2.6	6440	50	1.18E-02	179.4	-76.3	PBL04A	2.6	5835	50	1.66E-04	165.6	-67.8
PB005A	2.6	6440	100	1.14E-02	180.5	-76.7	PBL04A	2.6	5835	100	1.75E-04	169.4	-68.7
PBN01B	2.5	6340	0	1.01E-02	270.5	-79.4	PBL04A	2.6	5835	200	1.58E-04	166.6	-68.5
PBN01B	2.5	6340	100	8.95E-03	270.4	-79.6	PBL04A	2.6	5835	400	1.86E-04	270.0	-69.8
PBN01B	2.5	6340	200	6.31E-03	260.6	-79.3	PBL05A	2.6	5835	0	1.87E-04	168.3	-37.5
PBN02A	2.7	6340	0	1.12E-02	262.2	-78.2	PBL05A	2.6	5835	50	2.08E-04	171.2	-51.5
PBN02A	2.7	6340	100	9.91E-03	260.3	-77.9	PBL05A	2.6	5835	100	2.26E-04	174.1	-58.4
PBN02A	2.7	6340	200	6.73E-03	257.6	-77.4	PBL05A	2.6	5835	200	6.64E-04	266.0	-66.5
PBN03C	2.5	6340	0	1.04E-02	268.5	-77.0	PBL05A	2.6	5835	400	1.14E-04	180.8	-68.5
PBN03C	2.5	6340	100	9.20E-03	264.0	-76.8	PBY01A	2.6	5780	0	5.78E-04	56.5	62.9
PBN03C	2.5	6340	200	1.51E-03	260.4	-76.8	PBY01A	2.6	5780	50	9.50E-04	50.6	57.4
PBN04A	2.5	6340	0	1.10E-02	267.7	-77.8	PBY01A	2.6	5780	100	8.64E-05	27.9	39.3
PBN04A	2.5	6340	100	9.91E-03	262.6	-77.8	PBY01A	2.6	5780	200	2.19E-04	43.9	18.0
PBN04A	2.5	6340	200	6.72E-03	262.1	-77.6	PBY01A	2.6	5780	300	6.32E-05	28.4	12.1
PBN05A	2.5	6340	0	1.26E-02	280.0	-80.1	PBY01A	2.6	5780	400	1.45E-04	215.2	21.6
PBN05A	2.5	6340	100	1.12E-02	277.1	-79.3	PBY02A	2.6	5780	0	5.60E-04	101.5	53.2
PBN05A	2.5	6340	200	7.31E-03	270.8	-80.0	PBY02B	2.6	5780	50	4.77E-04	359.9	48.7
PBM01A	2.6	6160	0	2.21E-03	223.3	-62.3	PBY02B	2.6	5780	100	1.01E-04	311.7	27.7
PBM01A	2.6	6160	50	2.20E-03	222.9	-63.6	PBY02B	2.6	5780	200	3.82E-05	9.6	-3.5
PBM01A	2.6	6160	100	* 2.1E-03	223.0	-63.4	PBY02B	2.6	5780	300	6.13E-05	35.7	19.2
PBM02B	2.6	6160	0	2.03E-03	234.0	-62.8	PBY02B	2.6	5780	400	5.58E-05	2.3	12.8
PBM02B	2.6	6160	25	2.03E-03	234.6	-62.8	PBY03C	2.6	5780	0	8.94E-04	43.1	75.5
PBM02B	2.6	6160	50	2.05E-03	235.1	-62.8	PBY03C	2.6	5780	50	7.62E-04	27.5	52.3
PBM02B	2.6	6160	100	2.02E-03	235.3	-62.9	PBY03C	2.6	5780	250	4.74E-04	44.3	75.4
PBM02B	2.6	6160	200	1.86E-03	235.5	-63.0	PBY03C	2.6	5780	500	1.74E-04	72.6	61.9
PBM02B	2.6	6160	400	1.72E-03	229.7	-64.5	PBY03C	2.6	5780	1000	6.51E-05	36.7	38.9
PBM02B	2.6	6160	800	3.01E-04	146.7	-56.5	PBY03C	2.6	5780	2000	6.92E-05	17.6	12.5
PBM03A	2.6	6160	0	1.70E-03	218.7	-63.2	PBY03C	2.6	5780	3000	7.13E-05	37.2	19.9
PBM03A	2.6	6160	25	2.03E-03	214.6	-62.8	PBY03C	2.6	5780	4000	1.40E-05	22.4	-30.1
PBM03A	2.6	6160	50	2.05E-03	225.1	-62.8	PBY04C	2.6	5780	0	4.88E-04	44.3	75.4
PBM03A	2.6	6160	100	2.02E-03	235.1	-62.8	PBY04C	2.6	5780	50	7.32E-04	44.3	75.4
PBM03A	2.6	6160	200	1.86E-03	235.5	-63.0	PBY04C	2.6	5780	100	5.33E-04	106.0	46.9
PBM03A	2.6	6160	400	1.72E-03	229.7	-64.5	PBY04C	2.6	5780	200	2.06E-04	88.0	47.2
PBM03A	2.6	6160	800	3.01E-04	146.7	-56.5	PBY04C	2.6	5780	300	5.46E-05	35.9	35.5
PBM03A	2.6	6160	0	2.18E-03	216.0	-58.7	PBY04C	2.6	5780	400	1.58E-05	321.3	-20.3
PBM03A	2.6	6160	50	1.71E-03	216.7	-62.9	PBY04C	2.6	5780	0	1.40E-05	22.4	-30.1
PBM03A	2.6	6160	100	1.68E-03	216.6	-63.3	PBY05C	2.6	5780	50	7.13E-04	104.8	42.6
PBM03A	2.6	6160	200	1.62E-03	235.3	-62.9	PBY05C	2.6	5780	100	5.33E-04	106.0	46.9
PBM03A	2.6	6160	400	1.71E-03	216.1	-62.7	PBY05C	2.6	5780	200	2.06E-04	88.0	47.2
PBM03A	2.6	6160	800	3.01E-04	146.7	-56.5	PBY05C	2.6	5780	300	5.46E-05	35.9	35.5
PBM03A	2.6	6160	0	2.18E-03	216.0	-58.7	PBY05C	2.6	5780	400	1.58E-05	321.3	-20.3
PBM03A	2.6	6160	50	1.71E-03	216.7	-62.7	PBY05C	2.6	5780	0	1.40E-05	22.4	-30.1
PBL01A	2.6	5835	0	2.40E-04	77.7	49.1	PBY05C	2.6	5780	50	3.27E-04	1.9	26.8
PBL01A	2.6	5835	50	1.75E-03	216.1	-62.7	PBY05C	2.6	5780	100	2.54E-04	358.2	7.3
PBL01A	2.6	5835	100	1.72E-03	218.1	-62.2	PBY05C	2.6	5780	200	1.94E-04	355.7	-7.3
PBL01A	2.6	5835	200	1.70E-03	218.7	-62.2	PBY05C	2.6	5780	300	5.46E-05	359.9	-7.2
PBL01A	2.6	5835	400	1.71E-03	216.0	-58.7	PBY05C	2.6	5780	400	8.89E-05	297.4	-16.9
PBL01A	2.6	5835	0	2.14E-03	215.4	-58.5	PBY05C	2.6	5780	0	3.54E-04	14.5	29.1
PBL01A	2.6	5835	50	1.71E-03	218.3	-62.7	PBY05C	2.6	5780	50	4.14E-04	11.9	45.7
PBL01A	2.6	5835	100	1.70E-03	216.0	-62.7	PBY05C	2.6	5780	100	2.06E-04	88.0	47.2
PBL01A	2.6	5835	200	1.69E-03	218.1	-62.2	PBY05C	2.6	5780	200	5.46E-05	359.9	-7.2
PBL01A	2.6	5835	300	1.68E-03	216.0	-58.7	PBY05C	2.6	5780	300	1.40E-05	22.4	-30.1
PBL01A	2.6	5835	400	1.70E-03	214.6	-40.1	PBY05C	2.6	5780	400	3.54E-04	61.2	55.7
PBL01A	2.6	5835	0	1.99E-04	100.9	45.5	PBK01A	2.5	5745	50	1.66E-04	56.7	55.7
PBL01A	2.6	5835	50	1.41E-04	120.6	-36.7	PBK01A	2.5	5745	100	7.25E-05	22.8	41.7
PBL01A	2.6	5835	100	1.71E-04	143.0	-61.7	PBK01A	2.5	5745	200	6.53E-05	17.3	22.6
PBL01A	2.6	5835	200	1.61E-04	151.8	-67.1	PBK01A	2.5	5745	400	3.01E-05	350.4	30.4
PBL02B	2.7	5835	0	4.76E-04	99.1	59.9	PBK02A	2.5	5745	0	4.68E-04	344.7	73.2
PBL02B	2.7	5835	50	7.04E-04	224.9	59.9	PBK02A	2.5	5745	25	3.38E-04	349.6	71.6
PBL02B	2.7	5835	100	5.38E-05	205.4	39.8	PBK02A	2.5	5745	50	1.77E-04	346.6	80.3
PBL02B	2.7	5835	200	6.33E-05	194.6	-19.8	PBK02A	2.5	5745	100	7.52E-05	343.3	47.7
PBL03C	2.6	5835	0	7.04E-04	224.9	59.9	PBK02A	2.5	5745	25	1.77E-04	349.6	71.6
PBL03C	2.6	5835	50	5.38E-05	205.4	39.8	PBK02A	2.5	5745	50	1.77E-04	346.6	80.3
PBL03C	2.6	5835	100	6.33E-05	194.6	-19.8	PBK02A	2.5	5745	100	3.85E-05	343.3	47.7

INC	DEC	EMU	TREAT	ELEV	SITE
PBI05B	2.7	5675	100	1.82E-03	40.3
PBI05B	2.7	5675	200	1.04E-03	41.7
PBH01A	2.7	5655	0	3.19E-03	72.5
PBH01A	2.7	5655	50	2.53E-03	33.7
PBH01A	2.7	5655	100	2.38E-03	4.3
PBH01B	2.7	5655	0	2.48E-02	91.2
PBH01B	2.8	5655	50	1.73E-02	94.0
PBH01B	2.8	5655	100	1.82E-02	39.4
PBH01B	2.8	5655	200	2.25E-03	94.3
PBH01B	2.8	5655	400	6.51E-04	86.8
PBH01B	2.8	5655	1000	7.82E-03	70.2
PBH01B	2.8	5655	2000	1.17E-02	13.6
PBH01B	2.8	5655	5000	3.81E-03	4.6
PBH01B	2.8	5655	10000	5.10E-04	352.5
PBH03B	2.8	5655	0	5.10E-02	24.9
PBH03C	2.8	5655	100	1.35E-02	347.4
PBH03C	2.8	5655	200	8.28E-04	298.5
PBH03C	2.8	5655	400	5.36E-04	281.9
PBH03D	2.8	5655	0	8.44E-02	281.3
PBH03D	2.8	5655	25	4.63E-02	280.0
PBH03D	2.8	5655	50	1.82E-02	276.8
PBH03D	2.8	5655	100	4.01E-03	273.0
PBH03D	2.8	5655	200	1.86E-03	275.1
PBH03D	2.8	5655	400	7.85E-04	276.8
PBH03D	2.8	5655	800	1.12E-04	306.3
PBH03D	2.8	5655	1000	1.46E-04	299.6
PBH03D	2.8	5655	1200	2.88E-05	339.3
PBH04B	2.8	5655	0	4.17E-03	56.5
PBH04B	2.8	5655	50	1.59E-03	26.1
PBH04B	2.8	5655	100	1.51E-03	22.7
PBH04B	2.8	5655	200	2.41E-04	21.2
PBH04B	2.7	5655	0	4.46E-03	318.5
PBH05A	2.7	5655	50	2.76E-03	335.6
PBH05A	2.7	5655	100	1.91E-03	349.6
PBG01A	2.5	5580	0	2.83E-04	21.6
PBG01A	2.5	5580	100	2.71E-04	21.0
PBG01A	2.5	5580	200	2.41E-04	21.4
PBG01A	2.5	5580	500	3.19E-04	17.4
PBG02B	2.5	5580	0	4.46E-03	18.6
PBG02B	2.5	5580	50	2.50E-04	18.7
PBG02B	2.5	5580	200	2.32E-04	17.8
PBG02B	2.5	5580	500	1.17E-04	19.3
PBG02B	2.5	5580	1000	2.11E-04	-3.3
PBG02B	2.5	5580	2000	1.77E-04	19.4
PBG02B	2.5	5580	5000	3.88E-04	0.2
PBG02B	2.5	5580	10000	5.57E-04	4.7
PBG02B	2.5	5580	20000	2.97E-04	18.7
PBG02B	2.5	5580	50000	2.50E-04	18.7
PBG02B	2.5	5580	100000	2.32E-04	17.8
PBG02B	2.5	5580	200000	1.71E-04	6.4
PBG02B	2.5	5580	500000	1.21E-04	19.3
PBG02B	2.5	5580	1000000	2.11E-04	-2.7
PBG02B	2.5	5580	2000000	1.77E-04	19.4
PBG02B	2.5	5580	5000000	1.21E-04	0.5
PBG02B	2.5	5580	10000000	1.97E-04	19.1
PBG02B	2.5	5580	20000000	1.63E-04	22.4
PBG02B	2.5	5580	50000000	1.25E-04	13.7
PBG02B	2.5	5580	100000000	1.98E-04	23.2
PBG02B	2.5	5580	200000000	1.62E-04	-2.3
PBG02B	2.5	5580	500000000	2.07E-04	17.6
PBG02B	2.5	5580	1000000000	1.99E-04	20.0
PBG02B	2.5	5580	2000000000	1.54E-04	11.2
PBG02B	2.5	5580	5000000000	2.09E-04	13.6
PBG02B	2.5	5580	10000000000	1.84E-04	14.3
PBG02B	2.5	5580	20000000000	1.50E-04	13.2
PBG02B	2.5	5580	50000000000	2.29E-04	16.4
PBG02B	2.5	5580	100000000000	1.03E-04	-0.3
PBG02B	2.5	5580	200000000000	2.05E-04	22.9
PBG02B	2.5	5580	500000000000	8.04E-05	23.0
PBG02B	2.5	5580	1000000000000	1.03E-04	23.0
PBG02B	2.5	5580	2000000000000	2.05E-04	-3.5
PBG02B	2.5	5580	5000000000000	8.04E-05	23.0
PBG02B	2.5	5580	10000000000000	1.03E-04	23.0
PBG02B	2.5	5580	20000000000000	2.05E-04	-3.5
PBG02B	2.5	5580	50000000000000	8.04E-05	23.0
PBG02B	2.5	5580	100000000000000	1.03E-04	23.0
PBG02B	2.5	5580	200000000000000	2.05E-04	-3.5
PBG02B	2.5	5580	500000000000000	8.04E-05	23.0
PBG02B	2.5	5580	1000000000000000	1.03E-04	23.0
PBG02B	2.5	5580	2000000000000000	2.05E-04	-3.5
PBG02B	2.5	5580	5000000000000000	8.04E-05	23.0
PBG02B	2.5	5580	10000000000000000	1.03E-04	23.0
PBG02B	2.5	5580	20000000000000000	2.05E-04	-3.5
PBG02B	2.5	5580	50000000000000000	8.04E-05	23.0
PBG02B	2.5	5580	100000000000000000	1.03E-04	23.0
PBG02B	2.5	5580	200000000000000000	2.05E-04	-3.5
PBG02B	2.5	5580	500000000000000000	8.04E-05	23.0
PBG02B	2.5	5580	1000000000000000000	1.03E-04	23.0
PBG02B	2.5	5580	2000000000000000000	2.05E-04	-3.5
PBG02B	2.5	5580	5000000000000000000	8.04E-05	23.0
PBG02B	2.5	5580	10000000000000000000	1.03E-04	23.0
PBG02B	2.5	5580	20000000000000000000	2.05E-04	-3.5
PBG02B	2.5	5580	50000000000000000000	8.04E-05	23.0
PBG02B	2.5	5580	100000000000000000000	1.03E-04	23.0
PBG02B	2.5	5580	200000000000000000000	2.05E-04	-3.5
PBG02B	2.5	5580	500000000000000000000	8.04E-05	23.0
PBG02B	2.5	5580	1000000000000000000000	1.03E-04	23.0
PBG02B	2.5	5580	2000000000000000000000	2.05E-04	-3.5
PBG02B	2.5	5580	5000000000000000000000	8.04E-05	23.0
PBG02B	2.5	5580	10000000000000000000000	1.03E-04	23.0
PBG02B	2.5	5580	20000000000000000000000	2.05E-04	-3.5
PBG02B	2.5	5580	50000000000000000000000	8.04E-05	23.0
PBG02B	2.5	5580	100000000000000000000000	1.03E-04	23.0
PBG02B	2.5	5580	200000000000000000000000	2.05E-04	-3.5
PBG02B	2.5	5580	500000000000000000000000	8.04E-05	23.0
PBG02B	2.5	5580	1000000000000000000000000	1.03E-04	23.0
PBG02B	2.5	5580	2000000000000000000000000	2.05E-04	-3.5
PBG02B	2.5	5580	5000000000000000000000000	8.04E-05	23.0
PBG02B	2.5	5580	10000000000000000000000000	1.03E-04	23.0
PBG02B	2.5	5580	20000000000000000000000000	2.05E-04	-3.5
PBG02B	2.5	5580	50000000000000000000000000	8.04E-05	23.0
PBG02B	2.5	5580	100000000000000000000000000	1.03E-04	23.0
PBG02B	2.5	5580	20000000000000000000000000	2.05E-04	-3.5
PBG02B	2.5	5580	50000000000000000000000000	8.04E-05	23.0
PBG02B	2.5	5580	100000000000000000000000000	1.03E-04	23.0
PBG02B	2.5	5580	20000000000000000000000000	2.05E-04	-3.5
PBG02B	2.5	5580	50000000000000000000000000	8.04E-05	23.0
PBG02B	2.5	5580	100000000000000000000000000	1.03E-04	23.0
PBG02B	2.5	5580	20000000000000000000000000	2.05E-04	-3.5
PBG02B	2.5	5580	50000000000000000000000000	8.04E-05	23.0
PBG02B	2.5	5580	100000000000000000000000000	1.03E-04	23.0
PBG02B	2.5	5580	20000000000000000000000000	2.05E-04	-3.5
PBG02B	2.5	5580	50000000000000000000000000	8.04E-05	23.0
PBG02B	2.5	5580	100000000000000000000000000	1.03E-04	23.0
PBG02B	2.5	5580	20000000000000000000000000	2.05E-04	-3.5
PBG02B	2.5	5580	50000000000000000000000000	8.04E-05	23.0
PBG02B	2.5	5580	100000000000000000000000000	1.03E-04	23.0
PBG02B	2.5	5580	20000000000000000000000000	2.05E-04	-3.5
PBG02B	2.5	5580	50000000000000000000000000	8.04E-05	23.0
PBG02B	2.5	5580	100000000000000000000000000	1.03E-04	23.0
PBG02B	2.5	5580	20000000000000000000000000	2.05E-04	-3.5
PBG02B	2.5	5580	50000000000000000000000000	8.04E-05	23.0
PBG02B	2.5	5580	100000000000000000000000000	1.03E-04	23.0
PBG02B	2.5	5580	20000000000000000000000000	2.05E-04	-3.5
PBG02B	2.5	5580	50000000000000000000000000	8.04E-05	23.0
PBG02B	2.5	5580	100000000000000000000000000	1.03E-04	23.0
PBG02B	2.5	5580	20000000000000000000000000	2.05E-04	-3.5
PBG02B	2.5	5580	50000000000000000000000000	8.04E-05	23.0
PBG02B	2.5	5580	100000000000000000000000000	1.03E-04	23.0
PBG02B	2.5	5580	20000000000000000000000000	2.05E-04	-3.5
PBG02B	2.5	5580	50000000000000000000000000	8.04E-05	23.0
PBG02B	2.5	5580	100000000000000000000000000	1.03E-04	23.0
PBG02B	2.5	5580	20000000000000000000000000	2.05E-04	-3.5
PBG02B	2.5	5580	50000000000000000000000000	8.04E-05	23.0
PBG02B	2.5	5580	100000000000000000000000000	1.03E-04	23.0
PBG02B	2.5	5580	20000000000000000000000000	2.05E-04	-3.5
PBG02B	2.5	5580	50000000000000000000000000	8.04E-05	23.0
PBG02B	2.5	5580	100000000000000000000000000	1.03E-04	23.0
PBG02B	2.5	5580	20000000000000000000000000	2.05E-04	-3.5
PBG02B	2.5	5580	50000000000000000000000000	8.04E-05	23.0
PBG02B	2.5	5580	100000000000000000000000000	1.03E-04	23.0
PBG02B	2.5	5580	20000000000000000000000000	2.05E-04	-3.5
PBG02B	2.5	5580	50000000000000000000000000	8.04E-05	23.0
PBG02B	2.5	5580	100000000000000000000000000	1.03E-04	23.0
PBG02B	2.5	5580	20000000000000000000000000	2.05E-04	-3.5
PBG02B	2.5	5580	50000000000000000000000000	8.04E-05	23.0
PBG02B	2.5	5580	100000000000000000000000000	1.03E-04	23.0
PBG02B	2.5	5580	20000000000000000000000000	2.05E-04	-3.5
PBG02B	2.5	5580	50000000000000000000000000	8.04E-05	23.0
PBG02B	2.5	5580	100000000000000000000000000	1.03E-04	23.0
PBG02B	2.5	5580	20000000000000000000000000	2.05E-04	-3.5
PBG02B	2.5	5580	50000000000000000000000000	8.04E-05	23.0
PBG02B	2.5	5580	100000000000000000000000000	1.03E-04	23.0
PBG02B	2.5	5580	20000000000000000000000000	2.05E-04	-3.5
PBG02B	2.5	5580	50000000000000000000000000	8.04E-05	23.0
PBG02B	2.5</				

INC	DEC	SITE	DENS	ELEV	TREAT	EMU	SITE	DENS	ELEV	TREAT	EMU	SITE	DENS	ELEV	TREAT	EMU				
PAH01B	2.7	4300	0	7.37E-03	16.7	68.9	PAK01A	2.9	4170	100	2.90E-03	300.9	78.8	PAM05B	2.7	4135	100	2.77E-04	155.8	-32.2
PAH01B	2.7	4300	25	5.55E-03	13.5	68.4	PAK01A	2.9	4170	200	1.35E-03	298.1	79.2	PAM05B	2.7	4135	200	1.48E-04	160.3	-39.4
PAH01B	2.7	4300	50	3.84E-03	18.9	69.1	PAK02A	2.8	4170	0	1.27E-02	307.3	82.1	PAN01B	2.9	4125	0	2.71E-04	206.9	-7.5
PAH01B	2.7	4300	100	2.94E-03	17.5	68.1	PAK02A	2.8	4170	100	5.57E-03	305.0	81.5	PAN01B	2.9	4125	100	2.71E-04	165.3	-32.6
PAH01B	2.7	4300	200	1.65E-03	19.7	68.0	PAK03B	2.8	4170	200	2.64E-03	309.0	80.7	PAN01B	2.9	4125	200	2.73E-04	168.6	-33.0
PAH01B	2.7	4300	400	5.72E-04	26.9	69.2	PAK03B	2.8	4170	0	7.31E-03	324.1	77.0	PAN02C	2.8	4125	0	4.62E-04	187.3	-3.1
PAH01B	2.7	4300	800	1.57E-04	22.0	60.3	PAK03B	2.8	4170	25	6.03E-03	322.0	77.2	PAN02C	2.8	4125	100	4.92E-04	172.7	-47.7
PAH02B	2.4	4300	0	6.74E-03	17.7	63.5	PAK03B	2.8	4170	50	5.52E-03	318.9	78.9	PAN02C	2.8	4125	200	3.04E-04	173.0	-49.3
PAH02B	2.4	4300	100	1.90E-03	20.9	65.6	PAK03B	2.8	4170	100	5.59E-03	322.2	76.6	PAN03B	2.8	4125	0	1.47E-04	130.9	-14.5
PAH02B	2.4	4300	200	1.85E-03	21.1	66.3	PAK03B	2.8	4170	200	3.57E-03	319.3	77.3	PAN03B	2.8	4125	100	2.73E-04	152.2	-40.3
PAH03B	2.3	4300	0	7.32E-03	17.6	61.2	PAK03B	2.8	4170	400	2.03E-03	316.0	77.8	PAN03B	2.8	4125	200	3.50E-04	158.2	-46.9
PAH03B	2.3	4300	100	1.61E-03	23.1	62.8	PAK04A	2.8	4170	800	9.23E-04	330.2	73.5	PAN04B	2.7	4125	0	2.07E-04	149.5	-12.9
PAH03B	2.3	4300	200	9.12E-04	20.2	61.6	PAK04A	2.8	4170	0	5.02E-03	0.2	76.4	PAN04B	2.7	4125	100	4.63E-04	185.4	-42.7
PAH04B	2.7	4300	0	9.21E-03	1.2	67.2	PAK04A	2.8	4170	100	4.25E-03	12.0	75.0	PAN04B	2.7	4125	200	3.37E-04	183.8	-44.5
PAH04B	2.7	4300	100	8.11E-03	1.5	66.5	PAK04A	2.8	4170	200	8.25E-04	17.2	76.0	PAN05C	2.9	4125	0	1.97E-04	87.4	-33.6
PAH04B	2.7	4300	200	8.36E-04	3.0	66.4	PAK05A	2.8	4170	0	2.61E-03	104.3	76.3	PAN05C	2.9	4125	25	3.50E-04	139.1	-51.4
PAH05A	2.7	4300	0	7.32E-03	10.3	72.5	PAK05A	2.8	4170	100	1.07E-03	139.5	81.5	PAN05C	2.9	4125	50	3.55E-04	152.0	-52.1
PAH05A	2.7	4300	100	2.13E-03	14.3	69.8	PAK05A	2.8	4170	200	1.03E-03	139.4	81.6	PAN05C	2.9	4125	100	2.83E-04	158.3	-52.5
PAH05A	2.7	4300	200	1.30E-03	13.8	70.0	PAK05A	2.9	4155	0	7.84E-04	276.1	67.6	PAN05C	2.9	4125	200	1.76E-04	161.6	-55.5
PAI01C	2.7	4230	0	1.06E-03	323.4	62.5	PAI01B	2.9	4155	100	8.88E-05	287.9	67.3	PAI05C	2.9	4125	400	7.29E-05	152.1	-50.7
PAI01C	2.7	4230	25	8.36E-04	344.8	76.6	PAI01B	2.9	4155	200	4.88E-05	307.7	62.8	PAI05C	2.9	4125	800	4.16E-05	229.3	-37.6
PAI01C	2.7	4230	50	7.45E-04	344.8	82.0	PAI02B	3.0	4155	0	1.02E-03	281.9	80.0	PAI01C	2.9	4125	0	3.38E-03	181.3	-75.9
PAI01C	2.7	4230	100	5.14E-04	35.5	84.0	PAI02B	3.0	4155	25	4.13E-04	303.1	79.5	PAI01C	2.9	4125	100	1.68E-03	175.1	-74.6
PAI01C	2.7	4230	200	5.14E-04	35.5	84.0	PAI02B	3.0	4155	50	2.80E-04	313.3	74.7	PAI01C	2.9	4125	200	5.28E-04	178.9	-73.2
PAI01C	2.7	4230	400	1.36E-04	21.1	85.0	PAI02B	3.0	4155	100	1.39E-04	315.3	68.6	PAI02C	2.8	4115	0	3.43E-03	162.9	-77.5
PAI01C	2.7	4230	800	4.27E-05	176.5	82.1	PAI02B	3.0	4155	200	7.57E-05	302.9	71.2	PAI02C	2.8	4115	100	1.28E-03	166.9	-75.8
PAI02C	2.7	4230	0	1.05E-03	344.8	78.6	PAI02B	3.0	4155	400	3.36E-05	302.2	67.1	PAI02C	2.8	4115	200	1.28E-03	163.9	-75.8
PAI02C	2.7	4230	25	8.36E-04	344.8	78.6	PAI02B	3.0	4155	800	1.34E-05	305.1	31.2	PAI03C	2.8	4115	0	6.81E-03	165.6	-74.7
PAI02C	2.7	4230	50	7.45E-04	344.8	82.0	PAI02B	3.0	4155	100	1.26E-04	321.1	68.5	PAI03C	2.8	4115	100	1.53E-03	166.7	-74.4
PAI02C	2.7	4230	100	5.25E-04	35.5	84.0	PAI02B	3.0	4155	50	2.13E-04	313.3	74.7	PAI03C	2.8	4115	200	1.58E-03	171.8	-74.2
PAI03A	2.7	4230	200	4.23E-04	44.9	85.4	PAI02B	3.0	4155	100	1.26E-04	321.1	69.1	PAI04A	2.8	4115	0	4.1E-03	296.2	-23.3
PAI03A	2.7	4230	400	1.36E-04	21.1	85.0	PAI02B	3.0	4155	200	7.11E-05	330.3	60.2	PAI04A	2.8	4115	100	3.36E-03	174.3	-76.8
PAI03A	2.7	4230	800	4.27E-05	176.5	82.1	PAI02B	3.0	4155	100	7.57E-05	302.9	61.1	PAI04A	2.8	4115	200	1.28E-03	163.9	-75.8
PAI04C	2.7	4230	0	1.05E-03	344.8	78.6	PAI04B	2.9	4155	100	1.50E-04	299.5	73.8	PAI04B	2.6	4115	200	1.60E-03	295.4	-23.3
PAI04C	2.7	4230	100	3.46E-03	60.5	87.6	PAI04B	2.9	4155	200	9.29E-05	299.5	75.7	PAI04B	2.6	4115	0	9.30E-05	164.4	-10.4
PAI04C	2.7	4230	200	3.19E-03	82.0	88.0	PAI04B	2.9	4155	800	9.46E-04	315.6	68.5	PAI04B	2.6	4115	25	2.62E-04	154.1	-74.9
PAI05B	2.7	4230	400	1.24E-03	259.6	82.1	PAI05C	2.9	4155	100	1.26E-04	321.1	69.1	PAI05B	2.6	4115	50	2.60E-04	161.2	-74.2
PAI05B	2.7	4230	800	4.23E-04	47.9	87.8	PAI05C	2.9	4155	200	7.11E-05	330.3	60.2	PAI05B	2.6	4115	100	1.31E-04	159.0	-75.5
PAI05B	2.7	4230	200	3.55E-04	36.5	87.4	PAI05C	2.9	4155	100	5.97E-04	264.0	61.1	PAI05B	2.6	4115	200	5.30E-03	174.3	-76.8
PAI05B	2.7	4230	400	3.46E-03	60.5	87.6	PAI05C	2.9	4155	200	1.50E-04	299.5	73.8	PAI05B	2.6	4115	800	1.05E-05	128.5	-29.5
PAI05B	2.7	4230	800	2.42E-04	304.5	72.2	PAI05C	2.9	4155	800	8.18E-04	297.8	79.6	PAI05B	2.6	4115	25	2.62E-04	154.1	-74.9
PAI05B	2.7	4230	200	2.43E-04	304.5	72.2	PAI05C	2.9	4155	100	1.37E-04	318.9	69.2	PAI05B	2.6	4115	50	2.60E-04	161.2	-74.2
PAI05B	2.7	4230	400	1.01E-03	104.2	85.3	PAI05C	2.9	4155	200	5.57E-05	317.8	62.2	PAI05B	2.6	4115	100	1.31E-04	159.0	-75.5
PAI05B	2.7	4230	800	3.18E-03	114.2	85.9	PAI05C	2.9	4155	100	1.51E-03	165.2	38.3	PAI05B	2.6	4115	200	5.30E-03	174.3	-76.8
PAI05B	2.7	4230	200	4.39E-04	288.9	80.2	PAI05C	2.7	4135	100	1.50E-03	167.3	38.9	PAI05B	2.6	4115	800	1.05E-05	128.5	-29.5
PAI05B	2.7	4230	400	9.56E-03	336.3	80.6	PAI05C	2.7	4135	200	1.56E-04	164.7	49.4	PAI05B	2.6	4115	200	8.97E-05	121.9	-85.0
PAI05B	2.7	4230	800	4.38E-03	342.8	80.3	PAI05C	2.7	4135	800	1.30E-05	146.1	37.7	PAI05B	2.6	4115	0	3.09E-04	344.5	-20.3
PAI05B	2.7	4230	200	6.26E-02	78.4	88.2	PAI05C	2.7	4135	25	1.58E-04	129.9	38.1	PAI05B	2.6	4115	50	2.60E-04	163.9	-76.1
PAI05B	2.7	4230	400	3.36E-03	110.1	85.8	PAI05C	2.7	4135	50	2.65E-04	143.8	42.6	PAI05B	2.6	4115	200	1.27E-04	158.3	-83.7
PAI05B	2.7	4230	800	9.77E-03	314.6	67.9	PAI05C	2.7	4135	100	2.37E-04	155.9	47.6	PAI05B	2.6	4115	0	2.37E-04	158.3	-83.7
PAI05B	2.7	4230	200	9.73E-04	306.4	76.3	PAI05C	2.7	4135	100	1.50E-03	165.4	49.4	PAI05B	2.6	4115	200	1.26E-04	158.3	-83.7
PAI05B	2.7	4230	400	4.39E-04	288.9	80.2	PAI05C	2.7	4135	200	1.56E-04	164.4	51.8	PAI05B	2.6	4115	0	2.37E-04	158.3	-83.7
PAI05B	2.7	4230	800	9.56E-03	336.3	80.6	PAI05C	2.7	4135	400	1.53E-04	160.7	83.8	PAI05B	2.6	4115	200	1.01E-04	250.8	-79.5
PAI05B	2.7	4230	200	4.38E-03	342.8	80.3	PAI05C	2.7	4135	800	1.30E-05	146.1	37.7	PAI05B	2.6	4115	0	1.47E-03	344.5	-20.3
PAI05B	2.7	4230	400	2.42E-02	200	81.3	PAI05C	2.7	4135	0	5.07E-04	111.2	30.6	PAI05B	2.6	4115	0	1.50E-04	357.3	-75.1
PAI05B	2.7	4230	800	9.39E-03	300.8	80.2	PAI05C	2.8	4135	100	4.47E-04	158.3	46.3	PAI05B	2.6	4115	0	2.37E-04	358.8	-83.7
PAI05B	2.7	4230	200	1.4E-03	299.4	80.2	PAI05C	2.8	4135	200	2.81E-04	160.8	47.9	PAI05B	2.6	4115	0	2.37E-04	299.4	-83.7
PAI05B	2.7	4230	400	7.51E-03	333.4	78.5	PAI05C	2.8	4135	100	1.56E-03	161.4	50.1	PAI05B	2.6	4115	0	1.48E-04	266.4	-77.4
PAI05B	2.7	4230	800	3.99																

SITE	DENS	ELEV	TREAT	EMU	INC	DEC	SITE	DENS	ELEV	TREAT	EMU	INC	DEC
PAW02B	2.5	3700	800	3.58E-07	255.3	7.0	PAT04B	2.7	3650	0	3.63E-04	350.7	-65.3
PAW03A	2.7	3700	0	3.76E-04	4.9	10.3	PAT04B	2.7	3650	25	4.12E-04	358.9	-78.5
PAW03A	2.7	3700	50	3.20E-04	4.3	13.7	PAT04B	2.7	3650	50	4.26E-04	357.9	-83.5
PAW03A	2.7	3700	100	2.48E-04	2.9	16.3	PAT04B	2.7	3650	100	3.77E-04	311.3	-87.7
PAW04A	2.7	3700	0	1.01E-04	5.3	20.0	PAT04B	2.7	3650	200	1.90E-04	255.0	-87.8
PAW04A	2.7	3700	25	7.37E-04	3.4	29.1	PAT04B	2.7	3650	400	6.19E-05	145.4	-87.3
PAW04A	2.7	3700	50	5.71E-04	1.6	30.0	PAT04B	2.7	3650	600	1.53E-05	186.7	-55.2
PAW04A	2.7	3700	100	2.72E-04	0.3	1.8	PAT05B	2.7	3650	0	4.96E-04	81.2	-64.5
PAW04A	2.7	3700	200	6.64E-05	353.1	38.6	PAT05B	2.7	3650	100	5.23E-04	93.4	-78.7
PAW04A	2.7	3700	400	3.11E-05	356.4	45.2	PAT05B	2.7	3650	200	2.47E-04	100.7	-79.0
PAW04A	2.7	3700	600	1.15E-05	318.5	-17.3	PAT05B	2.7	3650	400	1.12E-04	99.6	-80.2
PAW05B	1.8	3700	0	3.59E-04	333.8	37.3	PAT05B	2.7	3650	600	1.12E-04	84.3	-81.4
PAW05B	1.8	3700	25	2.52E-04	357.5	30.0							
PAW05B	1.8	3700	50	2.37E-04	0.5	24.6							
PAW05B	1.8	3700	100	1.75E-04	1.2	19.7							
PAW05B	1.8	3700	200	5.46E-05	10.0	21.0							
PAW05B	1.8	3700	400	1.87E-05	105.3	6.2							
PAW05B	1.8	3700	600	4.07E-05	32.0	-73.6							
PAX01B	2.7	3675	0	6.38E-04	105.0	-69.3							
PAX01B	2.7	3675	50	6.99E-04	107.5	-83.0							
PAX01B	2.7	3675	100	5.85E-04	108.7	-84.6							
PAX01B	2.7	3675	200	5.83E-04	107.3	-85.1							
PAX01B	2.7	3675	400	1.52E-04	123.4	-84.4							
PAX02B	2.8	3675	0	9.64E-04	181.0	-79.5							
PAX02B	2.8	3675	50	1.03E-03	160.9	-85.5							
PAX02B	2.8	3675	100	7.08E-04	141.6	-86.1							
PAX02B	2.8	3675	200	3.88E-04	139.0	-86.2							
PAX02B	2.8	3675	400	3.75E-04	240.7	-88.2							
PAX03B	2.9	3675	0	1.08E-03	216.9	-82.1							
PAX03B	2.9	3675	50	1.16E-03	194.3	-85.1							
PAX03B	2.9	3675	100	1.03E-03	179.0	-85.6							
PAX03B	2.9	3675	200	5.62E-04	179.7	-86.1							
PAX04B	2.7	3675	0	6.37E-04	196.5	-80.0							
PAX04B	2.7	3675	50	8.08E-04	186.6	-84.8							
PAX04B	2.7	3675	100	5.54E-04	190.5	-86.9							
PAX04B	2.7	3675	200	2.01E-04	191.0	-86.2							
PAX05B	2.8	3675	0	2.56E-04	140.6	-78.4							
PAX05B	2.8	3675	25	4.59E-04	115.5	-86.2							
PAX05B	2.8	3675	50	5.08E-04	114.6	-87.2							
PAX05B	2.8	3675	100	3.71E-04	112.2	-88.9							
PAX05B	2.8	3675	200	1.55E-04	136.2	-88.5							
PAX05B	2.8	3675	400	3.38E-05	314.7	-49.9							
PAX05B	2.8	3675	600	9.91E-06	261.2	-83.8							
PAY01B	2.5	3650	0	3.14E-04	306.7	-68.0							
PAY01B	2.5	3650	100	4.06E-04	79.6	-9.1							
PAY01B	2.5	3650	200	2.04E-04	106.3	-87.7							
PAY02A	2.7	3650	0	3.20E-04	299.0	-53.2							
PAY02A	2.7	3650	100	3.10E-04	10.3	-84.5							
PAY02A	2.7	3650	200	1.60E-04	324.0	-86.3							
PAY03B	2.6	3650	0	3.31E-04	337.3	-50.1							
PAY03B	2.6	3650	100	3.18E-04	8.4	-82.1							
PAY03B	2.6	3650	200	1.62E-04	27.4	-83.8							
PAY03B	2.6	3650	400	5.68E-05	64.3	-85.1							
PAY03B	2.6	3650	600	1.89E-05	253.1	-79.9							



B30326